(12) INTERNATIONAL APPLICATION PUBLISHED UNDER THE PATENT COOPERATION TREATY (PCT)

(19) World Intellectual Property Organization
International Bureau

(43) International Publication Date
21 August 2014 (21.08.2014)

WIPO | PCT

(10) International Publication Number
WO 2014/125309 A2

(51) International Patent Classification:
B01J 21/08 (2006.01)

(21) International Application Number:
PCT/GB2014/050475

(22) International Filing Date:
18 February 2014 (18.02.2014)

(25) Filing Language: English

(26) Publication Language: English

(30) Priority Data:
1302778.4 18 February 2013 (18.02.2013) GB

(71) Applicant: **TEESSIDE UNIVERSITY** [GB/GB]; Middlesbrough, Cleveland TS1 3BA (GB).

(72) Inventors: **OLEA, Maria**; 12 Queens Road, Middlesbrough, Cleveland TS5 6EE (GB). **HODGSON, Simon, Nicholas**; 9 Northfield Drive, Stokesley, Yorkshire TS9 5PF (GB). **AHMED, Rawaz, Abdulrahman**; School of Science and Engineering, Teesside University, Middlesbrough, Cleveland TS1 3BA (GB).

(74) Agent: **HARRISON GODDARD FOOTE LLP**; Document Handling - (HGF) York, Belgrave Hall, Belgrave Street, Leeds Yorkshire LS2 8DD (GB).

(81) Designated States *(unless otherwise indicated, for every kind of national protection available)*: AE, AG, AL, AM, AO, AT, AU, AZ, BA, BB, BG, BH, BN, BR, BW, BY, BZ, CA, CH, CL, CN, CO, CR, CU, CZ, DE, DK, DM, DO, DZ, EC, EE, EG, ES, FI, GB, GD, GE, GH, GM, GT, HN, HR, HU, ID, IL, IN, IR, IS, JP, KE, KG, KN, KP, KR, KZ, LA, LC, LK, LR, LS, LT, LU, LY, MA, MD, ME, MG, MK, MN, MW, MX, MY, MZ, NA, NG, NI, NO, NZ, OM, PA, PE, PG, PH, PL, PT, QA, RO, RS, RU, RW, SA, SC, SD, SE, SG, SK, SL, SM, ST, SV, SY, TH, TJ, TM, TN, TR, TT, TZ, UA, UG, US, UZ, VC, VN, ZA, ZM, ZW.

(84) Designated States *(unless otherwise indicated, for every kind of regional protection available)*: ARIPO (BW, GH, GM, KE, LR, LS, MW, MZ, NA, RW, SD, SL, SZ, TZ, UG, ZM, ZW), Eurasian (AM, AZ, BY, KG, KZ, RU, TJ, TM), European (AL, AT, BE, BG, CH, CY, CZ, DE, DK, EE, ES, FI, FR, GB, GR, HR, HU, IE, IS, IT, LT, LU, LV,

[Continued on next page]

(54) Title: SUPPORTED METAL CATALYST

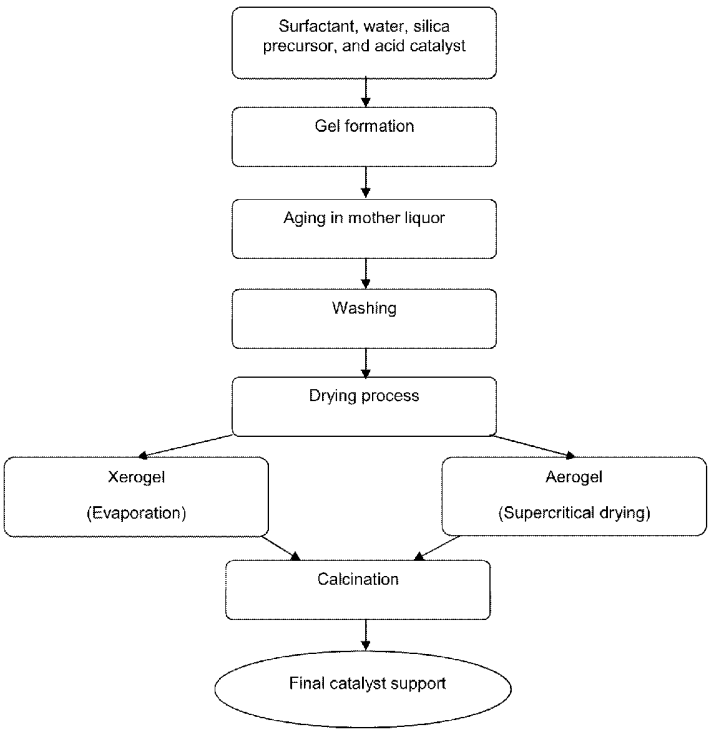

Fig. 1

(57) Abstract: The invention discloses a method of making a mesoporous material with hexagonaily arranged mesopores comprising the following steps: a) dissolving a surfactant in water to form a surfactant solution; b) adding an acid to the surfactant solution to form a mixture having pH less than 2; c) adding a silica precursor to said mixture to form a precipitate; d) aging the precipitate; e) filtering, washing and drying the aged precipitate of step d) and subjecting said precipitate to calcination. An alternative method of making the mesoporous material is also disclosed. The mesoporous material is suitable for supporting a catalyst. Furthermore, the invention describes a supported metal catalyst incorporating such a mesoporous material.

WO 2014/125309 A2

MC, MK, MT, NL, NO, PL, PT, RO, RS, SE, SI, SK, SM, TR), OAPI (BF, BJ, CF, CG, CI, CM, GA, GN, GQ, GW, KM, ML, MR, NE, SN, TD, TG).

Declarations under Rule 4.17:

— *of inventorship (Rule 4.17(iv))*

Published:

— *without international search report and to be republished upon receipt of that report (Rule 48.2(g))*

Supported Metal Catalyst

[0001] The present invention relates to a method of making a highly ordered mesoporous material suitable for supporting a catalyst. Furthermore, the invention describes a catalyst incorporating such a mesoporous material.

BACKGROUND

[0002] Currently, approximately 85% of the world's energy needs are met by the combustion of fossil fuels. The combustion of fossil fuels however, contributes to a multitude of harmful environmental effects including, and not limited to, the accumulation of greenhouse gases (particularly carbon dioxide and methane), water pollution, depletion of stratospheric ozone and acid rain. Although fossil fuels remain cheaper than renewable energy sources, it is predicted their price will soon significantly increase as reserves become depleted. Consequently, scientists around the world are striving to improve current renewable energy technologies.

[0003] Alternatives to fossil fuels have emerged from developments in biofuels whereby biogas, a useful synthetic fuel, can be produced via anaerobic digestion of biomass or organic waste. Generally the constituents of biogas comprise methane (50-70%), carbon dioxide (40-50%), low percentages of hydrogen and nitrogen together with ppm levels of hydrogen sulphide. Synthesis gas (syngas), consisting of hydrogen and carbon monoxide, can be produced from biogas via the carbon dioxide reforming of methane or, as the process is more commonly known, dry reforming of methane (DRM). Syngas produced by DRM represents an ideal raw material for the Fischer-Tropsch synthesis reaction which provides a route to numerous valuable synthetic fuels, including hydrocarbons. Furthermore, syngas is synthesized from methane and carbon dioxide and DRM therefore provides a means of reducing the environmental impact of greenhouse gases.

[0004] Key to the efficient production of syngas by DRM is the use of an effective catalyst. Presently, noble metal catalysts are used in such processes. However, noble metal catalysts suffer from several disadvantages including high cost and poor availability. Further research has shown that transition metal catalysts, such as nickel, may offer a suitable alternative as they are low cost, easily accessible and offer high activity and selectivity towards the production of syngas from DRM. Despite their apparent suitability, nickel catalysts are easily deactivated at temperatures higher than 700 ºC. Deactivation occurs through two mechanisms, one known as sintering which involves an increase in metal crystallite growth leading to the loss of exposed metal surface area and changes in the catalytic properties, and another known as coking which involves carbon and coke-forming processes (Bartholomew, 2001, Applied Catalysis A: General, 212, pp.17-60).

Due to these limitations, no sustainable catalytic technology to produce syngas via the DRM route has yet been demonstrated. To date, only one pilot plant study has been attempted and although high conversion of carbon dioxide were achieved, the process was considered commercially unattractive as the operating temperature was over 800 ºC (Tian et al.,2009, Energy & Fuels. 23, pp. 607-612).

[0005] In an effort to overcome these restrictions, numerous investigations have been conducted to explore modified nickel catalysts with high resistance to carbon formation and with lower operational temperatures (Li et al., 2011, Applied Catalysis A: General and Sokolov et al., 2011, Applied Catalysis B: Environmental). Many of the approaches have focused on the addition of other compounds to nickel or changing the interaction between the nickel component and the supporting material on which the catalyst is usually based. Porous materials typically form the basis of a catalyst support due to their large surface area. Such materials frequently incorporate silica and are characterized according to their pore size. According to the IUPAC definition, microporous materials comprise pores less than 2 nm in diameter, mesoporous materials comprise pores of 2 nm to 50 nm in diameter and macroporous materials have pores exceeding 50 nm in diameter.

[0006] The functionality of mesoporous silica supports suggests particular suitability for transition metal catalysis as they have a high surface area for the active site component, provide shape and mechanical strength for the catalyst, form a crystalline active phase and are low cost. Furthermore, when the metal component is confined to the mesoporous channels of the molecular sieve inherent to the silica support, the sintering rate can be reduced. Commonly used mesoporous silica supports are SBA-15 and MCM-41. SBA-15 exhibits particular suitability as it allows the pore size to be tailored, has a high degree of structural ordering and is simple and cheap to synthesize. In addition, SBA-15 has a high degree of hydrothermal/thermal stability, a large pore diameter providing good suitability for the catalysis of large molecules and demonstrates the fastest kinetics. SBA-15 is a mesoporous material with a hexagonally arranged mesoporous pore structure. Mesoporous materials comprising such a pore structure are thus known as SBA-15.

[0007] Although SBA-15 displays the appropriate functionality to support a metal catalyst suitable for the dry reforming of methane, the method of preparation of the support has a significant influence on the behaviour and ultimate performance of the catalyst. Commonly, SBA-15 supports are prepared using a sol-gel method. This method is an homogenous process which results in the continuous transformation of a solution into a hydrated solid precursor. Sol-gel methods are highly versatile allowing control of the texture, composition, homogeneity and structural properties of the final solids.

[0008] Despite the apparent suitability of SBA-15 for nickel-supported catalysis in DRM

and the versatility of the sol-gel preparation method, only one research group has adopted this approach to date (Zhang et al.,2006, Chinese Journal of Catalysis, 27(9), pp.777-782). This particular group followed the published method of Zhao (Zhao et al., 1998, Science, 279, pp.548-552 and Zhao et al., 1998, Journal of the American Chemical Society, 120, pp. 6024-6036 - hereinafter referred to as Zhao et al., 1998a and b) to prepare the SBA-15 support for the nickel catalyst. The results of the study indicated good stability and suggested SBA-15 possessed specific properties to avoid the sintering of nickel components. However, the optimal operational temperature of the catalyst was recorded as 750-800 °C which is prohibitively high for economical industrial use. Attempts to develop improved mesoporous support materials to provide catalysts with higher activity and other advantageous properties are hindered by the number of variables and codependent factors involved in their synthesis which determine the overall functionality of such materials. Identifying the combination of optimized variables to provide an improved catalyst support is therefore highly complex. Due to the potential industrial application of such materials, even small improvements in catalytic activity and performance over the currently available mesoporous catalysts are considered highly desirable.

[0009] In order to overcome the shortcomings of the prior art, what is therefore needed is an improved metal catalyst suitable for the dry reforming of methane on an industrial scale. Furthermore, an improved mesoporous material to support a metal catalyst and a method for making such a material is sought.

BRIEF SUMMARY OF THE DISCLOSURE

[0010] Embodiments of the present invention provide a mesoporous material with improved properties compared to those made by processes of the prior art. Mesoporous materials according to embodiments of the invention demonstrate improved catalytic performance as exhibited by higher carbon dioxide conversion in the dry reforming of methane reaction compared to materials made by the processes of the prior art.

[0011] According to a first aspect of the invention there is provided a method of making a mesoporous material with hexagonally arranged mesopores comprising the following steps:

a) dissolving a surfactant in water to form a surfactant solution;

b) adding an acid to the surfactant solution to form a mixture having pH less than 2;

c) adding a silica precursor to said mixture to form a precipitate;

d) aging the precipitate;

e) filtering, washing and drying the aged precipitate of step d) and subjecting said precipitate to calcination.

[0012] In the first aspect of the invention, dissolving the surfactant in water before the addition of acid in step b) is believed to promote the formation of cylindrical micelles in a highly ordered hexagonal structure. The highly ordered hexagonal cylindrical structure is believed to ensure that the mesoporous material of embodiments of the invention provides an improved framework for the addition of further moieties, such as a species with catalytic properties, than that formed by frameworks known from methods of the prior art.

[0013] In some preferred embodiments the surfactant may be a poly(alkyleneoxide) block co-polymer. In some preferred embodiments the block co-polymer may have a poly(ethylene oxide) – poly(propylene oxide) – poly(ethylene oxide) (EO-PO-EO) sequence. In further preferred embodiments the block copolymer may be a triblock co-polymer with a formula $EO_mPO_nEO_m$. In much preferred embodiments, the triblock co-polymer may have the formula $EO_{20}PO_{70}EO_{20}$. In these preferred embodiments the surfactant with the formula $EO_{20}PO_{70}EO_{20}$ may be Pluronic P123.

[0014] In some preferred embodiments, from 1% to 4% by weight surfactant may be dissolved in water. In some preferred embodiments between 2.5 and 3.5% by weight surfactant may be dissolved in water. In further preferred embodiments about 3% and in particular, about 3.2% by weight surfactant may be dissolved in water.

[0015] In some preferred embodiments, the acid in step b) is added after a set period. The period may be greater than 1 hour and in some preferred embodiments is at least 6 hours.

[0016] In further preferred embodiments, the acid may be selected from the group consisting of hydrochloric acid, hydroiodic acid, hydrobromic acid, nitric acid, sulphuric acid and phosphoric acid. In some preferred embodiments the acid may be hydrochloric acid. It is believed that the use of hydrochloric acid means that the mesoporous material is advantageously formed via a true-liquid crystal template mechanism and promotes the maintenance of a highly ordered cylindrical hexagonal structure of micelles.

[0017] In some preferred embodiments the mixture has pH less than 1.

[0018] In still further preferred embodiments, the silica precursor may be selected from tetramethoxysilane, tetraethoxysilane, tetrapropoxysilane, sodium silicate or a silica alkoxide. In some preferred embodiments the silica precursor may be tetraethoxysilane.

[0019] In some preferred embodiments the molar ratio of silica precursor/surfactant may be from 60 to 75. In further preferred embodiments, the molar ratio of silica

precursor/surfactant may be from 65 to 70 and in particular embodiments the molar ratio of silica precursor/surfactant may be about 67. The Inventor believes that the use of a molar ratio of silica precursor/surfactant according to the invention may facilitate the production of a mesoporous material with lower microporosity than that of the prior art and may provide a mesoporous material with high thermal stability.

[0020] In some preferred embodiments the silica precursor may be added dropwise.

[0021] Dropwise can be defined as adding the silica precursor at a rate low enough to ensure the ordered arrangement of the micelles is not disturbed to any disadvantageous extent and preferably is not significantly disturbed.

[0022] In some preferred embodiments steps a), b) and c) may be performed under heating. In further preferred embodiments, the solution of step a) may be heated to at least 35 ºC and the respective mixtures of step b) and step c) maintained at the same temperature of step a). In further preferred embodiments the solution of step a) may be heated to 40ºC and the respective mixtures of step b) and step c) maintained at a temperature of 40 ºC.

[0023] In some preferred embodiments aging may be performed at a temperature of at least 80 ºC. In further preferred embodiments aging may be performed at a temperature greater than 80 ºC and in still further embodiments aging is performed at a temperature of from 93 ºC to 97 ºC. In one preferred example aging may be performed at a temperature of 95 ºC. Increasing the aging temperature to from 93 ºC to 97 ºC, for example 95 ºC, is believed to facilitate the formation of a mesoporous material with low or negligible microporosity compared to mesoporous materials produced by the prior art.

[0024] In some preferred embodiments aging may be for a period of at least 12 hours and in further preferred embodiments aging may be for a period of about 24 hours.

[0025] In some preferred embodiments calcination may be performed at a temperature of at least 500 ºC. In further preferred embodiments calcination may be performed at a temperature of greater than 500 ºC and in still further embodiments calcination may be performed at a temperature of from 545 ºC to 555 ºC. In preferred examples calcination may be performed at a temperature of about 550 ºC.

[0026] In further preferred embodiments, calcination may be performed by heating at a rate of 1 ºC per minute and maintaining steady state conditions for 6 hours. In such preferred embodiments, calcination is thus performed by heating at rate of 1 ºC per minute until a specified temperature is reached followed by maintaining the specified temperature for the 6 hour period without changing any conditions.

[0027] In still further preferred embodiments the method further comprises the steps:

f) cooling the calcined precipitate of step e), rehydrating to form a suspension; and

g) filtering and drying the suspension. In some preferred embodiments, the method further comprises boiling the suspension of step f) before filtering and drying the suspension.

[0028] According to a second aspect of the invention there is provided a mesoporous material made by the method according to the first aspect of the invention.

[0029] In preferred embodiments, said mesoporous material comprises mesopores with a total pore volume of greater than 0.55 cm^3/g and an average micropore volume of less than 0.038 cm^3/g as measured from nitrogen adsorption isotherms using the methods specified herein.

[0030] In further preferred embodiments, said mesoporous material comprises mesopores with a total pore volume of greater than 0.92 cm^3/g and an average micropore volume of less than 0.038 cm^3/g as measured from nitrogen adsorption isotherms using the methods specified herein.

[0031] In some embodiments the volume of mesopores is determined from nitrogen adsorption isotherms using the BJH method and the volume of micropores is determined using α-, β- and *t*-plots.

[0032] In a third aspect of the invention there is provided a support for a catalyst comprising or consisting of a mesoporous material according to the second aspect of the invention.

[0033] According to a fourth aspect of the invention there is provided a method of making a mesoporous material with hexagonally arranged mesopores comprising the following steps:

a) dissolving a surfactant in a mixture of water and acid wherein the mixture has pH less than 2;

b) adding a silica precursor to said mixture to form a precipitate;

c) aging the precipitate;

d) filtering, washing and drying the aged precipitate of step c) and subjecting said precipitate to calcination;

e) cooling the calcined product of step d), rehydrating to form a suspension; and

f) filtering and drying the suspension.

[0034] In the fourth aspect of the invention the surfactant may be dissolved in a

combined mixture of water and acid. Thus in the fourth aspect of the invention, the surfactant does not have to be dissolved in water first before adding the acid. In embodiments of the invention the inclusion of the rehydration process as described in steps e) and f) is thought ultimately to provide a mesoporous material that, when impregnated with a metal precursor, may demonstrate enhanced carbon dioxide conversion when compared to a mesoporous material as prepared by methods of the prior art. It is believed that the re-hydrated mesoporous material may be less susceptible to cracking when subsequently impregnated with a metal precursor or other catalytic species.

[0035] In some preferred embodiments, the method of the fourth aspect of the invention further comprises boiling the suspension of step e) before filtering and drying the suspension.

[0036] In some preferred embodiments the surfactant may be a poly(alkyleneoxide) block co-polymer. In some preferred embodiments the block co-polymer may have a poly(ethylene oxide) – poly(propylene oxide) – poly(ethylene oxide) (EO-PO-EO) sequence. In further preferred embodiments the block copolymer may be a triblock co-polymer with a formula $EO_mPO_nEO_m$. In much preferred embodiments, the triblock co-polymer may have the formula $EO_{20}PO_{70}EO_{20}$. In these preferred embodiments the surfactant with the formula $EO_{20}PO_{70}EO_{20}$ may be Pluronic P123.

[0037] In some preferred embodiments, from 1% to 4% by weight surfactant may be dissolved in the mixture. In some preferred embodiments between 2 and 3% by weight surfactant may be dissolved in the mixture. In further preferred embodiments about 2.5% by weight surfactant may be dissolved in the mixture and in particular 2.6% by weight surfactant may be dissolved in the mixture.

[0038] In further preferred embodiments, the acid may be selected from the group consisting of hydrochloric acid, hydroiodic acid, hydrobromic acid, nitric acid, sulphuric acid and phosphoric acid. In some preferred embodiments the acid may be hydrochloric acid.

[0039] In some preferred embodiments the mixture has pH less than 1.

[0040] In still further preferred embodiments, the silica precursor may be selected from tetramethoxysilane, tetraethoxysilane, tetrapropoxysilane, sodium silicate or a silica alkoxide. In some preferred embodiments the silica precursor may be tetraethoxysilane.

[0041] In some preferred embodiments the molar ratio of silica precursor/surfactant may be from 60 to 75. In further preferred embodiments, the molar ratio of silica precursor/surfactant may be from 65 to 70 and in particular embodiments the molar ratio

of silica precursor/surfactant may be 67.

[0042] In some preferred embodiments the silica precursor may be added dropwise.

[0043] In some preferred embodiments steps a) and b) may be performed under heating. In further preferred embodiments, the mixture of step a) may be heated to at least 35 ºC and the mixture of step b) maintained at the same temperature of step a). In still further preferred embodiments the mixture of step a) may be heated to 40ºC and the mixture of step b) maintained at a temperature of 40 ºC.

[0044] In some preferred embodiments aging may be performed at a temperature of at least 80 ºC. In further preferred embodiments aging may be performed at a temperature of greater than 80 ºC and in still further embodiments aging is performed at a temperature of from 93 ºC to 97 ºC. In one preferred example aging may be performed at a temperature of 95 ºC.

[0045] In some preferred embodiments aging may be for a period of at least 12 hours and in further preferred embodiments aging may be for a period of about 24 hours.

[0046] In some preferred embodiments calcination may be performed at a temperature of at least 500 ºC. In further preferred embodiments calcination may be performed at a temperature of greater than 500 ºC and in still further embodiments calcination is performed at a temperature of from 545 ºC to 555 ºC. In preferred examples calcination may be performed at a temperature of about 550 ºC.

[0047] In further preferred embodiments, calcination may be performed by heating at a rate of 1 ºC per minute and maintaining steady state conditions for 6 hours. In such preferred embodiments, calcination is thus performed by heating at rate of 1 ºC per minute until a specified temperature is reached followed by maintaining the specified temperature for the 6 hour period without changing any conditions.

[0048] According to a fifth aspect of the invention there is provided a mesoporous material made by the method according to the fourth aspect of the invention.

[0049] In preferred embodiments, said mesoporous material comprises mesopores with a total pore volume of greater than 0.55 cm^3/g and an average micropore volume of less than 0.038 cm^3/g as measured from nitrogen adsorption isotherms using the methods specified herein.

[0050] In further preferred embodiments, said mesoporous material comprises mesopores with a total pore volume of greater than 0.92 cm^3/g and an average micropore volume of less than 0.038 cm^3/g as measured from nitrogen adsorption isotherms using the methods specified herein.

[0051] In a sixth aspect of the invention there is provided a support for a catalyst comprising or consisting of a mesoporous material according to the fifth aspect of the invention.

[0052] According to a seventh aspect of the invention there is provided a method of making a catalyst comprising the step of impregnating the mesoporous material of the second aspect, the fifth aspect or the support for a catalyst of the sixth aspect of the invention with a metal precursor.

[0053] In some preferred embodiments of the seventh aspect of the invention impregnating the material may comprise adding a solution containing the metal precursor to said material, drying the material and subjecting the material to calcination.

[0054] In some preferred embodiments the material may be impregnated using wet impregnation.

[0055] In some preferred embodiments wet impregnation may be performed under reflux conditions. Performing the wet impregnation step under reflux is believed to improve the mass transfer between the solution and the solid mesoporous material. In some preferred embodiments, the metal precursor has improved solubility in boiling solvent and this is believed to enable greater dispersion throughout the mesoporous material.

[0056] In some preferred embodiments calcination may be performed at a temperature of greater than 500 ºC and in still further embodiments calcination is performed at a temperature of from 545 ºC to 555 ºC. In preferred examples calcination may be performed at a temperature of about 550 ºC.

[0057] In some preferred embodiments the metal may be a transition metal.

[0058] In further preferred embodiments the metal may be nickel.

[0059] In still further preferred embodiments the metal precursor may be a metal salt. In some preferred embodiments the metal salt may be selected from the group consisting of acetate, citrate, nitrate, acetylacetonate, chloride, fluoride, carbonate and sulphate. In some preferred embodiments the metal precursor may be nickel acetate or nickel nitrate. The use of nickel acetate as the metal precursor is believed to advantageously increase the dispersion of the metal throughout the mesoporous material. The use of nickel nitrate may contribute to a high loading of the metal precursor onto the mesoporous material.

[0060] In an eighth aspect of the invention there is provided a supported metal catalyst made by the method of the seventh aspect of the invention.

[0061] In a ninth aspect of the invention there is provided a mesoporous material comprising SBA-15, wherein said SBA-15 has mesopores with a total pore volume of

greater than 0.92 cm^3/g and an average micropore volume of less than 0.038 cm^3/g as measured from nitrogen adsorption isotherms using methods specified herein. In some embodiments the volume of mesopores is determined from nitrogen adsorption isotherms using the BJH method and the volume of micropores is determined using *α*-, *β*- and *t*-plots. The mesoporous material comprising SBA-15 exhibits mesopores with a high total pore volume whilst ensuring low or negligible microporosity compared to mesoporous materials produced by the methods of the prior art.

[0062] In some preferred embodiments said SBA-15 may have mesopores with a total pore volume of greater than 1.0 cm^3/g and in further preferred embodiments said SBA-15 may have mesopores with a total pore volume of about 1.05 cm^3/g.

[0063] In some preferred embodiments said SBA-15 may further comprise mesopores with an average wall thickness of greater than 2.15 nm as measured using a method specified herein. In further preferred embodiments, said SBA-15 may comprise mesopores with an average wall thickness of about 3 nm. In some embodiments, the average wall thickness may be measured from nitrogen adsorption isotherms. In some preferred embodiments, the average wall thickness may be determined from nitrogen adsorption isotherms using the BJH method.The mesopores of the material according to the invention are believed to have a greater wall thickness and thus the material can exhibit improved thermostability compared to mesoporous materials produced by the methods of the prior art.

[0064] In some preferred embodiments said SBA-15 may have a pore size distribution centred around 3 nm as measured from nitrogen desorption isotherms using a method specified herein. In some preferred embodiments, said SBA-15 may have a pore size distribution centred around 4 nm as measured from nitrogen adsorption isotherms using a method specified herein. In further preferred embodiments, said SBA-15 may have a pore size distribution centred around 3.8 nm as measured from nitrogen adsorption isotherms. In some embodiments, the pore size distribution is determined from nitrogen isotherms using the BJH method. Advantageously, the mesopores of the material may demonstrate a narrow pore size distribution.

[0065] In some preferred embodiments said SBA-15 may have a *p6mm* hexagonal symmetry as measured by X ray diffraction.

[0066] In some preferred embodiments said SBA-15 may have an interplanar distance of about 9 nm and a unit cell parameter of about 11 nm. In further preferred embodiments said material may have an interplanar distance of about 9.2 nm and a unit cell parameter of about 10.6 nm.

[0067] In some preferred embodiments said SBA-15 may have a BET specific surface area of greater than 800 m^2/g. In further preferred embodiments said SBA-15 has a BET specific surface area of about 830 m^2/g, in particular 834 m^2/g.

[0068] In a tenth aspect of the invention there is provided a supported metal catalyst comprising SBA-15 impregnated with a metal, wherein said supported metal catalyst has a total pore volume of greater than 0.68 cm^3/g as measured from nitrogen isotherms using a method specified herein. In some preferred embodiments, said catalyst may exhibit a total pore volume of greater than 0.8 cm^3/g and in further preferred embodiments the catalyst may exhibit a total pore volume of greater than 0.9 cm^3/g. In some preferred embodiments said supported metal catalyst may have a total pore volume of 0.84 cm^3/g or greater and in other preferred embodiments said supported metal catalyst has a total pore volume of 1.0 cm^3/g or greater. In some preferred embodiments, the total pore volume is measured from nitrogen adsorption isotherms. In other preferred embodiments, the total pore volume is measured from nitrogen desorption isotherms. In some preferred embodiments, the total pore volume is measured from nitrogen isotherms using the BJH method. In some preferred embodiments the supported metal catalyst following impregnation may exhibit a higher total pore volume than metal catalysts of the prior art.

[0069] In some preferred embodiments said supported metal catalyst may have a BET specific surface area of greater than 400 m^2/g. In further preferred embodiments said supported metal catalyst may have a BET specific surface area of greater than 475 m^2/g. In some preferred embodiments the BET specific surface area may be greater than 500 m^2/g and in other preferred embodiments the BET specific surface area may be about 591 m^2/g. Thus in some preferred embodiments the supported metal catalyst according to the invention may have a BET specific surface area greater than supported metal catalysts of the prior art.

[0070] In some preferred embodiments said supported metal catalyst may comprise crystallites of said metal of less than 5 nm diameter. In such preferred embodiments, crystallites of the metal could not be detected by wide angle X ray diffraction and thus must have a diameter of less than 5 nm. As the supported metal catalyst comprises crystallites of a such a size, the supported metal catalyst is believed to demonstrate a better distribution of the metal species over the SBA-15 surface compared with supported metal catalysts prepared by methods of the prior art. The greater dispersion of the metal species is believed to increase the number of active sites available for the dry reforming of methane reaction.

[0071] In some preferred embodiments the metal is a transition metal.

[0072] In further preferred embodiments the metal is nickel.

[0073] In an eleventh aspect of the invention there is provided a supported metal catalyst comprising a mesoporous material, operable to attain 100% conversion of carbon dioxide from methane at a temperature lower than 700 ºC when performing the catalyst activity test as specified herein. In some preferred embodiments, the supported metal catalyst is operable to attain 100% conversion of carbon dioxide from methane at a temperature of 650 ºC when performing the catalyst activity test as specified herein. In further preferred embodiments, the supported metal catalyst is a supported metal catalyst according to the eighth aspect of the invention.

BRIEF DESCRIPTION OF THE DRAWINGS

[0074] Embodiments of the invention are further described hereinafter with reference to the accompanying drawings, in which:

Figure 1 shows a summary of the principal steps in a typical sol-gel preparation method;

Figure 2 shows low angle XRD spectra of modified and unmodified SBA-15 mesoporous silica;

Figure 3 shows an SEM image of A) modified SBA-15 and B) unmodified SBA-15 mesoporous silica;

Figure 4 shows low angle XRD spectra of 9Ni/modified SBA-15 and 9Ni/unmodified SBA-15 mesoporous silica;

Figure 5 shows a wide angle XRD spectra of 9Ni/modified SBA-15 and 9Ni/unmodified SBA-15 samples before and after CO_2 reforming of methane reaction. The labels 9Ni/modified SBA-15 and 9Ni/unmodified SBA-15 are the results before the reaction and 9Ni/modified SBA-15, spent, 650 ºC and 9Ni/unmodified SBA-15, spent, 650 ºC are the results after the reaction when conducted at 650 ºC.

Figure 6 shows SEM images of: A) 9Ni/modified SBA-15, fresh; B) 9Ni/modified SBA-15, spent; C) 9Ni-unmodified SBA-15, fresh; and D) 9Ni/unmodified SBA-15, spent for the samples before and after CO_2 reforming of methane reaction. The label “fresh” refers to the sample before the reaction and “spent” refers to the sample after the reaction when conducted at 650 ºC.

Figure 7 shows nitrogen adsorption (ads) – desorption (des) isotherms for SBA-15 mesoporous silica aged for 24hr wherein V (STP) represents the volume of

adsorbed (desorbed) N_2 at standard temperature and pressure and P/P^0 is relative pressure;

Figure 8 shows the BET transform plots of SBA-15 mesoporous silica;

Figure 9 shows pore size distribution plots of SBA-15 mesoporous silica, calculated from the nitrogen sorption isotherm during adsorption (ads) and desorption (des), respectively. The incremental change in the pore volume divided by the incremental change in the pore radius (dVp/dRp) is plotted against the pore radius (Rp);

Figure 10 shows nitrogen adsorption (ads) – desorption (des) isotherms of A) 9% IMPNiA-Bd, B) 9% IMPNiA-Bc, C) 12% IMPNiN-B, and D) 8% IMPNiC-B catalysts wherein V (STP) represents the volume of adsorbed (desorbed) N_2 at standard temperature and pressure and P/P^0 is relative pressure;

Figure 11 shows pore size distribution plots of A) 9% IMPNiA-Bd, B) 9% IMPNiA-Bc, C) 12% IMPNiN-B, and D) 8% IMPNiC-B catalysts. The incremental change in the pore volume divided by the incremental change in the pore radius (dVp/dRp) is plotted against the pore radius (Rp);

Figure 12 shows low angle XRD spectra of SBA-15-1.2-24-HCl, SBA-15-2-24-HCl and SBA-15-4-24-HCl samples;

Figure 13 shows SEM images of A) SBA-15-1.2-24-HCl, B) SBA-15-2-24-HCl and C) SBA-15-4-24-HCl samples;

Figure 14 shows TEM micrographs of the SBA-15-4-24-HCl sample;

Figure 15 shows nitrogen adsorption (ads) – desorption (des) isotherms of SBA-15-1.2-24-HCl, SBA-15-2-24-HCl and SBA-15-4-24-HCl samples wherein V (STP)represents the volume of adsorbed (desorbed) N_2 at standard temperature and pressure and P/P^0 is relative pressure;

Figure 16 shows pore size distribution plots of SBA-15-1.2-24-HCl, SBA-15-2-24-HCl and SBA-15-4-24-HCl samples, calculated from the nitrogen sorption isotherm during adsorption (ads) and desorption (des), respectively. The incremental change in the pore volume divided by the incremental change in the pore radius (dVp/dRp) is plotted against the pore radius (Rp);

Figure 17 shows the BET transform plots of SBA-15-1.2-24-HCl, SBA-15-2-24-HCl and SBA-15-4-24-HCl samples;

Figure 18 shows *t-, α- and β-plots,* respectively for the SBA-15-4-24-HCl sample;

Figure 19 Shows the formation of mesoporous materials by structure-directing agents via: a) true liquid-crystal template mechanism and b) cooperative self-assembly template mechanism; with reference to Beck et al., 1992, Journal of the American Chemical Society, 114, pp.10834-10843; Edler et al., Australian Journal of Chemistry, 58, pp.627-643; Hoffmann et al., 2006, Angewandte Chemie International Edition, 45, pp.3216-3251;

Figure 20 shows low angle XRD spectra of formation SBA-15 after addition of TEOS at 0 min, 10 min, 30 min, 60 min, 90 min and 120 min;

Figure 21 shows low angle XRD spectra of SBA-15-4-24-HCl and SBA-15-4-48-HCl samples;

Figure 22 shows SEM images of: A) SBA-15-4-24-HCl and B) SBA-15-4-48-HCl;

Figure 23 shows low angle XRD spectra of SBA-15-4-24-HCl and SBA-15-4-24-HNO_3 samples;

Figure 24 shows SEM images of A) SBA-15-4-24-HCl and B) SBA-15-4-24-HNO_3 samples;

Figure 25 shows nitrogen adsorption (ads) – desorption (des) isotherms for SBA-15-4-24-HCl and SBA-15-4-24-HNO_3 samples, wherein V (STP) represents the volume of adsorbed (desorbed) N_2 at standard temperature and pressure and P/P^0 is relative pressure;

Figure 26 shows pore size distribution plots of SBA-15-4-24-HCl and SBA-15-4-24-HNO_3 samples, calculated from the nitrogen sorption isotherm during adsorption and desorption, respectively. The incremental change in the pore volume divided by the incremental change in the pore radius (dVp/dRp) is plotted against the pore radius (Rp);

Figure 27 shows the BET transform plots of SBA-15-4-24-HCl and SBA-15-4-24-HNO_3 samples;

Figure 28 shows low angle XRD spectra for formation of the mesoporous structure in sample SBA-15-4-0-HNO_3, after addition of TEOS at 90 min and 120 min;

Figure 29 shows SEM images for the formation of the mesoporous structure in sample SBA-15-4-0-HCl, after addition of TEOS at, A) 0 min, B) 10 min, C) 30 min, D) 60 min, E) 90 min, and F) 120 min;

Figure 30 shows SEM images for the formation of the mesoporous structure in sample SBA-15-4-0-HNO_3, after addition of TEOS at, A) 0 min, B) 10 min, C) 30 min, D) 60 min, E) 90 min, and F) 120 min;

Figure 31 shows low angle XRD spectra of the SBA-15-4-24-HCl sample calcined at 650 ºC, 750 ºC, 850 ºC and 1000 ºC;

Figure 32 shows SEM images of A) 9%IMPNiA-Bd, B) 9%IMPNiA-Bc, C) 12%IMPNiN-B, and D) 8% IMPNiC-B catalyst samples;

Figure 33 shows TEM micrographs of A) 9% IMPNiA-Bd, B) 9%IMPNiA-Bc, C) 12%IMPNiN-B and D) 8%IMPNiC-B catalyst samples;

Figure 34 shows low angle XRD spectra of A) 9%IMPNiA-Bd, B) 9% IMPNiA-Bc, C) 12% IMPNiN-B, D) 8% IMPNiC-B catalyst samples;

Figure 35 shows wide angle XRD spectra of A) 9%IMPNiA-Bd, B) 9% IMPNiA-Bc, C) 12% IMPNiN-B, D) 8% IMPNiC-B catalyst samples;

Figure 36 shows a TEM micrograph of 8% IMPNiA-5 catalyst sample calcined at 550°C, after each of the five impregnation cycles;

Figure 37 shows A) a low angle XRD spectrum of 8% IMPNiA-5 and B) a wide angle XRD spectrum of 8% IMPNiA-5 catalyst samples;

Figure 38 shows A) nitrogen adsorption (ads) – desorption (des) isotherms of 8% IMPNiA-5 wherein V (STP) represents the volume of adsorbed (desorbed) N_2 at standard temperature and pressure and P/P^0 is relative pressure and B) pore size distribution of the 8% IMPNiA-5 catalyst sample calculated from the nitrogen sorption isotherm during adsorption and desorption, respectively. The incremental change in the pore volume divided by the incremental change in the pore radius (dVp/dRp) is plotted against the pore radius (Rp).

DETAILED DESCRIPTION

[0075] In order to produce an improved support which ultimately enhances the properties of a metal catalyst for DRM, the inventors have made a series of improvements to the general protocol for the synthesis of SBA-15 mesoporous silica materials as previously disclosed by Zhao (Zhao et al.,1998a and b).

[0076] The method used to form SBA-15 mesoporous silica materials described in the prior art procedure of Zhao is as follows:

> "In a typical preparation, 4.0 g of Pluronic P123 was dissolved in 30 g of water and 120 g of 2 M HCl solution with stirring at 35 °C. Then 8.50 g of TEOS was added

into that solution with stirring at 35 °C for 20 h. The mixture was aged at 80 °C overnight without stirring. The solid product was recovered, washed, and air-dried at RT. Calcination was carried out by slowly increasing temperature from room temperature to 500 °C in 8 h and heating at 500 °C for 6 h."

[0077] Any reference made to the "method of the prior art", "the method Zhao" or the "procedure of Zhao" is therefore to be interpreted as referring to that outlined above unless stated otherwise. Furthermore, any reference to a mesoporous material of the prior art is to be interpreted as a material made following said method.

[0078] A summary of the principal steps in a typical sol-gel preparation method as used in known methods of the prior art shown in Figure 1.

[0079] To synthesize a mesoporous material, such as SBA-15, a hydrogel is first formed via hydrolysis and condensation of a silica source in the presence of a surfactant to form a reticulate, metastable polymer with an open structure. Surfactants are generally classified as cationic, anionic, and non-ionic species. Previously, few non-ionic surfactants were used in hydrogel synthesis. These non-ionic surfactants are available in a wide variety of different structures and are frequently used in industry because of attractive characteristics such as low price, non-toxicity and biodegradability. In addition, non-ionic surfactants exhibit rich phase behaviour and their self-assembly produces mesophases with different geometries and arrangements. Due to such properties, non-ionic surfactants are especially appropriate for the syntheses of mesoporous solids. The first mesoporous silicas were synthesized with non-ionic triblock co-polymers in 1998 (Zhao et al.,1998a and b). These particular materials are named SBA-*X*, wherein *X* is a number corresponding to a specific pore structure and a surfactant capable of producing such a pore structure (e.g. SBA-15 has hexagonally ordered cylindrical pores and can be synthesized with Pluronic P123). The ethylene oxide/ propylene oxide (EO/PO) ratio of the co-polymer has a large effect on the formation of the silica mesophase. For example, it is known that using triblock co-polymers with smaller ratios (<0.07) such as $EO_5PO_{70}EO_5$, favours the formation of lamellar mesostructured silica, while larger EO/PO ratio (>1.5) tends to favour the formation of cubic mesoporous silica structures. An EO/PO ratio around (0.28) favours an hexagonal arrangement for the silica mesostructure.

[0080] The mesoporous silica support of the invention may be made using a surfactant capable of forming hexagonally ordered cylindrical pores. Preferably, the surfactant for the invention is an amphillic triblock co-polymer such as Pluronic® P123 ($EO_{20}PO_{70}EO_{20}$, M = 5800). Throughout this specification, the terms Pluronic P123 and P123 are used interchangeably and will be understood as referring to the same thing (Pluronic is a registered trademark of BASF). The surfactant should be present in a concentration

sufficient to allow micelles to form, namely, above a critical micelle concentration. The size of the micelles influences the ordered structure of mesoporous silica and ultimately affects the performance of the catalyst. The concentration of surfactant in solution can be altered to maximize the size of the micelles formed. In the process of the invention, between 1 and 4% by weight surfactant is used and preferably between 2.5 and 3.5% by weight surfactant is used. Most preferably about 3% by weight surfactant is used and optimally, 3.2% by weight surfactant is used. In one preferred embodiment, the surfactant solution comprises the surfactant dissolved in water. The percentage expressed by weight thus relates to the percentage by weight of surfactant dissolved in water. For example, 4.0 g surfactant dissolved in 120 g water equates to 3.2% by weight surfactant in water. In alternative embodiments, the surfactant solution comprises a mixture containing water and acid. In such embodiments, the percentage expressed by weight surfactant thus relates to the percentage by weight of surfactant dissolved in the water and acid mixture. For example, 4.0 g surfactant dissolved in 30 g water and 120 g acid equates to 2.6% by weight surfactant in the mixture.

[0081] The inventors have discovered that substantially dissolving the surfactant in water is an important step in some preferred embodiments of the optimized method. In one preferred embodiment of the invention, water is first added to the surfactant to form a surfactant solution before adding the acid. The surfactant solution is stirred at 40 °C until the solution is clear indicating the surfactant is fully dissolved. Thus in a preferred embodiment the acid is only added after a set period when a clear solution has been formed. Typically this period is 6 hours. This is in contrast to the method of the prior art where the surfactant and acid are added in combination. First mixing in an appropriate amount of water ensures that the surfactant is completely dissolved and enables the formation of spherical micelles. The spherical micelles then undergo a transition from a spherical to a cylindrical shape. Following this transition, the elongated cylindrical micelles arrange themselves in a hexagonal pattern. Substantially dissolving the surfactant in water before the addition of acid promotes the formation of a highly ordered hexagonal structure. If the acid and water are added in combination with the surfactant, such as in the method of the prior art, some of the spherical micelles form aggregates leading to a less ordered hexagonal structure.

[0082] Once the surfactant is fully dissolved, indicated by the presence of a clear solution, acid is added to reduce the pH of the solution. Acid acts as a catalyst for the hydrolysis and polycondensation reactions which occur on the addition of a silica precursor. Suitable acids are those which promote the maintenance of the hexagonally ordered structure formed following the dissolution of the surfactant and are selected from

hydrochloric acid (HCl), hydroiodic acid (HI), hydrobromic acid (HBr), nitric acid (HNO_3), sulphuric acid (H_2SO_4) and phosphoric acid (H_3PO_4). Particularly preferred is HCl. The rate and extent of the hydrolysis reaction is influenced by the concentration and strength of the acid. Before adding the acid, the pH of the solution is around 8.5. As the precipitation of silica only occurs below its isoelectric point of pH 2, sufficient acid is added to reduce the pH below this value. Preferably the pH of the acidified mixture after the addition of acid is below pH 1.

[0083] After the addition of the acid, the acidified mixture is left for about 10 to 20 minutes. Following this, a silica precursor is then added to the mixture. Suitable silica precursors include any silica precursor suitable for the formation of sol-gel processes known in the art, for example, tetramethoxysilane (TMOS), tetraethoxysilane (TEOS), tetrapropoxysilane or other silica alkoxides with longer alkyl chains. Alternatively, sodium silicate may be used either alone or in combination with alkoxides. Preferably the silica precursor is TEOS.

[0084] The silica precursor is advantageously added in a dropwise fashion. The silica precursor is thus added at such a rate so as not to disturb the hexagonal arrangement of micelles.

[0085] In embodiments of the invention wherein the acid catalyst is HCl, the formation of the mesoporous material occurs via a true-liquid crystal template mechanism (TLCT). The true liquid-crystal template mechanism is defined as when the surfactant in solution forms a lyotropic liquid crystal phase (LC). When formation of the mesoporous material occurs via such a mechanism, inorganic precursors (i.e. silica precursors) are deposited on the micelle rods of a preformed liquid crystalline phase. Subsequent polymerization of the inorganic precursors leads to the formation of an organic-inorganic mesostructure. Adding silica dropwise when the mesostructure is formed by a TLCT mechanism ensures the ordered arrangement of the micelles is not disturbed.

[0086] When the silica precursor is added to the acidified mixture, silica infiltrates the hydrophobic portion of the micelles resulting in hydrolysis. The amount of the silica precursor added influences the rate of the hydrolysis reaction. In some embodiments of the invention, preferably from 6 to 7% by weight silica precursor is added and optimally about 6.4% by weight silica precursor is added. In contrast, the method of the prior art teaches 5.5% by weight solution of silica precursor. It is thus clear that, in comparison with the prior art a greater proportion of silica precursor is added in accordance with the present invention. Increasing the amount of silica precursor by weight solution increases the rate of the hydrolysis reaction by providing more silanol moieties and increases the probability that the condensation reaction between silanol moieties will occur. Ultimately

the advantageous effect of such a rate increase is a mesoporous material with thicker walls and therefore greater thermal stability. The final step in the gel formation process is completion of the hydrolysis and condensation reactions which is ensured by stirring the mixture continuously under heating at 40 °C for approximately 20 hours.

[0087] The inventors have further noted that both the amount of surfactant and the silica precursor can be advantageously adjusted together to provide an SBA-15 material with improved properties. By tuning the molar ratio of silica precursor to surfactant appropriately, an SBA-15 material can be obtained with low or negligible microporosity and a high thermal stability. Furthermore, the inventors have noted that such an effect can be achieved without significantly reducing the available surface area of the mesoporous material. This effect has been attained by using a molar ratio of silica precursor/surfactant (*r*) higher than those used in the methods of the prior art. High quality large pore mesoporous materials for the invention can be attained by selecting a molar ratio of silica precursor/surfactant in the range of 60 to 75. Preferably, the molar ratio of silica precursor/surfactant is in the range of 65 to 70 and optimally the molar ratio of silica precursor/surfactant molar ratio is 67. In preferred embodiments, the silica precursor comprises SiO_2 and the surfactant is P-123.

[0088] Hydrogel formation results in the creation of a precipitate which is subsequently subjected to aging. The precipitate is transferred to an oil bath and heated without stirring. In the aging process, the particle size is continually increased and the structure and properties of the network of micelles formed during the gel formation step continue to change up to the point that yields the target gel density. The aging step respectively comprises four processes: polycondensation; syneresis; coarsening; and phase transformation. Further polycondensation reactions occur due to a large concentration of hydroxyl groups, creating more cross linked structures. During syneresis shrinkage of the gel occurs due to expulsion of liquid from the pores as a result of the creation of new chemical bonds by polycondensation reactions and through reduction of the huge solid-liquid interface. This can be controlled by reducing the temperature and by selecting the correct solvents, which form hydrogen bonds with the hydroxyls. Coarsening or Ostwald ripening is caused by formation of a solid network with non-uniform surface curvature. The dissolution and reprecipitation of dissolved material into regions of negative curvature causes a growth of necks between particles, filing the small pores. This reduces the microporosity and surface area due to redistribution of the pore volume between the different pore size ranges. To influence the coarsening and other aging processes, the temperature and solution pH that control the material's solubility can be modified.

[0089] The aging step of the invention is performed at a temperature above 80 °C.

[0090] Preferably, aging is performed at a temperature of 95 °C. A variety of aging temperatures are taught in the method of the prior art including 80, 90 and 100 °C. A higher aging temperature (i.e. greater than 80 °C) reduces the microporosity of the mesoporous material. High microporosity is undesirable and adversely affects catalyst performance following impregnation of the catalyst support with a suitable catalytic species. By following the process of the invention, mesoporous materials suitable for a catalyst support can be produced with negligible microporosity. However, increasing the aging temperature to above 80 °C may reduce the thickness of the walls in the mesoporous silica. Consequently, in the case that the aging temperature is to be increased to above 80 °C, 6 to 7% by weight silica precursor can be added to ensure the wall thickness is not reduced. Thus the thermal stability of the catalyst support is not adversely impacted by the higher aging temperature. Furthermore, the aging step of the invention facilitates the preparation of uniform nano-sized porous silica with a uniform pore size.

[0091] Following the aging step, the precipitate from the solute is filtered and washed with water to remove the residual surfactant. The precipitate is then dried using evaporative drying in which a xerogel is formed or alternatively, supercritical drying in which an aerogel is formed. Preferably, the process of the invention uses evaporative drying as this is cheaper and easier to control compared to supercritical drying. The drying step can influence the porosity of the material, its uniformity and the constancy of the unit cell parameter. Optimally, the drying step of the process of the invention is performed at about 60 °C for approximately 24 hours. The drying step is conducted under these conditions to ensure gradual evaporation of the water.

[0092] After drying, the precipitate is placed in a furnace to be calcined. Calcination involves a high temperature treatment in air. The purpose of calcination is to decompose and volatilize the various precursors formed in the preparation stages, such as hydroxides, nitrates, and chlorides along with any other moieties that would be undesirable in the final catalyst support. Another important role of the calcination step is to remove all residual surfactant. Calcinations are typically conducted in methods known in the art at temperatures of above 350 °C but with a temperature low enough to prevent the structural collapse caused by local overheating. Heat treatment of the dried gel at increasing temperature causes chemical modification of its surface, crystallographic transformations of the solid matter and reorganization of the pore geometry. The calcination temperature should be lower than the stable temperature for mesoporous materials and higher than 350 °C to totally remove PEO-PPO-PEO type surfactants or at least 550 °C to remove long-chain alkyl surfactants. In order to completely remove the P123 surfactant, the

temperature should be at least 500 °C and optimally is 550 °C. In some preferred embodiments, the optimized process for the calcination step of the invention involves heating the dried product to 550 ºC at a heating rate of 1 °C per minute and then maintaining the temperature at 550 °C for 6 hours under steady state conditions (i.e. without changing any conditions for the 6 hour period). Steady state conditions mean the conditions of the reaction are kept constant over the stated period. Thus the optimized step in the calcination process when under steady state conditions involves maintaining the temperature at 550 ºC for 6 hours, without changing any conditions. In one embodiment of the invention, the final catalyst support product was yielded following calcination by cooling the sample to a temperature below 100 ºC, preferably 60 ºC, at a cooling rate of 10 ºC per minute.

[0093] In another preferred embodiment of the invention, once the calcination step has been completed and the sample cooled to 60 ºC at a cooling rate of 10 ºC per minute, the sample is re-hydrated in water to form a suspension. The hydrated suspension is then heated in an oil bath at 105 ºC and left to boil under gentle stirring. After 2 hours, the suspension is filtered and the final product dried at 120 ºC for 6 hours. The re-hydration step further improves the properties of the SBA-15 material. One particular advantage is that the re-hydrated SBA-15 material is less susceptible to cracking when subsequently impregnated with a metal precursor or other catalytic species.

[0094] In less preferred embodiments of the invention, the catalyst support may first be prepared by the method of the prior art and then re-hydrated after the calcination step by performing the re-hydration as described above.

[0095] A supported metal catalyst can be formed by incorporating a metal species into the catalyst support as prepared by embodiments of the invention. Once the mesoporous catalyst support has been prepared, an appropriate metal is incorporated into the catalyst support by an impregnation step. In the process of the invention, a wet impregnation method is used wherein a solution containing a metal precursor of the active phase, as an inorganic or organic salt, is added to the support. The active phase is the phase carrying the active sites of the catalyst. The metal precursor may be a metal salt. Inclusion of a metal species as the active phase confers activity to the catalyst, yet it is the combined chemical properties of the active phase and the catalyst support that determines its functionality. Wet impregnation can be defined as impregnating the solid mesoporous material such that the solid material is saturated with an excess of solution containing the catalytic species. Thus the amount of solution added containing the active phase exceeds the pore volume of the catalyst support. This ensures the metal precursor is impregnated first on the external surface of the mesoporous catalyst support and then in the pore

interior. Thus a wet impregnation method ensures the metal precursor is not localized only to the pore interior. In some embodiments, to improve the mass transfer between the solution and the solid support, the reaction may be carried out under reflux conditions and a reflux condenser may be used. Reflux can be described as a process whereby reactants are boiled using a refluxing apparatus to produce vapour and are partially condensed such that the vapour returns to the refluxing apparatus as a liquid. Thus in some preferred embodiments, the metal precursor has improved solubility in boiling solvent and as such, higher dispersion can be obtained. Suitable solutions or solvents containing the metal precursor include water or organic solvents such as ethanol, iso-propanol and acetonitrile. Preferably water is used due to its low cost, availability and as water causes minimal agglomeration of the metal phase of the metal precursor.

[0096] Careful selection of the metal precursor is important as this has a large impact on the ultimate dispersion of the active phase on and in the support. Preferably the metal precursor of the invention is a transition metal. Most preferably the transition metal may be nickel. In such embodiments, either an organic nickel salt or an inorganic nickel salt can be selected. Examples of suitable organic nickel salts include nickel acetate, nickel citrate and nickel acetylacetonate. Examples of suitable inorganic nickel salts include nickel nitrate, nickel chloride, nickel fluoride, nickel carbonate and nickel sulphate. Preferably nickel acetate is used as the metal precursor as this provides the best dispersion of metallic species throughout the catalyst support. The metal precursor may be added in solution to the catalyst support at a specified temperature. The impregnation temperature will be dependent on the nature of the metal precursor.

[0097] To effectively incorporate the metal species into the mesoporous material, the catalyst support is dried to remove the solution or solvent allowing the precursor of the active phase to adhere to its surface. The final step of the impregnation process is calcination in air which facilitates conversion of the soluble salt of the metal into the insoluble oxide. Calcination is conducted at 550 ºC as at low temperatures (e.g. 200 ºC) the metal salt does not undergo complete decomposition to form the metal oxide, whereas at too high calcination temperature (e.g. 800 ºC) the sintering and/or fusing of active sites through annealing effects can occur.

[0098] The invention will now be exemplified by way of illustration by the following examples.

Experimental details describing optimized SBA-15 catalyst support preparation procedure

[0099] A general experimental procedure for the preparation of mesoporous silica was

previously described in detail by the method of Zhao as outlined above. Various modifications were made to this procedure and the optimized methods are thus described below.

Protocol 1

[00100] An electronic weighing balance was used to measure 4 g of P123 (Sigma-Aldrich; product number 435465) and 120 g of deionized (DI) water. The measured P123 was placed into a polyethylene bottle and the DI water was added. Then the bottle was placed into a water bath which was heated on a hot plate at 40 °C and kept for 6 hours until a clear solution was observed as a result of the complete mixing of P123 into water. To intensify the mixing, a magnetic stirrer at 540 rpm was used. Then 20 ml of HCl was measured using a 50 ml measuring cylinder and added to the dissolved P123 in water to reduce the pH of the solution. The pH of the solution was measured with a pH meter before and after the addition of HCl. Before the addition of HCl, pH 8.5 was recorded and after the addition of HCl, the pH was lower than 1 (between 0.4 to 0.6). Approximately 10 minutes later, 9.25 g of TEOS was slowly added, at a rate of 25-30 drop/min, to the solution under vigorous stirring. The solution was then kept under stirring at approximately 540 rpm for 20 hours on the hot plate at 40ºC to complete hydrolysis and condensation reactions. A white precipitate was formed in the polyethylene bottle. The polyethylene bottle and precipitate were transferred to an oil bath and kept at 95 °C for 24 hours to age without stirring. The white solute precipitate was then filtered, washed sufficiently with approximately 600 ml of DI water to remove the template (P123) and afterwards the white precipitate was dried at 60 °C in an oven for 24 hours using a glass watch vessel.

[00101] Following drying, the white precipitate was removed from the oven and transferred into a crucible and placed in a furnace to be calcined by heating to 550 °C at a heating rate of 1 °C per minute then maintaining the temperature at 550 °C for 6 hours under steady state conditions. After calcination, the sample was cooled to 60 ºC at a cooling rate of 10 ºC / min. Once cooled, the sample was transferred to a round bottom flask comprising a short condenser and re-hydrated using 50 g of DI water to form a suspension. The suspension was then placed in an oil bath at 105 °C and boiled under gentle stirring. After 2 hours, the suspension was filtered and pure 2g of SBA-15 sample was collected by filtration and dried at 120 ºC for 6 hours.

Protocol 2

[00102] An electronic weighing balance was used to measure 4g of P123 (Sigma-Aldrich; product number 435465) and 120 g of DI water. The measured P123 was placed into a polyethylene bottle and the DI water was added. Then the bottle was placed into a water

bath which was heated on a hot plate at 40 °C and kept for 6 hours until a clear solution was observed as a result of the complete mixing of P123 into water. To intensify the mixing, a magnetic stirrer at 540 rpm was used. Then 20 ml of HCl was measured using a 50 ml measuring cylinder and added to the dissolved P123 in water to reduce the pH of the solution. The pH of the solution was measured with a pH meter before and after the addition of HCl. Before the addition of HCl, pH 8.5 was recorded and after the addition of HCl, the pH was lower than 1 (between 0.4 to 0.6). Approximately 10 minutes later, 9.25 g of TEOS was slowly added, at a rate of 25-30 drop/min to the solution under vigorous stirring. The solution was then kept under stirring at approximately 540 rpm reactions for 20 hours on the hot plate at 40 ºC to complete hydrolysis and condensation reactions. A white precipitate was formed in the polyethylene bottle. The polyethylene bottle and precipitate were transferred to an oil bath and kept at 95 °C for 24 hours to age without stirring. The white solute precipitate was then filtered, washed sufficiently with approximately 600 ml of DI water to remove the template (P123) and afterwards the white precipitate was dried at 60 °C in an oven for 24 hours using a glass watch vessel.

[00103] Following drying, the white precipitate was removed from the oven and transferred into a crucible and placed in a furnace to be calcined by heating to 550 °C at a heating rate of 1 °C per minute then maintaining the temperature at 550 °C for 6 hours under steady state conditions. After calcination, the sample was cooled to 60 ºC at a cooling rate of 10 ºC / min.

Protocol 3

[00104] A mesoporous silica was prepared in accordance with the prior art method as described in Zhao and outlined above with the exception that the sample was further rehydrated.

[00105] 4.0 g of Pluronic P123 (Sigma-Aldrich; product number 435465) was dissolved in 30 g of water and 120 g of 2 M HCl solution with stirring at 35 °C. Then 8.50 g of TEOS was added into that solution with stirring at 35 °C for 20 h. The mixture was aged at 80 °C overnight without stirring. The solid product was recovered, washed, and air-dried at RT. Calcination was carried out by slowly increasing temperature from room temperature to 500 °C in 8 h and heating at 500 °C for 6 h.

[00106] After calcination, the sample was cooled to 60 ºC at a cooling rate of 10 ºC / min. Once cooled, the sample was transferred to a round bottom flask comprising a short condenser and re-hydrated using 50 g of deionized water to form a suspension. The suspension was then placed in an oil bath at 105 °C and boiled under gentle stirring. After 2 hours, the suspension was filtered and pure 2g of SBA-15 sample was collected by filtration and dried at 120 ºC for 6 hours.

Method for impregnation of nickel into the SBA-15 catalyst support

[00107] A wet impregnation method was followed by adding a solution containing a nickel precursor in the form of nickel acetate, nitrate or citrate. The precursor was dissolved in water. When the precursor solution contained nickel acetate, the reaction was performed under reflux conditions and a reflux condenser was used in order to improve the mass transfer between the solution and the solid. Impregnation was carried out at different temperatures, for different impregnation times and different impregnation treatments. Samples were dried and calcined in air. The following samples were prepared and labeled as shown in Table 1.

Table 1 – Prepared metal catalyst samples

Precursor	SBA-15: Ni-salt: DI water	Impregnation time (hr)	Impregnation treatment Calcined at 550° C, 2hr, 5^0C/min		Label *
			Impregnation temp (°C)	Drying conditions	
Ni-acetate (diluted)	3:1:30	20	90-95	vacuum oven, 100°C, 1hr	4%IMPNiA-Ad
	3:2:30				9%IMPNiA-Bd
	3:3:30				11%IMPNiA-Cd
Ni-acetate (concentrated)	3:1:10	10	90-95	dried at 120 °C, 10hr	4%IMPNiA-Ac
	3:2:10				9%IMPNiA-Bc
	3:3:10				12%IMPNiA-Cc
Ni-nitrate	3:1:10	10	50-55	dried at 120ºC, 10 hr	6% IMPNiN-A
	3:2:10				12%IMPNiN-B
	3:3:10				29%IMPNiN-C
Ni-citrate	3:2:10	1-2	Room Temperature	vacuum oven, 100 °C, 1hr	8%IMPNiC-B
	3:3:10				15% IMPNiC-C
Ni-acetate (multiple impregnation)	3:1:10	1-2	Room Temperature	vacuum oven, 100°C, 1hr	8%IMPNiA-5

*The percentage in front of the label means wt % of nickel loaded as nickel oxide, determined from energy dispersive X-ray (EDX) measurements.

[00108] The impregnation temperature was higher for nickel acetate than for nickel nitrate because of its lower solubility in water. For example, at 20°C, the solubility of nickel nitrate is 94g/100 ml in water while for nickel acetate the solubility is only 17g/100 ml. As for

nickel citrate, the impregnation was possible at room temperature because an already prepared solution of nickel citrate was used. The nickel citrate solution was prepared by the reaction between nickel carbonate hexahydrate and citric acid (equal molar ratio) in DI water at 100°C, as the nickel citrate has a very low solubility in water, 0.05 mol/100 ml water at 18 °C. Calcinations were conducted at 550 ºC as at low temperatures (e.g. 200 ºC) the nickel salt does not undergo complete decomposition to form nickel oxide, whereas at too high calcination temperature (e.g. 800 ºC) the sintering and/or fusing of nickel active sites through annealing effects can occur.

Characterization techniques for the SBA-15 support and metal catalyst samples

[00109] Scanning electron microscopy (SEM) was used to monitor the morphology of the support and of the prepared catalyst samples as well. SEM examination was performed using a Hitachi S-3400N electronic microscope. A beam of highly energetic electrons (0.1-50 keV) is focused on the sample surface. The microscope is equipped with a secondary electron detector, a backscattered electron (BSE) detector, and X-rays energy dispersive spectroscopy (EDS or EDX). A secondary electron detector records topography of the surface under observation with high resolution imaging on the order of 1-2 nm and magnification range from 10x to 500,000x.

[00110] Transmission electron microscope (TEM) characterization was performed on JEOL, JEM-1010 at an accelerating voltage of 100 kV. The samples were prepared in the following way; 0.02 g of each sample was dispersed in 3 ml of ethanol solution, and the suspension was sonicated for 30 min. A drop of the suspension was transferred to a copper mesh grid covered with carbon film. The grid was dried in vacuum at room temperature for 24 hours.

[00111] X-ray diffraction (XRD) patterns were recorded on a Bruker D8 (25 kV, 20 mA) powder X-ray diffractometer, using Cu Kα (λ=0.15406 nm) radiation, the tube voltage 40 kV, and the current was 20 mA. The data were collected from 0.5–4° (2θ) with a resolution step size of 0.01° or angular increment of 0.01° (low angle XRD patterns) and from 10–100° (2θ) with a resolution step size of 0.02° (conventional wide angle XRD patterns). Low angle XRD gives information on the mesoporous structure while wide angle XRD gives information on the crystalline structure.

[00112] The pore structure and the specific surface area were determined by the B.J.H and B.E.T method using volumetric adsorption equipment (BEL JAPAN, INC. BELSORP-mini). All samples were pre-treated under He stream at 200ºC for 2 hr before the measurement.

Catalyst activity test

[00113] The CO_2 reforming of methane reaction was conducted under atmospheric pressure and constant temperature, namely 550, 600, 650 and 700°C respectively, in the CATLAB system. About 25 mg of each sample was firstly reduced under a 5 vol. % H_2 in Ar flow at 20ml/min and then exposed to the reaction mixture 100 ml/min flow, with CH_4/CO_2 = 1.5:1, for 3 hr. The analysis of the effluent was carried out using the quadrupole mass spectrometer, QIC20. The following amu were measured: 2 (H_2), 40 (Ar), 18 (H_2O), 15 (CH_4), 28 (CO), 32 (O_2), and 44 (CO_2). The integrated software allowed the conversion of intensity of the amu into partial pressure and as such, in this work, the conversions, X, of limiting reactant, CO_2, was calculated according to the following equations:

$$X_{CO2} = \frac{P^0_{CO2} - P_{CO2}}{P_{CO2}} \times 100$$

where, P^0_{CO2} is the initial pressure of CO_2 and X_{CO2} is the CO_2 fractional conversion, while P_{CO2} is the pressure of CO_2 leaving the reactor.

Characterization of the SBA-15 support and comparison to prior art

[00114] To assess the impact of the inventor's optimized protocol for the preparation of the supported metal catalyst, various comparisons were made with those produced method of Zhao. Firstly, two SBA-15 support samples were prepared. One SBA-15 sample was prepared using the optimized preparation method in accordance with Protocol 1 as described above (hereinafter referred to as "modified sample" equating to the invention). The other SBA-15 sample was prepared following Zhao's published procedure (hereinafter referred to as "unmodified sample" equating to the prior art).

Each of the samples, modified and unmodified, were characterized using low angle XRD and SEM.

[00115] The low angle XRD spectra are shown in Figure 2. For both samples, XRD data revealed peaks indexable as (100) (110), (200) reflections associated with a *p6mm* hexagonal symmetry a indicative of hexagonally arranged mesopores. However, XRD data analysis showed differences in the interplanar distance, *d*, which was higher for the modified sample, 9.2 nm, compared to 8.1 nm for the unmodified sample. Accordingly, the unit cell parameter, *a*, was also higher for the modified sample at a value of 10.6 nm compared to 9.35 nm. The larger inter-planar distance coupled with the higher unit cell parameter, is indicative of the fact that the method of the present invention produces micelles of increased size compared to those produced following the prior art procedure of

Zhao. In addition, the wall thickness of the pores (E) is equal to the difference between the unit cell, *a*, and the pore diameter, D_P, ($E = a - D_P$). According to this mathematical relationship, the wall thickness is directly proportional to the unit cell and inversely proportional to the pore diameter of mesoporous materials. The measured diameter of the pores of the unmodified sample was 7.2 nm compared to 7.60 nm for the modified sample. Consequently, the respective wall thickness was found to be 2.15 nm for the unmodified sample and 3.0 nm for the modified sample. As the wall thickness of the pores is a property linked to the thermal stability of the support, the modified sample of the invention with thicker walls will have greater thermal stability.

[00116] Referring now to Figure 3, the SBA-15 support as prepared by Protocol 1 exhibited morphological differences compared to the sample as prepared by the method of Zhao. SEM measurements show that the modified sample has a more uniform morphology, which is of a fibre-like type, with longer fibers than the unmodified sample. The fibres for the modified sample consist of cylindrical rods, which, from the SEM images, seem to be longer and wider than for the unmodified sample. The final morphology of the given product is essentially is thought to be governed by the interaction between the charged inorganic silica species and the surfactant. Depending on the synthesis conditions used, a number of morphologies can be attained. The uniform morphology observed for the modified sample is indicative of a more ordered structure. Without wishing to be bound by any particular theory, the inventors believe that the more ordered structure in the modified sample is a consequence of dissolving the P-123 surfactant in aqueous solution before adding the acid. In addition, the inventors believe that the dropwise addition of the TEOS silica precursor also contributes to the further ordering of the SBA-15 mesostructure compared to the unmodified SBA-15 silica as prepared by the procedure of Zhao. In particular, dropwise addition of the silica template ensures that the ordered structure formed via the TLCT mechanism when HCl is used as an acid, is not disturbed.

Characterization of the SBA-15 support impregnated with nickel in comparison to prior art

[00117] SBA-15 support samples prepared by Protocol 1 of the invention as described above and those prepared in accordance with the published procedure of Zhao were impregnated with nickel using nickel acetate solutions. The impregnation procedure was followed using the conditions as described for sample 9%IMPNiA-Bd in Table 1 above. Nickel loading as determined through SEM-EDS was 9 wt%. After calcinations, the catalyst samples were characterized by low angle XRD (Figure 4) to assess the effect of nickel impregnation on the SBA-15 support. Then the CO_2 reforming of methane reaction

was conducted in accordance with the conditions specified for the catalyst activity test as stated above. Wide angle XRD (Figure 5) spectra were obtained and SEM images (Figure 6) taken for fresh SBA-15 nickel impregnated catalysts before the CO_2 reforming of methane reaction and spent SBA-15 nickel impregnated catalysts after the reaction was completed. Samples with a catalyst support made by the invention are labeled as 9Ni/modified SBA-15 and those with a catalyst support made by the method of the prior art are labeled 9Ni/unmodified SBA-15.

[00118] Referring now to Figure 4, the low angle XRD spectrum for both the modified and unmodified samples shows that the mesoporous structure was not destroyed by impregnation as the three reflection peaks associated with the hexagonal structure were still present. These results demonstrate that the catalyst support prepared by the present invention is highly stable. Only minor changes in the interplanar distance, *d*, and unit cell parameter, *a*, were induced by impregnation thus indicating that the highly ordered mesoporous structure is maintained. The results also suggest that some of the nickel was loaded to the walls of the pores and incorporated into the silica framework, whereas most of the nickel was dispersed over the external surface.

[00119] With reference to Figure 5, the wide angle XRD spectra show that the diffraction patterns of the catalysts changed with nickel loading for the modified and unmodified SBA-15 silica samples. Diffraction peaks for the 9Ni/modifiedSBA-15 sample were almost entirely absent, whereas the 9Ni/unmodfiedSBA-15 sample showed strong diffraction peaks characteristic of nickel oxide. Only broad peaks were observed for the 9Ni/modified SBA-15 sample and this was indicative of very small nickel oxide particles. Conversely, the narrow peaks observed in the spectra for the 9Ni/unmodified SBA-15 were indicative of large crystallites of nickel oxide. The nickel oxide crystallite size was calculated from the Scherrer equation, [$L = K\lambda / \beta \cos(\Theta)$], where, λ is the wavelength of the X-ray source, Θ is the angle between the extrapolated incident ray and the scattered ray, L is diameter of the crystal grain (grain size), β is the full width at half maximum (FWHM), and K is the shape factor (with a typical value of 0.9)]. The calculated crystallite size was 10.5 nm for 9Ni/unmodifiedSBA-15 sample. In comparison, the crystallite size was too low to be detected by wide angle XRD for the modified sample and thus was lower than 5 nm. This data therefore demonstrates that nickel oxide is well dispersed for the modified sample of the invention following impregnation with a better distribution over the support surface compared with the unmodified sample produced following the procedure of Zhao. The Inventor believes that increased dispersion of the nickel oxide species in the modified sample means that there are a greater number of active sites available for performing the reforming reaction. In addition, the results in Figure 5 show no nickel crystallites for the

modified sample whereas crystallites were detected at 6.5 nm for the unmodified sample which were likely formed due to sintering. The results of Figure 5 therefore suggest the modified sample is more resistant to sintering.

[00120] As shown in Figure 6, minor changes in morphology were observed after impregnation for both the modified and unmodified samples, however these are not considered to be significant.

Carbon dioxide conversion over the SBA-15 support impregnated with nickel in comparison to prior art

[00121] A further experiment was conducted wherein SBA-15 samples were independently prepared following the method of the prior art and protocol 1, 2 and 3 of the invention respectively. The samples were then impregnated using a nickel acetate solution according to the conditions as described for sample 9%IMPNiA-Bd in Table 1. The carbon dioxide conversion was then measured and recorded in accordance with the catalyst activity test as specified above.

Table 2 – Carbon dioxide conversion

Supported metal catalyst	550 °C	600 °C	650 °C	700 °C
	X_{CO2} (%)	X_{CO2} (%)	X_{CO2} (%)	X_{CO2} (%)
Nickel impregnated SBA-15 support as prepared by the method of Zhao	70	81	92	100
Nickel impregnated SBA-15 support as prepared by Protocol 1 of the invention	80	89	100	100
Nickel impregnated SBA-15 support as prepared by Protocol 2 of the invention	75	90	100	100
Nickel impregnated SBA-15 support as prepared by Protocol 3 of the invention	75	85	95	100

*X_{CO2}, is the fractional conversion of CO_2.

[00122] Referring now to Table 2, the carbon dioxide conversion is depicted for nickel impregnated samples of SBA-15 prepared by the process of Protocols 1, 2 and 3 for the invention and an SBA-15 sample prepared by the method of Zhao. The carbon dioxide fractional conversion was higher for the nickel impregnated SBA-15 samples when prepared by Protocols 1, 2 and 3 of the invention at temperatures 550 °C, 600 °C and 650 °C than nickel impregnated SBA-15 when prepared by the method of the prior art. At 550 °C, at least a 5% improvement was noted over the prior art for all the metal catalysts prepared by the invention. Conversion was noted to be at least 10% higher for the catalyst as prepared by Protocol 1 of the invention at a temperature of 550 °C and at least 8% higher at temperatures of 600 °C and 650 °C. Conversion was noted to be at least 5% higher at 550 °C and at least 8% higher at temperatures of 600 °C and 650 °C for the catalyst as prepared by Protocol 2 of the invention. In addition, conversion was noted to be at least 5% higher at 550 °C, at least 4% higher at 600 °C and at least 3% higher at 650 °C for the catalyst when SBA-15 was prepared by Protocol 3 of the invention. Furthermore, 100% conversion was obtained at 650 °C for the catalyst prepared by the optimized methods of Protocol 1 and Protocol 2 of the invention whereas an operating temperature of 700 °C for 100% conversion of carbon dioxide was required for the catalyst prepared using the method of Zhao.

Nitrogen adsorption-desorption results for the SBA-15 and nickel impregnated catalyst supports

[00123] Nitrogen physisorption provides the bulk averaged information of the porous materials. Referring to Figure 7, the SBA-15 support produced by Protocol 1 of the invention was observed to follow the type IV isotherm and H1 hysteresis loop, according to IUPAC classification. Hysteresis is observed only for large pores with a diameter of greater than 4 nm. Pores with this size show capillary condensation and evaporation at relative pressure values greater than 0.45. Thus the steep capillary condensation step at high relative pressure (P/P^0 around 0.7) in Figure 7 is indicative of a high-quality large pore SBA-15 material.

[00124] The method of Brunauer, Emmett and Teller (BET) can be used to determine the surface area and was calculated using the following procedure. If the adsorption isotherm, described by the BET equation, is plotted as a straight line, with $P/(V(P^0 - P))$ on the y-axis and P/P^0 on the x-axis (as shown in the Figure 8), the V_m (volume of monolayer adsorption) and C, a constant, can be determined.

$$BET\ equation: \frac{p}{V(P^0 - P)} = \frac{1}{V_m C} + \frac{C-1}{V_m C} * \frac{P}{P^0}$$

Knowing V_m and the cross sectional area of adsorbed N_2, the BET surface area can be calculated using the following equation:

$$BET\ surface\ area = \frac{V_m}{Molar\ volume} * N_{Avogadro} * cross\ sectional\ area\ of\ adsorbed\ N_2$$

For the SBA-15 support as prepared by Protocol 1 of the present invention, V_m was 1.92E-4 m^3, the cross sectional area of N_2 is 1.62E-19 m^2 thus providing a calculated BET surface area of 834 m^2/g.

[00125] The Barrett-Joyner- Halenda Method (BJH) is a method for calculating pore size distributions of mesopores from experimental isotherms. Using the BJH method, the volume and the size and pore size distribution of the mesopores was determined for the SBA-15 support and is depicted in Figure 9. The SBA-15 support as prepared by Protocol 1 of the invention has a unimodal narrow pore size distribution, centred around 3 nm (from desorption data) and 3.8 nm (from adsorption data).

[00126] BET and BJH results as calculated from the adsorption and desorption data are shown in Table 3 for the SBA-15 catalyst support as prepared by Protocol 1 of the invention both before and after impregnation with the nickel component. The labels for the nickel impregnated SBA-15 samples correspond to those listed in Table 1 above.

Table 3 – Properties of mesoporous SBA-15 support as prepared by Protocol 1 and nickel impregnated samples

	BET Method		BJH Method					
			Calculated from adsorption data					
samples	^{S}BET (m^2/g)	C value	^{V}pore (mm^3/g)	a (nm)	^{R}peak (nm)	D_P (nm)	E (nm)	^{A}pore (m^2/g)
SBA-15	834	261	1046	10.62	3.80	7.60	3.02	666
4%IMPNiA-Ad	446	150	1064	9.81	4.90	9.80	0.01	485
9%IMPNiA-Bd	436	160	943	9.826	4.47	8.94	0.89	491
4%IMPNiA-Ac	442	155	822	9.11	3.80	7.60	1.51	480
9%IMPNiA-Bc	512	142	1116	9.53	4.11	8.22	1.31	546
6%IMPNiN-A	482	176	955	9.36	3.80	7.60	1.76	497
12%IMPNiN-B	591	188	904	9.36	3.80	7.60	1.76	545
29%IMPNiN-C	462	144	946	10.41	4.47	8.94	1.47	470
8%IMPNiC-B	526	128	1106	9.02	4.11	8.22	0.80	527
15%IMPNiC-C	584	122	931	9.722	4.11	8.22	1.50	569
8%IMPNiA-5	472	125	846		3.29	6.58		475
	BET Method		BJH Method					
			Calculated from desorption data					
samples	^{S}BET (m^2/g)	C value	^{V}pore (mm^3/g)	^{R}peak (nm)	D_P (nm)	E (nm)	^{A}pore (m^2/g)	
SBA-15	834	261	960	3.08	6.16	4.46	591	
4%IMPNiA-Ad	446	150	1030	4.11	8.22	1.59	518	
9%IMPNiA-Bd	436	160	992	3.53	7.06	2.77	545	
4%IMPNiA-Ac	442	155	804	3.08	6.16	2.95	511	
9%IMPNiA-Bc	512	142	1068	3.29	6.58	2.95	587	
6%IMPNiN-A	482	176	844	3.08	6.16	3.20	510	
12%IMPNiN-B	591	188	878	3.29	6.58	2.20	551	
29%IMPNiN-C	462	144	836	3.29	6.58	3.83	465	
8%IMPNiC-B	526	128	969	3.29	6.58	2.44	511	
15%IMPNiC-C	584	122	838	3.29	6.58	3.14	513	
8%IMPNiA-5	472	125	686	2.73	5.46		460	

S_{BET} = Specific surface area calculated by BET method, V_{Pore} = total pore volume obtained by N_2 adsorption volume at p/p_0 in the range 0.05-0.3, C = constant in BET equation, a = the unit cell parameter was calculated from $a = 2d_{100}/\sqrt{3}$, R_{Peak} = the pore radius at the peak of distribution curve measured by BJH method, A_{Pore} = the surface area of the mesopores, D_P is the pore diameter, E is the wall thickness of the pores, $E = a - D_P$.

[00127] A major issue of the impregnated catalysts is the maintenance of the mesoporous structure during preparation and calcinations steps. As seen from Table 3, after impregnation, the BET specific area significantly decreased for all samples. However, the mesoporous structure is not destroyed after impregnation, as evidenced by N_2 adsorption isotherms in Figure 10 for samples A, B, C, and D. All samples show the same sorption type IV isotherms with H1 hysteresis (a proof of well-defined cylindrical-like pore channel). Although not shown, the behaviour was the same for all prepared samples. The lower nickel loading showed much sharper capillary condensation steps, evidence of a more uniform distribution of the pore diameters.

[00128] Although Table 3 shows a significant decrease in BET specific area for all samples following impregnation, generally only minor changes are noted in the total pore volume. The reduction in BET specific surface area is most likely due to the dispersion of nickel oxide over the external surface of the catalyst support (as suggested by the wide angle XRD results in Figure 4). However, as the total pore volume is minimally affected by impregnation of the metal component, advantageously the internal surface remains virtually the same before and after impregnation. This is in contrast to equivalent known catalysts, such as those exemplified in Zhang (Zhang et al.,2006, Chinese Journal of Catalysis, 27(9), pp.777-782), wherein the total pore volume of can be reduced by greater than 25 per cent as a consequence of impregnation. As shown in Table 3, the total pore volume for SBA-15 is 1046 mm^3/g (or 1.046 cm^3/g) yet none of the samples demonstrate a reduction in total pore volume of the scale noted in the prior art following impregnation. Furthermore, the BET specific area measured for SBA-15 in Zhang (Zhang et al.,2006, Chinese Journal of Catalysis, 27(9), pp.777-782) is considerably lower (630.9 m^2/g) compared to that measured for the invention which was 834 m^2/g. In addition, Zhang reports a BET specific area of 474.5 m^2/g for an SBA-15 sample impregnated with nickel nitrate. All of the nickel nitrate samples listed in Table 3 (i.e. 6% IMPNiN-A, 12%IMPNiN-B and 29%IMPNiN-C) show higher BET specific areas and greater total pore volumes than those in Zhang which further demonstrates the SBA-15 impregnated samples of the invention demonstrate improved properties compared to the prior art.

[00129] Impregnation has little impact on the pore size or the pore size distribution, as shown in Figure 11. However, impregnated catalysts have a slightly broad pore size distribution, which is centred on 4.47 nm, 4.11 nm, 3.8 nm, and 4.47 nm for samples A, B, C and D respectively.

Studies investigating the effect of surfactant concentration, acid source and the aging time on the SBA-15 catalyst support

[00130] Samples were prepared according to Protocol 1 as described above aside from the fact that the concentration of P123, the aging time and the acid source were independently varied. The prepared samples were labeled as SBA-15-X-Y-Z, wherein X represents the amount of P123 used, Y corresponds to the aging time and Z refers to the acid source.

Table 4 – Reactants and conditions to prepare mesoporous SBA-15 support

Samples	P123, g	DI water, g	Concentration P123 in water	Acid source	TEOS, g
SBA-15-1.2-24-HCl	1.2	120	1 wt%	20 ml HCl	9.25
SBA-15-2-24-HCl	2.0	120	1.6wt%	20 ml HCl	9.25
SBA-15-4-24-HCl	4.0	120	3.2wt%	20 ml HCl	9.25
SBA-15-4-48-HCl	4.0	120	3.2wt%	20 ml HCl	9.25
SBA-15-4-24-HNO_3	4.0	120	3.2wt%	20 ml HNO_3	9.25

Effect of surfactant concentration

[00131] The structural changes induced by using increased concentration of P123 in DI water, namely from 1 wt% to 3.2 wt%, were assessed through XRD measurements. Low angle XRD of the SBA-15-1.2-24-HCl, SBA-15-2-24-HCl, and SBA-15-4-24-HCl samples respectively, revealed hexagonally arranged mesopores as the peaks, indexable as (100) (110), (200) reflections associated with a *p6mm* hexagonal symmetry were present. Thus, SBA-15 with a well ordered hexagonal structure was obtained for all P123 concentrations. However, the intensity of the peaks increased with P123 concentration. As the intensity of a given reflection is proportional to the number of hkl planes in reflecting condition, the higher the P123 concentration the better long-range hexagonal channel packing (or the packing approaches a perfect 2D hexagonal symmetry). Moreover, by increasing the P123 concentration, the interplanar distance, d-spacing, increases from 7.8 nm to 9.2 nm, as calculated from the d_{100} reflection peak, using Bragg's law: [$n\lambda = 2d_{100}sin(\Theta)$] where, n is an integer (1 here), λ is the wavelength of the X-rays, d is the inter-planar spacing generating the diffraction and, Θ is the diffraction angle. The interplanar distance, along with the size of the micelles, increases as more micelles aggregate together. The size of the micelles increases when the concentration of P123 dissolved in water also increases.

As *d*-spacing increases, the unit cell parameter (distance between pore centers), *a*, increases accordingly, as [$a = 2d_{100}/\sqrt{3}$].

[00132] For P123 to form micelles in water, its concentration should be higher than the critical micellar concentration (CMC). When the surfactant concentration is low, separate molecules of P123 are present in the air/water interface. The critical micellar concentration of P123 is around $3*10^{-4}$ wt% at 43 °C, the micelles aggregation number is 287 at 40 °C (Wanka et al., 1994, Macromolecules, 27, pp.4145-4159). Once the CMC is reached separate molecules of P123 aggregate together to form micelles. As shown in Table 4 for all samples, the P123 concentration was much higher than the CMC.

[00133] The results in Figure 12 demonstrate the formation of imperfect to perfect 2D hexagonal mesoporous silicas as the P123 concentration was increased. By increasing the amount of the P123 and keeping constant the amount of the other components, the volume ratio between the copolymer and inorganic components of the silica precursor was increased. Knowing the volume fraction of the copolymer it is possible to predict directly the final mesostructural ordering and macroscopic morphology adopted by silica. A quantitative comparison can be made between the phase behavior of the SiO_2-block copolymer system and the observed non-equilibrium mesostructures based on the volume fraction of the block copolymer. For volume fraction between 63 to 75, lamellar mesophases have been observed. Hexagonal mesophases have been observed for 40 to 55 and cubic mesostructures formed for volume fraction 30 to 36. The volume fraction of P123 in SiO_2 was calculated for each of the SBA-15 samples following the procedure described by Alberius (Alberius et al., 2002, Chemical Materials., 14, pp.3284-3294). The calculated volume fraction was 49.25%. Thus for the highest P123 concentration, in which all three XRD peaks were well resolved, the long-range mesoscopic ordering of the pores is improved and a perfect hexagonal structure is formed.

[00134] The effect of the P123 concentration on the morphology of SBA-15 was assessed through SEM measurements. Figure 13 A, B, and C shows the SEM images of the prepared SBA-15-1.2-24-HCl, SBA-15-2-24-HCl and SBA-15-4-24-HCl samples. For all concentrations a fiber-like morphology was obtained. The fibrous structure is an agglomerate of fibers that are constituted from small rod-like sub-particles 0.5 – 1.0 μm in length and about 0.5 μm in diameter. As described below in Table 5, the diameter of the pores was 7.6 nm and the wall-thickness was 3 nm. Therefore one silica channel is about 10.6 nm. For the sample with the highest P123 concentration, each nano-rod thus spans 47-50 mesoporous silica channels, indicating homogenous particle size distribution. The same result was obtained by analyzing the TEM data (see Figure 14). For low P123 concentrations, the fibrous structure is non-uniform and quite short. By increasing the

P123 concentration, uniform and long fibrous structure with several tens of micrometers in length was obtained.

[00135] Additional measurements were performed to assess the influence of the P123 concentration on the pore size and BET surface area of SBA-15. As such, N_2 adsorption-desorption isotherms at 77 K were recorded and are shown in Figure 15. For all three samples, SBA-15-2-24-HCl, SBA-15-2-24-HCl and SBA-15-4-24-HCl, the isotherms are type IV with H1 hysteresis loop, which is characteristic for SBA-15, corresponding to the filling of ordered mesopores. The relative pressure of pore filling is almost the same for the 1 and 1.6 wt% P123 samples, yet is higher for the 3.2 wt% P123 sample. As can be seen from Figure 15, all isotherm curves exhibit steep condensation steps which reflect a high uniformity of mesopores. However, for the highest P123 concentration, the condensation step is sharper which indicates an even narrower and more uniform distribution of the pore size. As illustrated in the Figure 16, the pore size distribution is determined by plotting the incremental change in pore volume (dVp) divided by the incremental change in the pore radius (dRp) versus the pore radius (Rp) and confirms the narrow pore size and uniform distribution for the sample with highest P123 concentration.

[00136] The BET specific area was calculated using the method as described above with the results depicted in Figure 17. The mesopores size and volume were determined using the BJH method. Furthermore, by combining N_2 adsorption-desorption isotherms and XRD data, the thickness of the wall (silica) was calculated. Results describing the properties of the various SBA-15 samples as prepared according to the conditions in Table 4 above are shown in Table 5.

Table 5 – Properties of the various mesoporous SBA-15 catalyst support samples

			BJH Method								
	BET method		Calculated from adsorption data						Cal. of desorption data		
Samples	^{S}BET (m^2/g)	C value	Vpore (cm^3/g)	Vmicro (cm^3/g)	D_p (nm)	^{A}pore (m^2/g)	a (nm)	E (nm)	Vpore (cm^3/g)	D_p (nm)	E (nm)
SBA-15-1.2-24-HCl	681	641	0.55	0.037	13.30	447	9.02	/	0.61	8.60	0.42
SBA-15-2-24-HCl	730	591	0.60	0.037	12.80	493	9.40	/	0.67	8.20	1.20
SBA-15-4-24-HCl	834	261	1.05	0.035	7.60	666	10.60	3.00	0.96	6.00	4.60
SBA-15-4-24-HNO_3	808	181	0.96	0.014	14.60	630	10.80	/	0.99	10.6	0.20

^{S}BET = Specific surface area calculated by BET method, Vpore = total pore volume obtained by N_2 adsorption volume at p/p_0 in the range 0.05-0.3, Vmicro = micropore volume calculated from β plot, C = constant in BET equation, a = the unit cell parameter was calculated from a $=2d_{100}/\sqrt{3}$, R_{Peak} = the radius at the peak of distribution curve measured by BJH method, ^{A}pore = the surface area of the mesopores, E is the wall thickness of the pores, E = a-D_p

[00137] Very thin walls were produced at low P123 concentrations for which larger pore diameters were determined, while for the highest P123 concentration, thicker walls were produced as the same amount of TEOS was used during preparation for all three samples. The wall thickness for the 3.2 wt% P123 sample was found to be 3 nm as calculated from the adsorption data and further confirmed by TEM measurements. The pore diameter increased with decreasing P-123 concentration.

[00138] Further data analysis was performed in order to determine the microporosity, if any, of the prepared samples. Three methods were used in this respect, namely *t-*, *α-* and *β*-plots by using the following equations:

$$t = 3.54\left[\frac{V_{ads}}{V_m}\right]\text{Å} \quad , \quad \alpha = \frac{V_{ads}}{V_{ads\ at\ P/p0}} \quad and \quad \beta = \left[\frac{Ln(0.4)}{Ln\left(\frac{P}{P0}\right)}\right]^{1/2.7}$$

All three methods demonstrated that the SBA-15 prepared samples have almost no microporosity. From the *β*-plots, an average micropore volume of 0.037 cm^3/g was calculated whereas t- and *α*-plots showed no microporous volume at all. Figure 18 A, B, and C shows the results for the SBA-15-4-24-HCl sample only. The same procedure was applied for the other samples and their respective micropore volumes are presented in Table 5.

[00139] In a further experiment the respective mesopore and micropore volumes were

measured for an additional SBA-15 sample prepared following the prior art procedure of Zhao. Nitrogen adsorption/desorption isotherms (data not shown) were obtained and surface areas were calculated using the BET method. The pore size distribution and volume of mesopores were obtained from the desorption branch of the isotherm using the BJH method. The pore volume of the mesopores was calculated as 0.92 cm^3/g. Following further data analysis, the volume of the micropores was calculated as 0.74 cm^3/g. Thus the micropore volume of the sample produced by the procedure of Zhao is considerably greater than the samples produced following the process of the invention as all the micropore volumes depicted in Table 5 are 0.037 cm^3/g or less as calculated from the β-plots. Low microporosity is particularly desirable to ensure optimal impregnation of the SBA-15 support with a metal precursor. If microporosity is high, such as is the case for the sample prepared using the procedure of Zhao, micropores can become blocked following impregnation leading to a loss of the internal surface of the catalyst. If microporosity of the support is low the volume of the pores will not be affected by impregnation and consequently none of the internal surface will be lost.

[00140] When HCl is used as the acid, the formation of the ordered mesoporous silica material was believed to be through a "true" liquid crystal template mechanism (TLCT), as shown in Figure 19(a). According to this mechanism, silica inserted itself into a preformed surfactant aggregate which had already the liquid-crystalline structure corresponding to that observed in the final material. To confirm this supposition, XRD measurements were taken at different times after adding TEOS with the results depicted in Figure 20. As shown in Figure 20, an almost perfect 2D hexagonal mesoporous structure was formed immediately after adding TEOS thus supporting the hypothesis that the formation of the structure proceeds via a TLCT mechanism. No major structural changes were seen with increasing reaction time.

Effect of aging time

[00141] Figure 21 shows the XRD results of two of the prepared supports described in Table 4, one sample aged for 24 hr and the other one for 48 hr. Low angle XRD pattern for the two SBA-15 samples show three peaks, indexable as (100) (110), (200) reflections associated with a *p6mm* hexagonal symmetry. By increasing the aging time, the *d*-spacing is decreased, from 9.20 nm to 8.1 nm, as calculated from the d100. The d110 and d200 values also decrease when the aging time is increased from 24 hr to 48 hr. As the *d*-spacing (interplanar distance) is decreased, the unit cell parameter (distance between pore centers), *a*, is also decreased. The aging temperature can affect the gel chemistry of silica and the interaction forces between the surfactant and the inorganic precursors. By increasing the aging temperature to as high as 95 °C, the length of the hydrophilic

segment (PEO) of the non-ionic surfactant (P123) most probably shortened by dehydration. This might lead either to the redistribution of the PEO from the silica framework to the region adjacent to the cores of the micelles or to the aggregation of the PEO segment within the silica structure. Either way should lead to the decrease of the wall thickness. As the formation of the mesoporous structure was through the "true" liquid crystal template mechanism, the diameter of the pores should remain the same regardless of an aging time of 24 or 48 hours. Although the thickness of the wall could not be directly measured for the sample aged for 48 hours, the cell parameter, *a*, which consists of 2 X (mesoporous radius plus wall thickness) decreases by increasing the aging time. As such, the thickness of the wall decreased with aging time. Therefore, the wall thickness can be controlled by controlling the aging time. Figure 22 shows the SEM images of the prepared SBA-15-4-24-HCl and SBA-15-4-48-HCl support samples. Different morphologies were observed. A uniform and long fibrous structure with several tens of micrometers in length was obtained for synthesised SBA-15 aged at 24 hours (see Figure 22A).The fibrous structure is an agglomerate of fibers that are constituted from small rod-like sub-particles 0.5 – 1.0 μm in length and about 0.5 μm in diameter. The sample aged for 48 hr (Figure 22B) displays a different shape, a little bit disordered, with very small rods, which are not aggregated to form long fibers.

Effect of acid source

[00142] The effect of acid source was assessed through low angle XRD, SEM and nitrogen-adsorption isotherms. Figure 23 presents the low angle XRD spectra for the SBA-15-4-24-HCl and SBA-15-4-24-HNO_3 samples. The interplanar distance and the cell parameter were slightly higher in the presence of HNO_3.

[00143] SEM images of the SBA-15-4-24-HCl and SBA-15-4-24-HNO_3 samples are displayed in Figure 24. Slightly different morphologies were observed for the two samples. For SBA-15 sample prepared using HCl, fiber-like morphology was observed. The morphology of the SBA-15 sample prepared using HNO_3 was of rod-like form, with relatively non-uniform size of ca. 2-4 μm in length. This size is bigger than that of SBA-15-4-24-HCl rods but these rods do not aggregate to form long fibers. Close examination of these rods indicated that they are stacked to each other and look like random or multi-dispersed particles. It is postulated that the enhanced hydrophilicity of the NO_3^- ion induces the formation of more elongated micelles stacked to form a hexagonal rod-like morphology with longer length.

[00144] Almost identical shapes of nitrogen isotherms were observed for both samples, SBA-15-4-24-HCl and SBA-15-4-24-HNO_3 (see Figure 25). These results demonstrate that the homogeneity and order of the hexagonal pores were not altered by using different

acids. However, a wider hysteresis loop was observed for the SBA-15-4-24-HNO_3 sample, indicative that the HNO_3 sample had larger pores. Indeed, the data analysis showed that the pore diameter was 14.60 nm which is almost twice that of the equivalent sample prepared using HCl (see Figure 26 and Table 5). It is suspected that the order of the pores in the SBA-15-4-24-HNO_3 sample decreased due to the increased interaction of the highly hydrophilic NO_3^- anion with the head group of P123. As the pore size was higher for the SBA-15-4-24-HNO_3 the BET surface and pore volume are expected to be smaller. Indeed, the analysis of the adsorption data supported this assumption (see Figure 27 and Table 5).

[00145] As stated above it is hypothesized that the formation of the mesoporous silica material occurs via a "true" liquid crystal template mechanism for the samples prepared using HCl. Measurements were conducted to assess if the same mechanism could be proposed for the formation of the mesoporous materials prepared using HNO_3. First, low-angle XRD were taken at different reaction times after adding TEOS to the P123 acid solutions. In contrast to the results for samples prepared using HCl (see Figure 20), it took 120 min for an imperfect hexagonal structure to be formed when the SBA-15 support was prepared using HNO_3 (Figure 28). However for both HCl and HNO_3 samples a perfect 2D hexagonal structure was formed within the 20 hr of reaction time as shown in Figure 22. The different behaviour for the SBA-15 supports prepared using HNO_3 suggested a different mechanism towards the formation of the mesoporous silica material. Based on this data, it is postulated a cooperative self-assembly mechanism, as illustrated in Figure 19 (b), is adopted by materials prepared using NO_3^- due to the difference in hydrophillicity compared to Cl^-.

[00146] SEM measurements support the theory of different mechanisms for materials comprising HNO_3 and HCl. Figures 29 and 30 present the SEM micrographs taken at 0, 10, 30, 60, 90 and 120 min after adding TEOS, for SBA-15 supports prepared using HCl and HNO_3 respectively. For the samples prepared using HCl, fiber-like morphology was formed immediately and the fibers continued to grow and re-organize themselves with increasing reaction time (Figure 29 A-F).

[00147] The morphology of the SBA-15 support prepared using HNO_3^- was completely different in the earlier stages of reaction, namely for the reaction time up to 2 hrs. As seen in Figure 30 A-F, a sponge-like morphology was formed and continued to grow with reaction time. However, after 20 hrs, the differences in morphology were not that significant, as seen in Figure 23. For the sample prepared with HCl, a uniform and well organized fiber-like structure was formed, with fibers consisting of rods, while for the HNO_3 sample, only a rod-like structure was formed. In summary, SBA-15 supports prepared

using HCl showed a preferable structure, texture and morphology compared to the SBA-15 supports prepared using HNO_3^-.

Effect of calcination temperature

[00148] To investigate the effect of calcination temperature on the mesoporous structure, experiments were conducted on sample SBA-15-4-24-HCl by performing calcination at 650 ºC, 750 ºC, 850 ºC and 1000 ºC. The results from the low angle XRD spectra are shown in Figure 31 wherein the well-ordered mesoporous structure was destroyed at 1000 ºC.

Effect of impregnation conditions and metal precursor salt

[00149] With reference to Table 1 and Table 3 above, the influence of the impregnation solution concentration and impregnation time, and of the nature of nickel precursors on the catalyst morphology can be assessed by comparing, on one hand, samples A and B, and on the other hand, samples B, C, and D. Figure 32 A, B, C and D shows the SEM images of 9% IMPNiA-Bd, 9%IMPNiA-Bc, 12%IMPNiN-B, and 8% IMPNiC-B catalyst, respectively. As observed, the morphologies are very different. A grey colour evidences the presence of nickel oxide, while a white colour evidences the presence of silica. For the catalyst derived from nickel acetate, with low concentration but longer time of impregnation (Figure 32A), the SEM image shows homogeneous particles, with a folding laminar structure. For the sample obtained by impregnation with high concentration but for shorter impregnation time (Figure 32B), the SEM image shows organized short bundles of shapes with primary particle diameters in the range of 250-300 nm. In the SEM image of the catalyst obtained from nickel nitrate (Figure 32C), the morphology appears to be as a short fiber-like structure, while for nickel citrate as the precursor, the SEM image shows rod-like morphology (Figure 32D). Although the SEM images for the other samples are not shown, it was concluded that for impregnation with low concentration solutions, irrespective to the nature of the precursor, homogeneous morphologies were obtained. In addition, EDX measurements were performed along with SEM. As can be seen from Table 3, the highest loadings were obtained by using the nickel nitrate as precursor, i.e. 12 wt% versus 9 wt% in the case of acetate and 8 wt% for citrate.

[00150] TEM micrographs for samples of 9% IMPNiA-Bd, 9%IMPNiA-Bc, 12%IMPNiN-B, and 8% IMPNiC-B catalyst are shown in Figure 33 A, B, C and D. They show the nickel oxides particles (dark zones) with different sizes between 5 and 50 nm over the mesoporous structure of SBA-15 support (long parallel channels in hexagonal array). Some of the particles show an irregular shape that seems to adapt to the porous structure of the support, while other ones show either cubic or very small spherical shape, probably

being placed over the external surface of the support, as assigned by the arrow. If impregnation was carried out with diluted nickel acetate solutions, the TEM micrograph shows very small aggregated spheres of nickel oxide (Figure 33A), while the size of these aggregates increased by increasing concentration (Figure 33B). In the nitrate case (Figure 33C), the size of nickel oxide particles is even bigger, while by using citrate (Figure 33D) one big particle, with a few small fragments on the top is formed. The TEM micrograph reveals that some nickel oxide is located inside the pores, whilst the others are present on the external surface (Figure 33 A & B). This means that the nickel oxide particles are larger than the mesoporous diameter of the SBA-15 support. Heat treatment such as drying at 120 ºC, for 10 hours, which is quite a slow drying process, would favour nickel species in the mesopores to move out and aggregate as shown in the Figure 33C.

[00151] According to the low angle XRD results as shown in Figure 34A, B, C and D for the 9% IMPNiA-Bd, 9%IMPNiA-Bc, 12%IMPNiN-B, and 8% IMPNiC-B SBA-15 catalyst samples, the mesoporous structure of the support is maintained after nickel impregnation. All the samples display at least three reflections: (100), (110) and (200), characteristics of a hexagonal array of mesochannels. The nature of the nickel precursor influences the interplanar distance, d_{100}, and the size of unit cell, a, as shown in Table 3.

[00152] The wide angle XRD spectra shown in Figure 35A, B, C and D for the 9% IMPNiA-Bd, 9%IMPNiA-Bc, 12%IMPNiN-B, and 8% IMPNiC-B SBA-15 catalyst samples display reflections of nickel oxide at 2Θ = 37, 43, 62, and 79º. Although the wide angle XRD results for the other samples are not shown, the nickel oxide reflections appeared only for samples with loadings higher than 5 wt%, and the intensity of the reflections increased with increasing nickel loading. The particle size of nickel oxide can be determined from Scherrer equation as described above. The sample prepared with citrate precursor displays well-resolved nickel oxide peaks, indicating that relatively large nickel oxide particles (19.45 nm in average as from Scherrer equation) are present. This result is again in good agreement with TEM results. For sample prepared with nitrate as precursor, the average nickel oxide particle size was 10.03 nm, while for concentrated nickel acetate solution was 8.69 nm. In the case of diluted nickel acetate solution, only very weak and broad reflections are obtained, indicating that exclusively uniformly dispersed, very small nickel oxide particles are formed, which is again, in good agreement with TEM observations. These results therefore demonstrate that nickel acetate was the most well dispersed species. This is most likely due to the size and geometry of the acetate component. Acetic acid is larger than nitric acid, for example, and due to its comparatively large size, increased dispersion of the nickel species is favoured when acetate is incorporated as part of the nickel salt.

Effect of multiple step impregnation

[00153] A multiple step impregnation, as opposed to single step impregnation, was performed to obtain high nickel loadings into SBA-15 whilst maintaining the mesostructure of silica support and high dispersion of nickel species over the area of catalyst.

[00154] Figure 36 shows the micrograph of the multiple step impregnation of the nickel acetate salt, sample 8 % IMPNiA-5 as described in Table 3. No large agglomerates of nickel precursor were formed during the preparation of the catalyst and consecutive calcinations of the catalyst after each of the five cycles of impregnation. Therefore, high and homogeneous dispersion of nickel particle into the framework of SBA-15 occurred. It could be explained that some of the nickel particles are incorporated into the pores of SBA-15 silica after each impregnation cycle so that the incorporatation of nickel into all pores of SBA-15 could be achieved after five cycles of impregnation.

[00155] The low angle and wide angle XRD spectra in Figure 37 show that the mesoporous structure of the support is well conserved, only slight shrinkage occurred. This can be attributed to the thicker and therefore more robust framework walls of SBA-15 which offers good hydrothermal and thermal stability during the preparation.

[00156] Figure 38 shows the nitrogen adsorption isotherm for the catalyst prepared by multiple step impregnation of nickel acetate salt. The mesoporous structure is not destroyed after five impregnation cycles as the sorption isotherm is still described through a H1 hysteresis type IV (a proof of well-defined cylindrical-like pore channels) as shown in Figure 38A. After five consecutive impregnation cycles of nickel oxide species, a very narrow pore size distribution is still observed, which is centred at 3.29 nm (Figure 38B). However, the total pore volume and pore diameter significantly decreased, as shown in Table 3. This is probably due to the partial blockage of SBA-15 pores.

[00157] Throughout the description and claims of this specification, the words “comprise” and “contain” and variations of them mean “including but not limited to”, and they are not intended to (and do not) exclude other moieties, additives, components, integers or steps. Throughout the description and claims of this specification, the singular encompasses the plural unless the context otherwise requires. In particular, where the indefinite article is used, the specification is to be understood as contemplating plurality as well as singularity, unless the context requires otherwise.

[00158] Features, integers, characteristics, compounds, chemical moieties or groups described in conjunction with a particular aspect, embodiment or example of the invention are to be understood to be applicable to any other aspect, embodiment or example described herein unless incompatible therewith. All of the features disclosed in this

specification (including any accompanying claims, abstract and drawings), and/or all of the steps of any method or process so disclosed, may be combined in any combination, except combinations where at least some of such features and/or steps are mutually exclusive. The invention is not restricted to the details of any foregoing embodiments. The invention extends to any novel one, or any novel combination, of the features disclosed in this specification (including any accompanying claims, abstract and drawings), or to any novel one, or any novel combination, of the steps of any method or process so disclosed.

[00159] The reader's attention is directed to all papers and documents which are filed concurrently with or previous to this specification in connection with this application and which are open to public inspection with this specification, and the contents of all such papers and documents are incorporated herein by reference.

CLAIMS

1. A method of making a mesoporous material with hexagonally arranged mesopores comprising the following steps:

a) dissolving a surfactant in water to form a surfactant solution;

b) adding an acid to the surfactant solution to form a mixture having pH less than 2;

c) adding a silica precursor to said mixture to form a precipitate;

d) aging the precipitate;

e) filtering, washing and drying the aged precipitate of step d) and subjecting said precipitate to calcination.

2. The method of claim 1, wherein the surfactant is a poly(alkyleneoxide) block co-polymer.

3. The method of claim 1 or 2, wherein the surfactant is a triblock co-polymer with the formula $EO_{20}PO_{70}EO_{20}$.

4. The method of claim 1 or 2, wherein the surfactant is Pluronic P123.

5. The method of any preceding claim, wherein from 1% to 4% by weight surfactant is dissolved in water.

6. The method of any preceding claim, wherein about 3% by weight surfactant is dissolved in water.

7. The method of any preceding claim, wherein the acid is added after a set period.

8. The method of claim 7, wherein the acid is added after at least 6 hours.

9. The method of any preceding claim, wherein the acid is selected from the group consisting of hydrochloric acid, hydroiodic acid, hydrobromic acid, nitric acid, sulphuric acid and phosphoric acid.

10. The method of any preceding claim, wherein the acid is hydrochloric acid.

11. The method of any preceding claim, wherein the mixture has pH less than 1.

12. The method of any preceding claim, wherein the silica precursor is selected from tetramethoxysilane, tetraethoxysilane, tetrapropoxysilane, sodium silicate or a silica alkoxide.

13. The method of any preceding claim, wherein the silica precursor is tetraethoxysilane.

14. The method of any preceding claim, wherein the molar ratio of silica precursor/surfactant is from 60 to 75.

15. The method of any preceding claim, wherein the molar ratio of silica precursor/surfactant is from 65 to 70.

16. The method of any preceding claim, wherein the silica precursor is added dropwise.

17. The method of any preceding claim, wherein steps a), b) and c) are performed under heating.

18. The method of claim 17, wherein the solution of step a) is heated to at least 35 °C and the respective mixtures of step b) and step c) are maintained at the same temperature of step a).

19. The method of any preceding claim, wherein aging is performed at a temperature of at least 80 °C.

20. The method of any preceding claim, wherein aging is performed at a temperature of from 93 °C to 97 °C.

21. The method of any preceding claim, wherein aging is for a period of at least 12 hours and preferably for a period of about 24 hours.

22. The method of any preceding claim, wherein calcination is performed at a temperature of at least 500 °C.

23. The method of any preceding claim, wherein calcination is performed at a temperature of from 545 to 555 °C.

24. The method of claims 22 or 23, wherein calcination is performed by heating at a rate of 1 °C per minute and maintaining steady state conditions for 6 hours.

25. The method of any preceding claim further comprising the steps:

f) cooling the calcined precipitate of step e), rehydrating to form a suspension; and g) filtering and drying the suspension.

26. A method of making a mesoporous material with hexagonally arranged mesopores comprising the following steps:

a) dissolving a surfactant in a mixture of water and acid wherein the mixture has pH less than 2;

b) adding a silica precursor to said mixture to form a precipitate;

c) aging the precipitate;

d) filtering, washing and drying the aged precipitate of step c) and subjecting said precipitate to calcination;

e) cooling the calcined precipitate of step d), rehydrating to form a suspension; and

f) filtering and drying the suspension.

27. The method of claim 26, wherein the surfactant is a poly(alkyleneoxide) block co-polymer.

28. The method of claim 26 or 27, wherein the surfactant is a triblock co-polymer with the formula $EO_{20}PO_{70}EO_{20}$.

29. The method of claims 26 or 27, wherein the surfactant is Pluronic P123.

30. The method of any of claims 26 to 29, wherein from 1% to 4% by weight surfactant is dissolved in the mixture.

31. The method of claim 30, wherein about 2.5% by weight surfactant is dissolved in the mixture.

32. The method of any of claims 26 to 31, wherein the acid is selected from the group consisting of hydrochloric acid, hydroiodic acid, hydrobromic acid, nitric acid, sulphuric acid and phosphoric acid.

33. The method of any of claims 26 to 32, wherein the acid is hydrochloric acid.

34. The method of any of claims 26 to 33, wherein the mixture has pH less than 1.

35. The method of any of claims 26 to 34, wherein the silica precursor is selected from tetramethoxysilane, tetraethoxysilane, tetrapropoxysilane, sodium silicate or a silica alkoxide.

36. The method of any of claims 26 to 35, wherein the silica precursor is tetraethoxysilane.

37. The method of any of claims 26 to 36, wherein the molar ratio of silica precursor/surfactant is from 60 to 75.

38. The method of any of claims 26 to 36, wherein the molar ratio of silica precursor/surfactant is from 65 to 70.

39. The method of any of claims 26 to 38, wherein the silica precursor is added dropwise.

40. The method of any of claims 26 to 39, wherein steps a) and b) are performed under heating.

41. The method of claim 26, wherein the mixture of step a) is heated to at least 35 ºC and the mixture of step b) is maintained at the same temperature of step a).

42. The method of any of claims 26 to 41, wherein aging is performed at a temperature of at least 80 ºC.

43. The method of any of claims 26 to 42, wherein aging is performed at a temperature of from 93 ºC to 97 ºC .

44. The method of any of claims 26 to 43, wherein aging is for a period of at least 12 hours and preferably wherein aging is for a period of about 24 hours.

45. The method of any of claims 26 to 44, wherein calcination is performed at a temperature of at least 500 ºC.

46. The method of any of claims 26 to 45, wherein calcination is performed at a temperature of from 545 to 555 ºC.

47. The method of claims 45 or 46, wherein calcination is performed by heating at a rate of 1 ºC per minute and maintaining steady state conditions for 6 hours.

48. A mesoporous material made by the method of any of the claims 1 to 47.

49. The mesoporous material of claim 48, wherein said mesoporous material comprises mesopores with a total pore volume of greater than 0.55 cm^3/g and an average micropore volume of less than 0.038 cm^3/g as measured from nitrogen adsorption isotherms using the methods specified herein.

50. The mesoporous material of claim 48, wherein said mesoporous material comprises mesopores with a total pore volume of greater than 0.92 cm^3/g and an average micropore volume of less than 0.038 cm^3/g as measured from nitrogen adsorption isotherms using the methods specified herein.

51. A support for a catalyst comprising or consisting of the mesoporous material according to any of claims 48 to 50.

52. A method of making a catalyst comprising the step of impregnating the mesoporous material of any of claims 48 to 51 with a metal precursor.

53. The method of claim 52, wherein impregnating the mesoporous material comprises adding a solution containing the metal precursor to said mesoporous material, drying the material and subjecting the material to calcination.

54. The method of claim 52 or 53, wherein the material is impregnated using a wet impregnation method.

55. The method of claim 54, wherein wet impregnation is performed under reflux conditions.

56. The method of any of claims 53 to 55, wherein calcination is performed at a temperature of greater than 500 ºC and preferably wherein calcination is performed at a temperature of from 545 ºC to 555 ºC.

57. The method of any of claims 52 to 56, wherein the metal is a transition metal.

58. The method of any of claims 52 to 57, wherein the metal is nickel.

59. The method of any of claims 52 to 58, wherein the metal precursor is a metal salt.

60. The method of claim 59, wherein the salt is selected from the group consisting of acetate, citrate, nitrate, acetylacetonate, chloride, fluoride, carbonate and sulphate.

61. The method of any of claims 52 to 60, wherein the metal precursor is nickel acetate or nickel nitrate.

62. A supported metal catalyst made by the method of any of claims 52 to 61.

63. A mesoporous material comprising SBA-15, wherein said SBA-15 has mesopores with a total pore volume of greater than 0.92 cm^3/g and an average micropore volume of less than 0.038 cm^3/g as measured from nitrogen adsorption isotherms using the methods specified herein.

64. The mesoporous material of claim 63, wherein said SBA-15 has mesopores with a total pore volume of greater than 1.0 cm^3/g as measured from nitrogen adsorption isotherms.

65. The mesoporous material of claims 63 or 64, wherein said SBA-15 comprises mesopores with an average wall thickness of greater than 2.15 nm as measured from nitrogen adsorption isotherms.

66. The mesoporous material of claim 65, wherein said SBA-15 comprises mesopores with an average wall thickness of about 3 nm as measured from nitrogen adsorption isotherms.

67. The mesoporous material of any of claims 63 to 66, wherein said SBA-15 has a pore size distribution centred around 3 nm as measured from nitrogen desorption isotherms using a method specified herein.

68. The mesoporous material of any of claims 63 to 67, wherein said SBA-15 has a *p6mm* hexagonal symmetry as measured by X ray diffraction.

69. The mesoporous material of any of claims 63 to 68, wherein said SBA-15 has an interplanar distance of about 9 nm and a unit cell parameter of about 11 nm.

70. The mesoporous material of any of claims 63 to 69, wherein said SBA-15 has a BET specific surface area of greater than 800 m^2/g.

71. The mesoporous material of any of claims 63 to 69, wherein said SBA-15 has a BET specific surface area of about 830 m^2/g.

72. A supported metal catalyst comprising SBA-15 impregnated with a metal, wherein said supported metal catalyst has a total pore volume of greater than 0.68 cm^3/g as measured from nitrogen adsorption isotherms using a method specified herein.

73. The supported metal catalyst of claim 72, wherein said supported metal catalyst has a total pore volume of 0.84 cm^3/g or greater.

74. The supported metal catalyst of claims 72 or 73, wherein said supported metal catalyst has a total pore volume of 1.0 cm^3/g or greater.

75. The supported metal catalyst of any of claims 72 to 74, wherein said supported metal catalyst has a BET specific surface area of greater than 400 m^2/g.

76. The supported metal catalyst of any of claims 72 to 75, wherein said supported metal catalyst has a BET specific surface area of greater than 475 m^2/g.

77. The supported metal catalyst of any of claims 72 to 76, wherein said supported metal catalyst comprises crystallites of said metal of less than 5 nm diameter.

78. The supported metal catalyst of any of claims 72 to 77, wherein the metal is a transition metal.

79. The supported metal catalyst of claims 72 to 78, wherein the metal is nickel.

80. A supported metal catalyst comprising a mesoporous material, operable to attain 100% conversion of carbon dioxide from methane at a temperature lower than 700 °C when performing the catalyst activity test as specified herein.

81. The supported metal catalyst of claim 80, operable to attain 100% conversion of carbon dioxide from methane at a temperature of 650 °C when performing the catalyst activity test as specified herein.

82. A supported metal catalyst according to claim 80 or 81 wherein said catalyst is a catalyst according to claim 62.

83. A method of making a mesoporous material as herein described with reference to the description and accompanying drawings.

84. A method of making a supported metal catalyst as herein described with reference to the description and accompanying drawings.

85. A mesoporous material as herein described with reference to the description and accompanying drawings.

86. A catalyst support as herein described with reference to the description and accompanying drawings.

87. A supported metal catalyst as herein described with reference to the description and accompanying drawings.

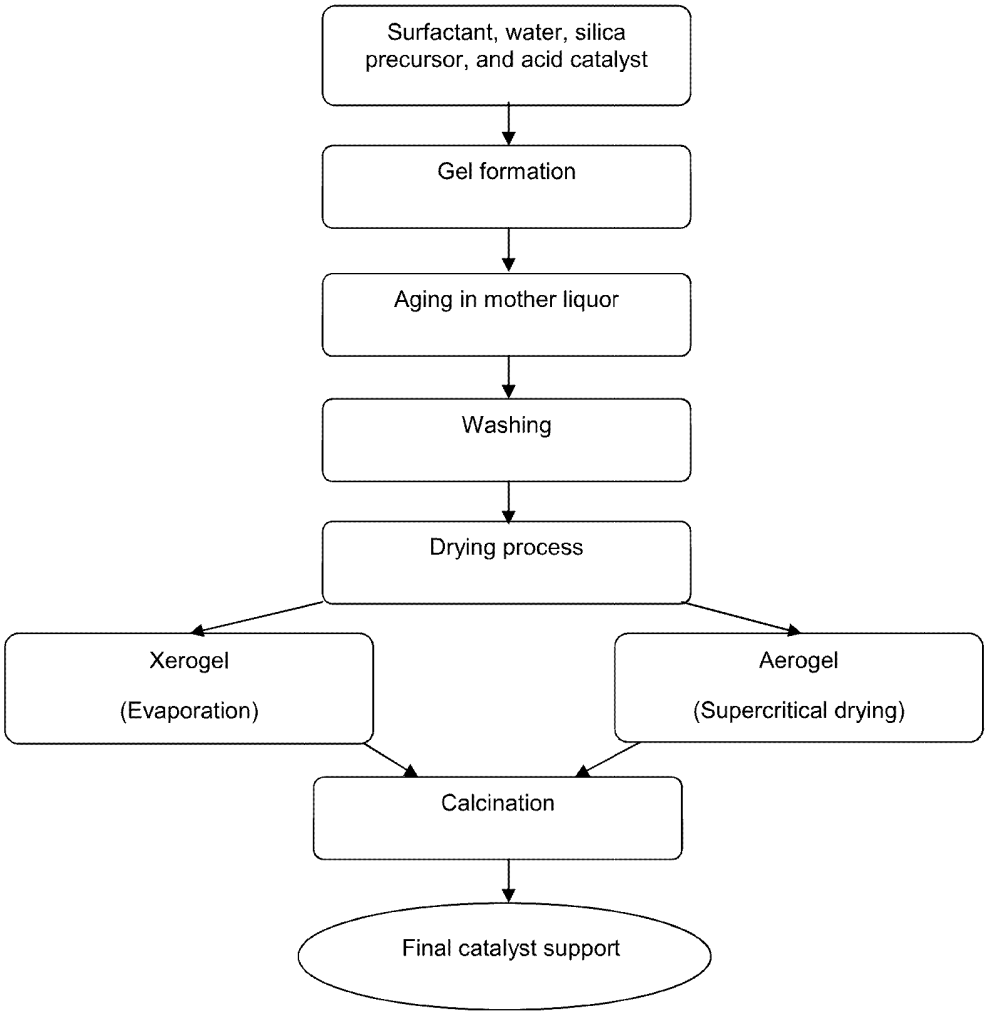
Surfactant, water, silica precursor, and acid catalyst
Gel formation
Aging in mother liquor
Washing
Drying process
Xerogel
(Evaporation)
Aerogel
(Supercritical drying)
Calcination
Final catalyst support

Fig. 1

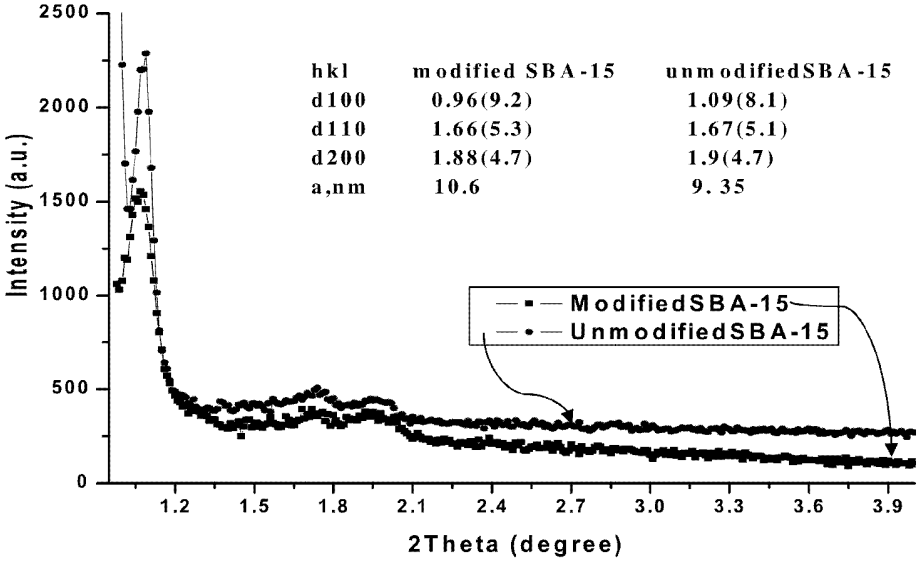
hkl modified SBA-15 unmodifiedSBA-15
d100 0.96(9.2) 1.09(8.1)
d110 1.66(5.3) 1.67(5.1)
d200 1.88(4.7) 1.9(4.7)
a,nm 10.6 9. 35
ModifiedSBA-15
UnmodifiedSBA-15
Intensity (a.u.)
2Theta (degree)
2500
2000
1500
1000
500
0
1.2
1.5
1.8
2.1
2.4
2.7
3.0
3.3
3.6
3.9

Fig. 2

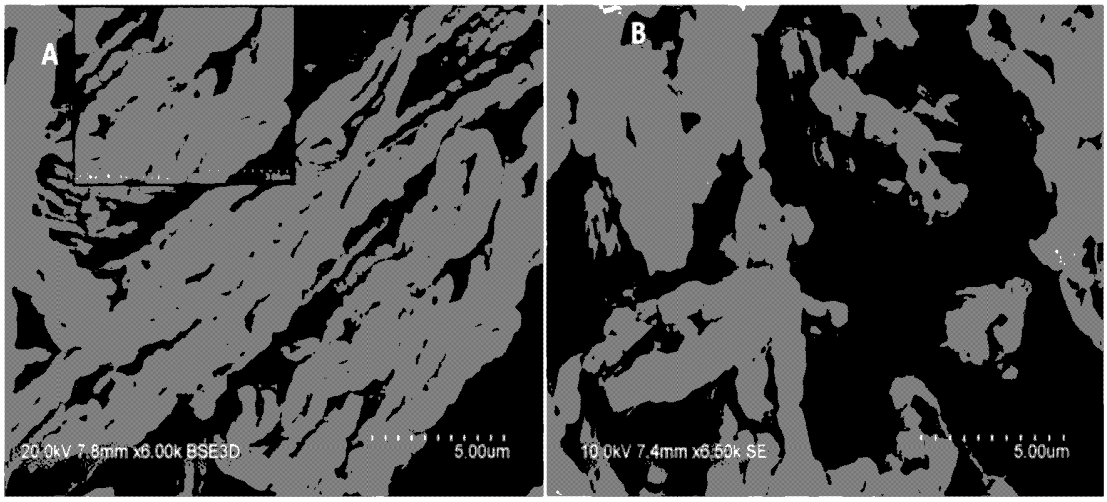

Fig. 3

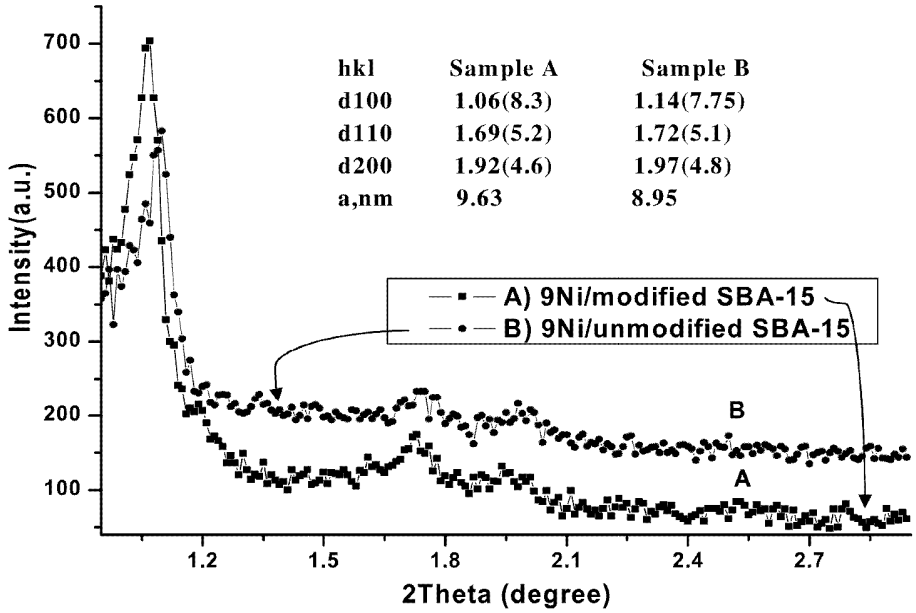
hkl Sample A Sample B
d100 1.06(8.3) 1.14(7.75)
d110 1.69(5.2) 1.72(5.1)
d200 1.92(4.6) 1.97(4.8)
a,nm 9.63 8.95
A) 9Ni/modified SBA-15
B) 9Ni/unmodified SBA-15
B
A
Intensity(a.u.)
2Theta (degree)
700
600
500
400
300
200
100
1.2
1.5
1.8
2.1
2.4
2.7

Fig. 4

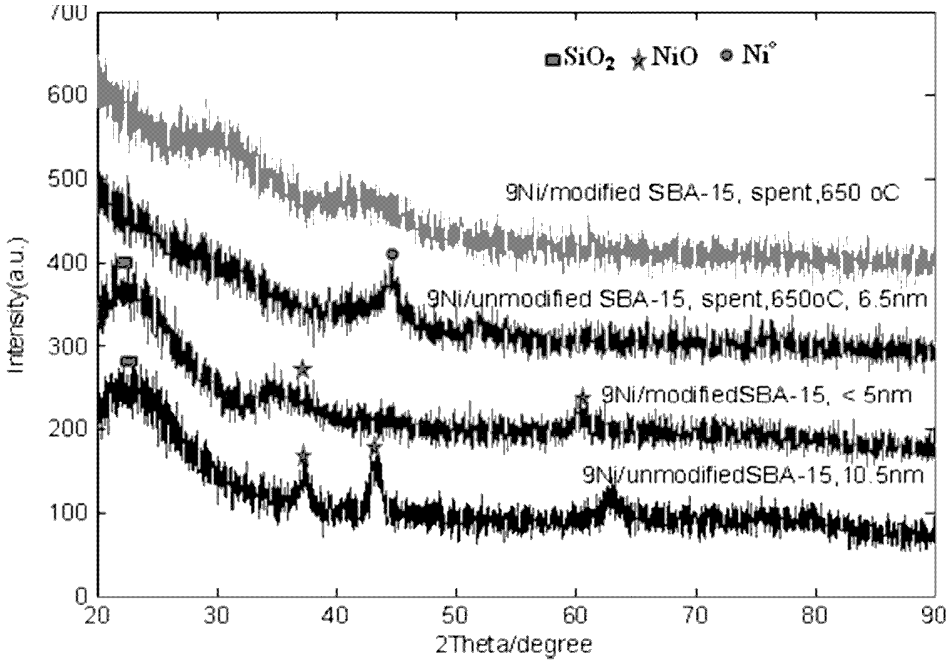
700
600
500
400
300
200
100
0
Intensity(a.u.)
20
30
40
50
60
70
80
90
2Theta/degree
SiO2
NiO
Ni°
9Ni/modified SBA-15, spent,650 oC
9Ni/unmodified SBA-15, spent,650oC, 6.5nm
9Ni/modifiedSBA-15, < 5nm
9Ni/unmodifiedSBA-15,10.5nm

Fig. 5

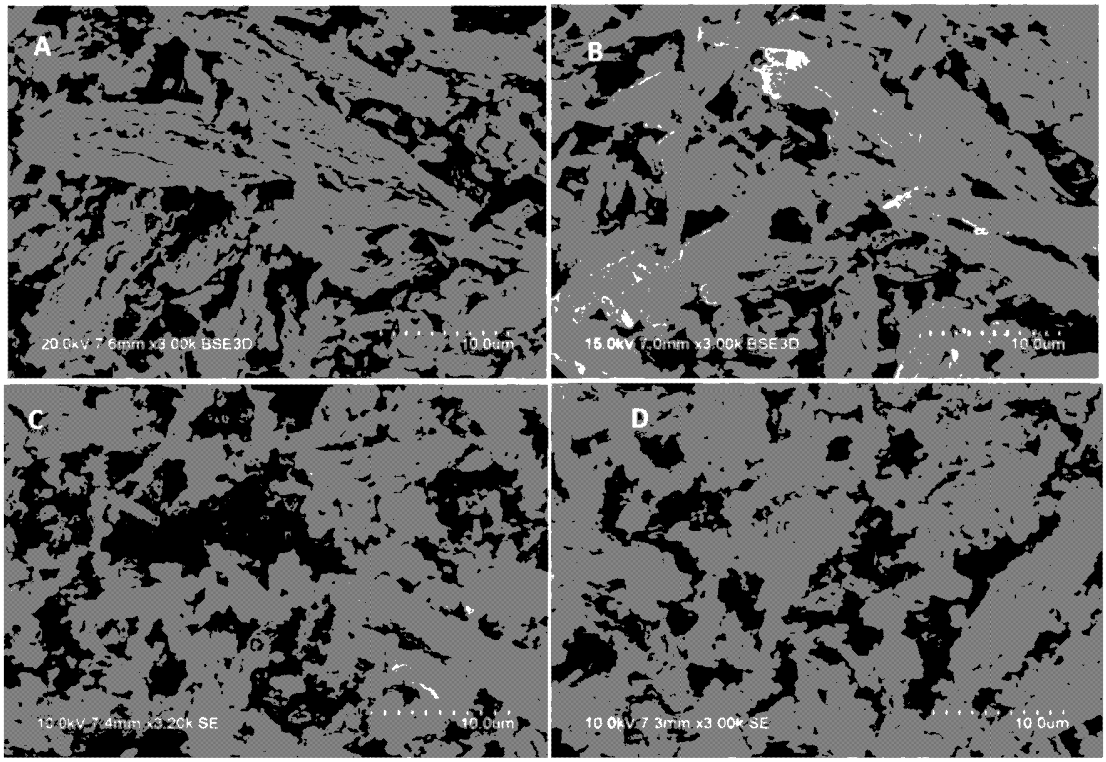
A
20.0kV 7.6mm x3.00k BSE3D
10.0um
B
15.0kV 7.0mm x3.00k BSE3D
10.0um
C
10.0kV 7.4mm x3.20k SE
10.0um
D
10.0kV 7.3mm x3.00k SE
10.0um

Fig. 6

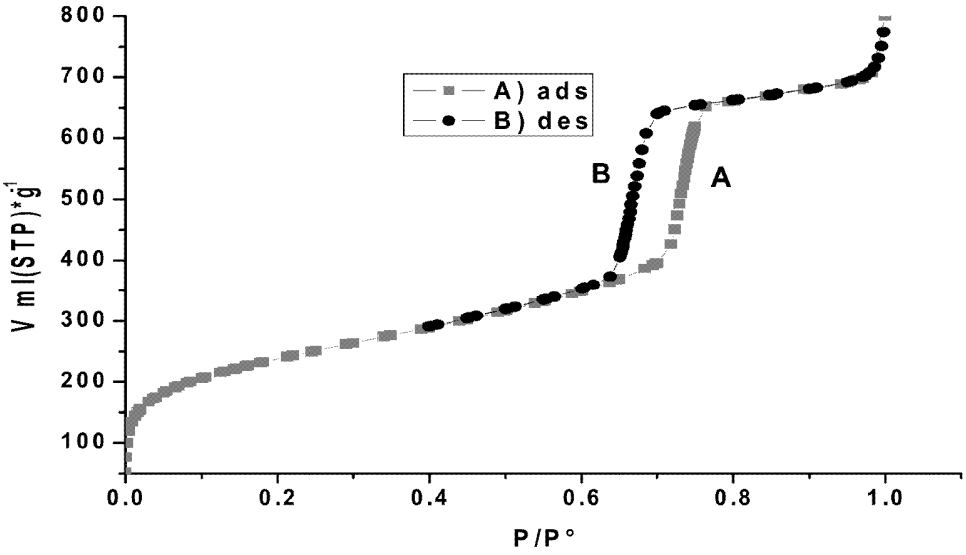
800
700
600
500
400
300
200
100
V ml(STP)*g-1
0.0
0.2
0.4
0.6
0.8
1.0
P/P°
A) ads
B) des
B
A

Fig.7

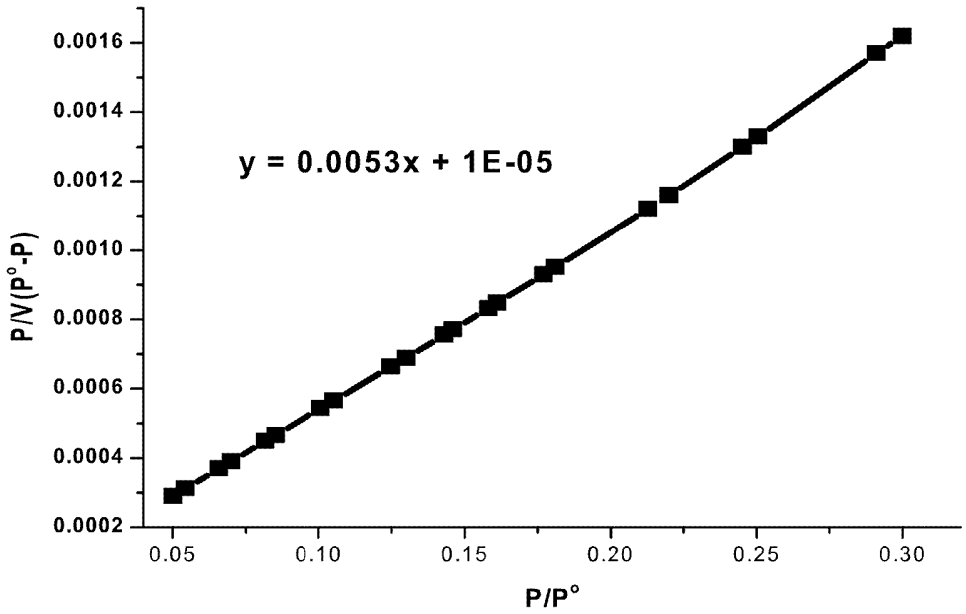
y = 0.0053x + 1E-05
P/V(P°-P)
P/P°
0.0002
0.0004
0.0006
0.0008
0.0010
0.0012
0.0014
0.0016
0.05
0.10
0.15
0.20
0.25
0.30

Fig. 8

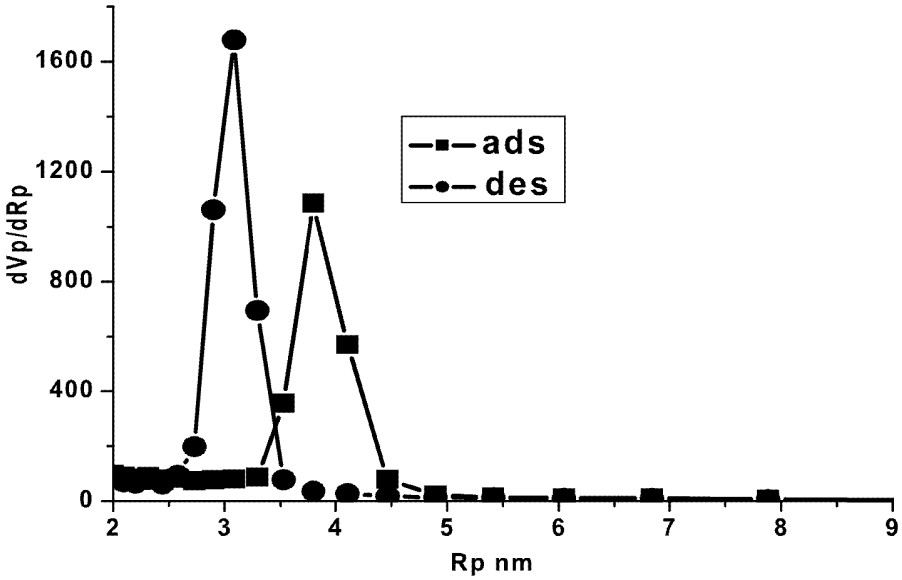

Fig. 9

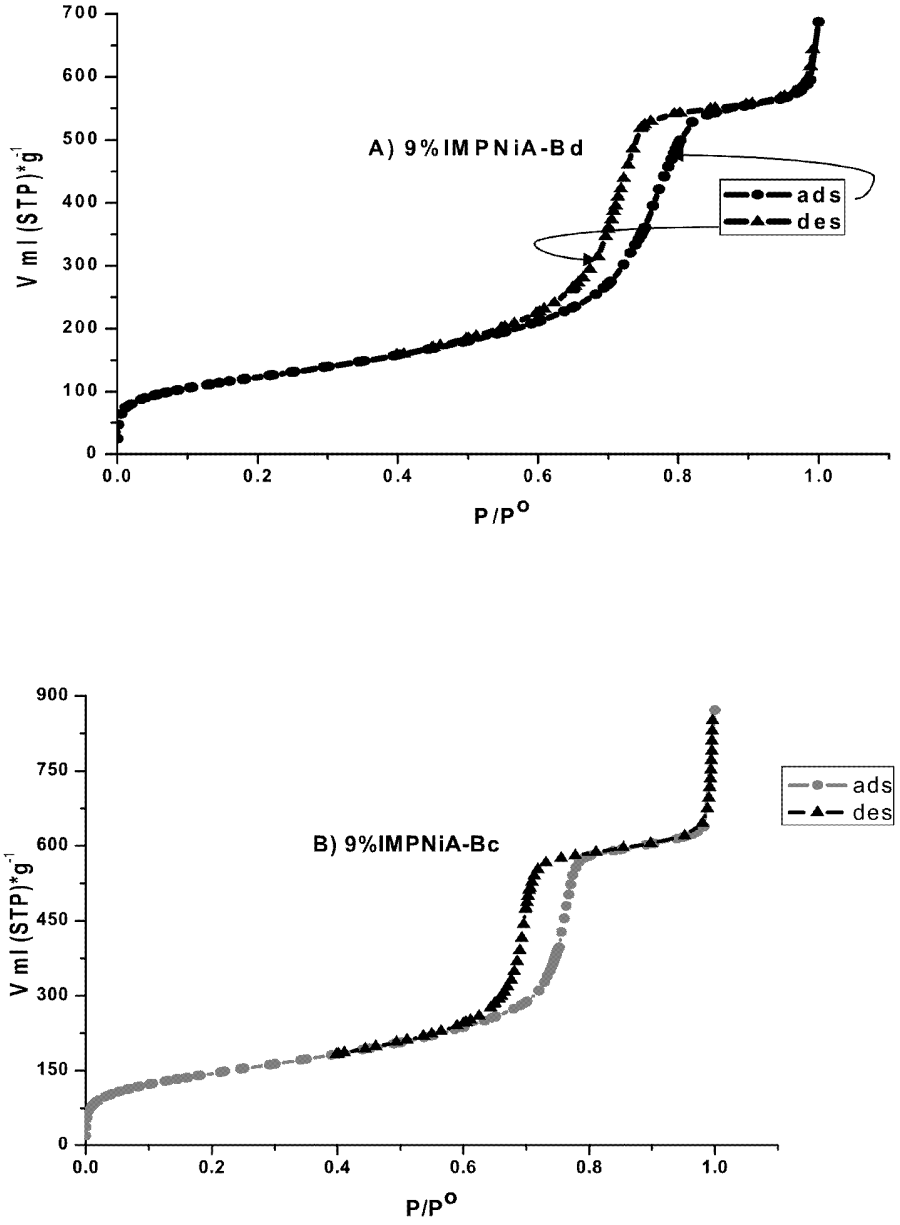
A) 9%IMPNiA-Bd
ads
des
V ml (STP)*g-1
P/PO
0
100
200
300
400
500
600
700
0.0
0.2
0.4
0.6
0.8
1.0
B) 9%IMPNiA-Bc
ads
des
V ml (STP)*g-1
P/PO
0
150
300
450
600
750
900

Fig. 10

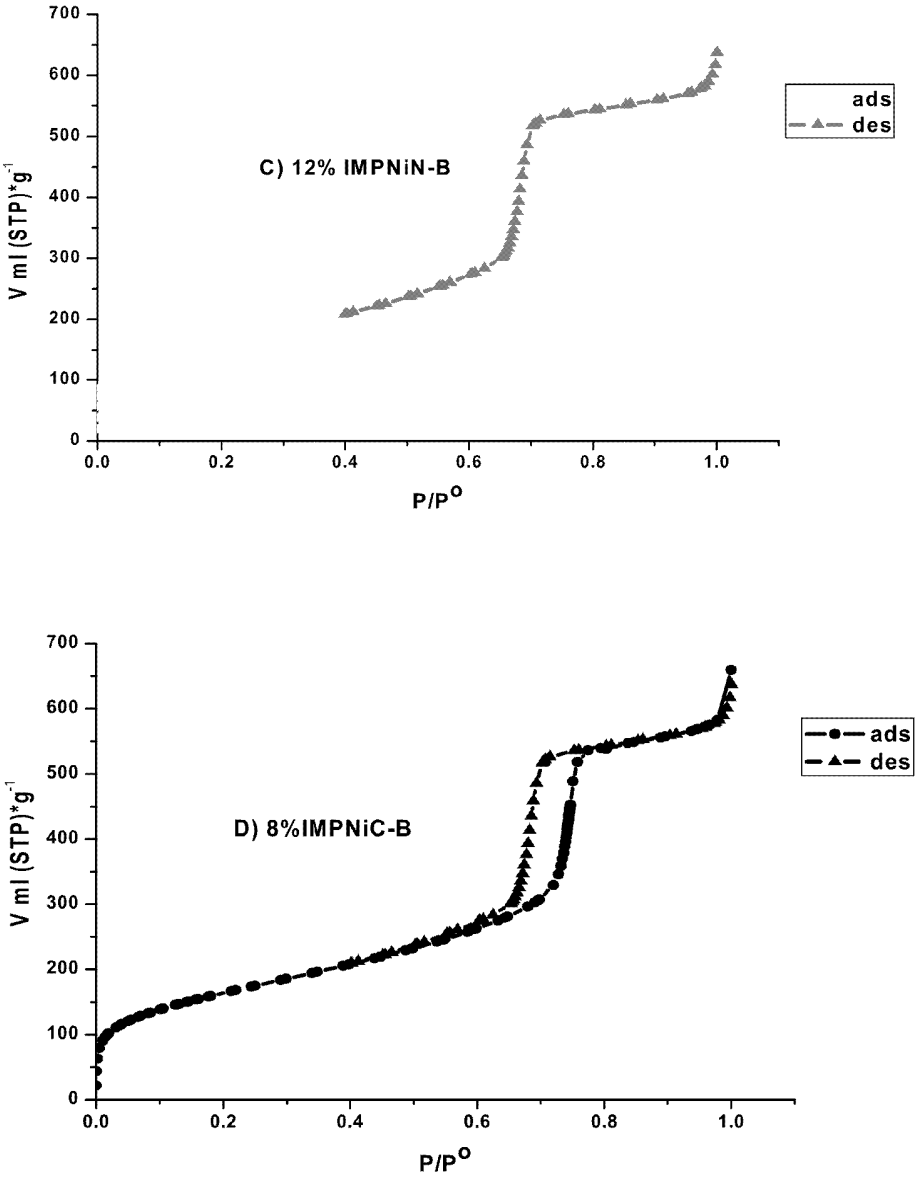
C) 12% IMPNiN-B
ads
des
V ml (STP)*g-1
P/PO
D) 8%IMPNiC-B
ads
des
V ml (STP)*g-1
P/PO

Fig. 10

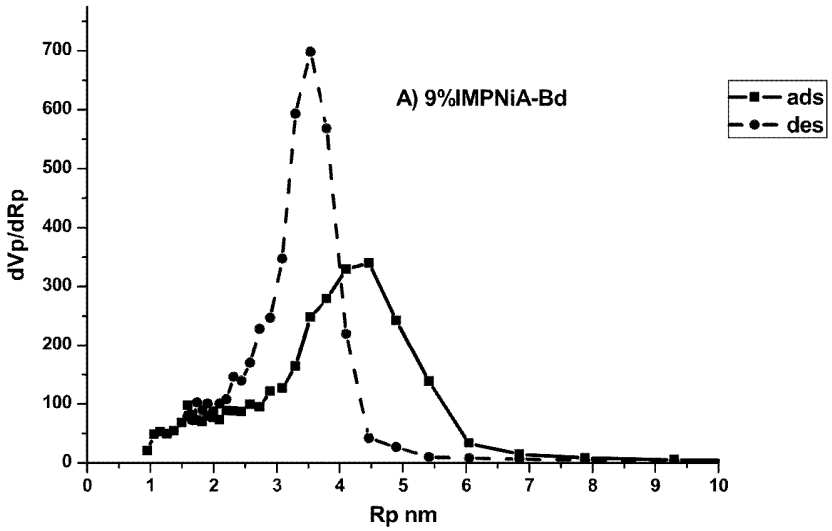
A) 9%IMPNiA-Bd
ads
des
dVp/dRp
Rp nm
0
100
200
300
400
500
600
700
0
1
2
3
4
5
6
7
8
9
10

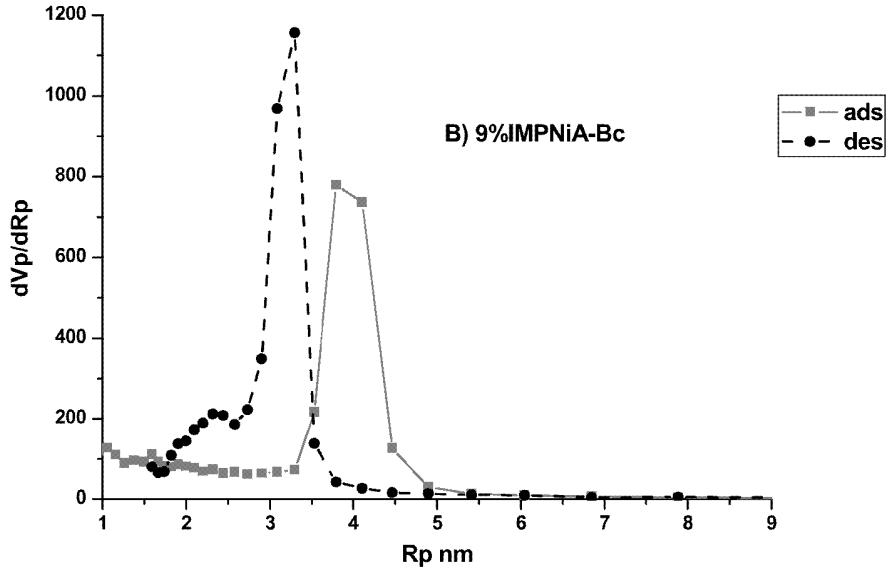
B) 9%IMPNiA-Bc
ads
des
dVp/dRp
Rp nm
0
200
400
600
800
1000
1200
1
2
3
4
5
6
7
8
9

Fig. 11

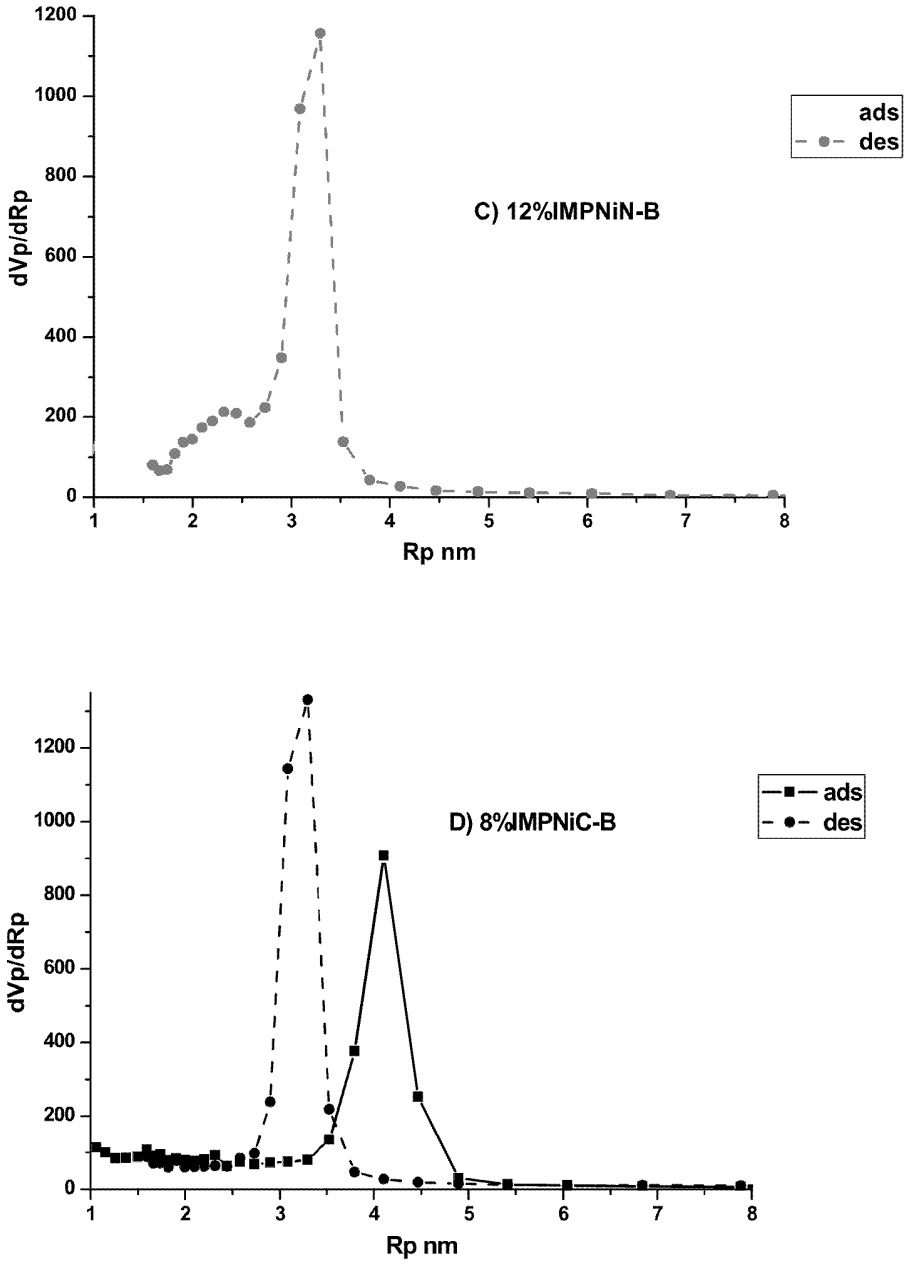
C) 12%IMPNiN-B
ads
des
dVp/dRp
Rp nm
D) 8%IMPNiC-B
ads
des
dVp/dRp
Rp nm

Fig. 11

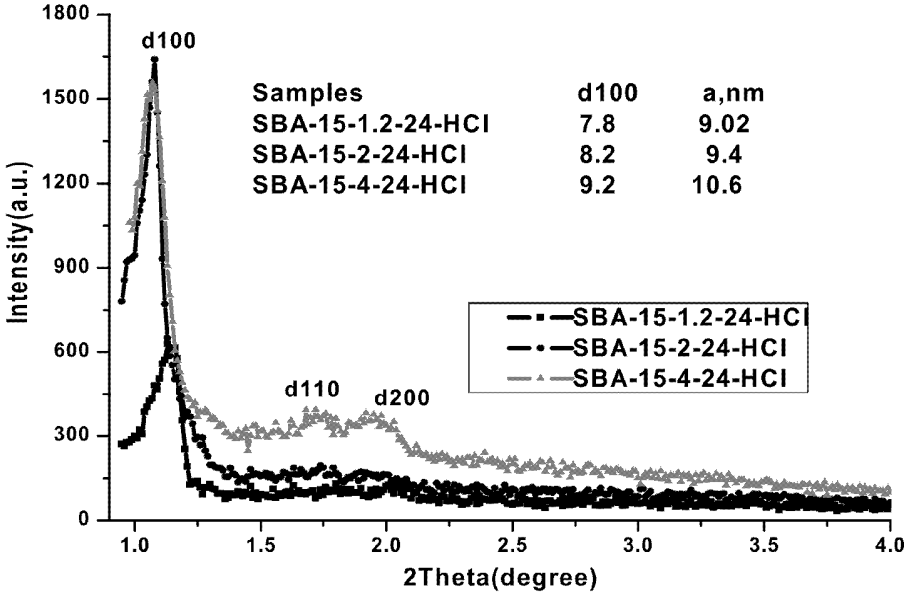
1800
1500
1200
900
600
300
0
Intensity(a.u.)
d100
d110
d200
Samples d100 a,nm
SBA-15-1.2-24-HCl 7.8 9.02
SBA-15-2-24-HCl 8.2 9.4
SBA-15-4-24-HCl 9.2 10.6
SBA-15-1.2-24-HCl
SBA-15-2-24-HCl
SBA-15-4-24-HCl
1.0
1.5
2.0
2.5
3.0
3.5
4.0
2Theta(degree)

Fig. 12

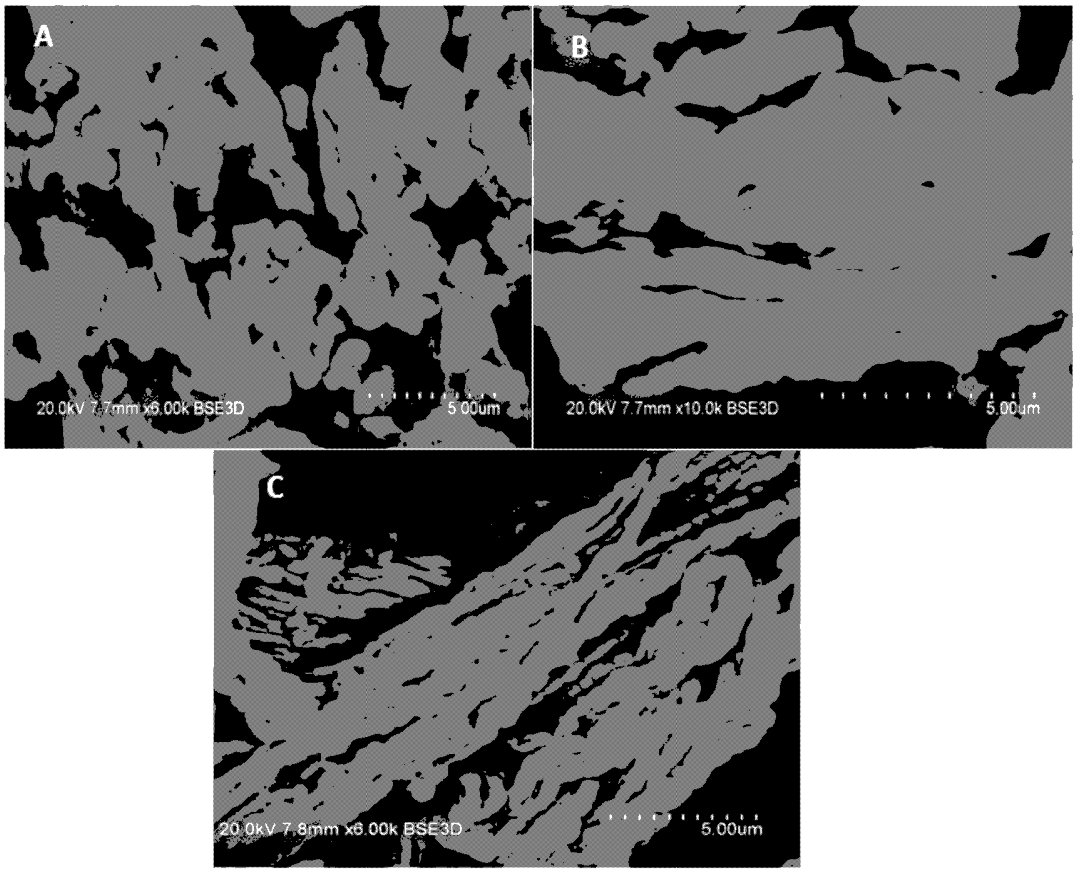
A
20.0kV 7.7mm x6.00k BSE3D
5.00um
B
20.0kV 7.7mm x10.0k BSE3D
5.00um
C
20.0kV 7.8mm x6.00k BSE3D
5.00um

Fig. 13

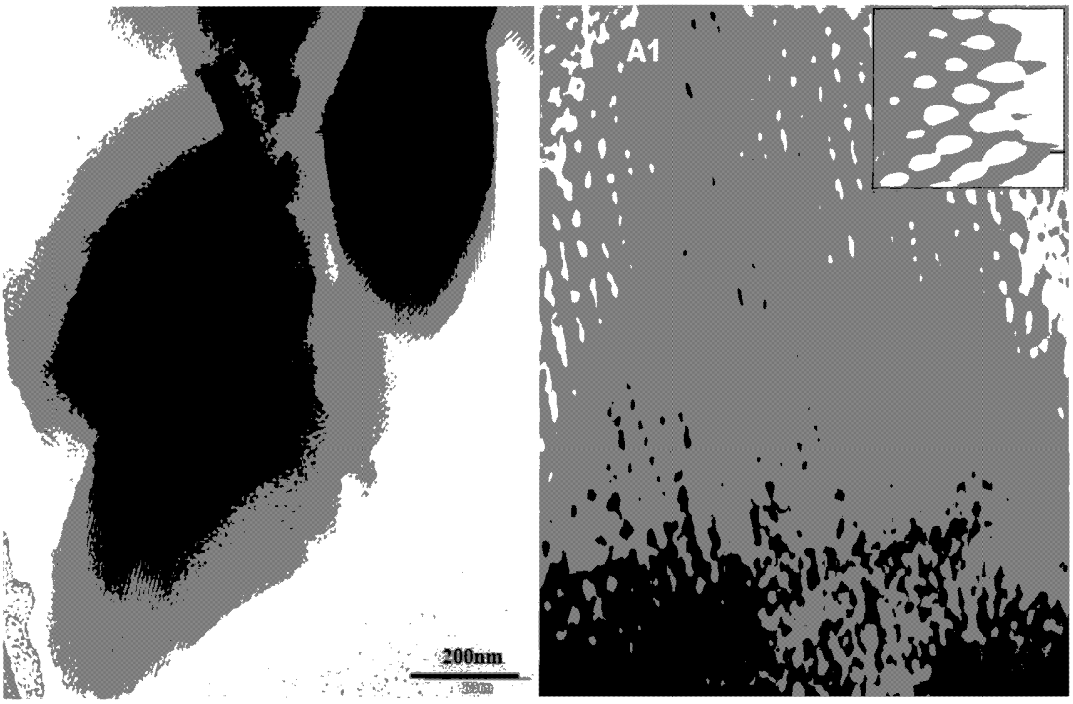

Fig. 14

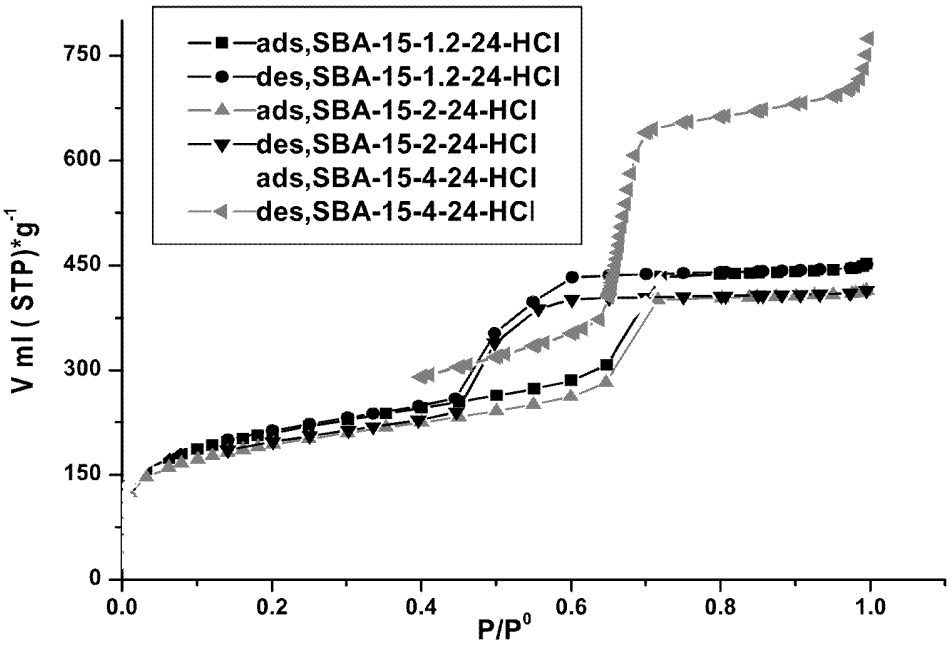
ads,SBA-15-1.2-24-HCl
des,SBA-15-1.2-24-HCl
ads,SBA-15-2-24-HCl
des,SBA-15-2-24-HCl
ads,SBA-15-4-24-HCl
des,SBA-15-4-24-HCl
V ml (STP)*g-1
P/P0
0
150
300
450
600
750
0.0
0.2
0.4
0.6
0.8
1.0

Fig. 15

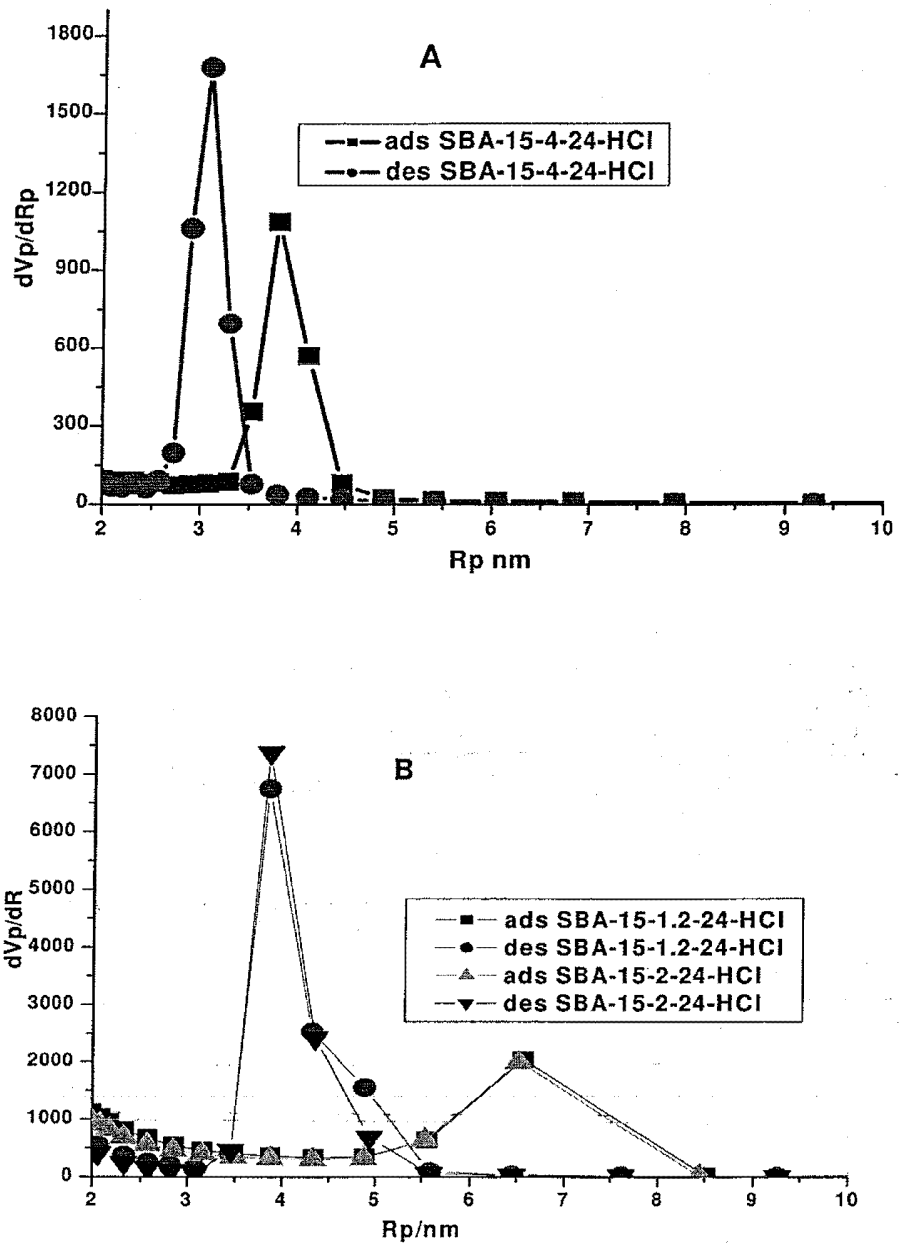
A
ads SBA-15-4-24-HCl
des SBA-15-4-24-HCl
dVp/dRp
Rp nm
B
ads SBA-15-1.2-24-HCl
des SBA-15-1.2-24-HCl
ads SBA-15-2-24-HCl
des SBA-15-2-24-HCl
dVp/dR
Rp/nm

Fig. 16

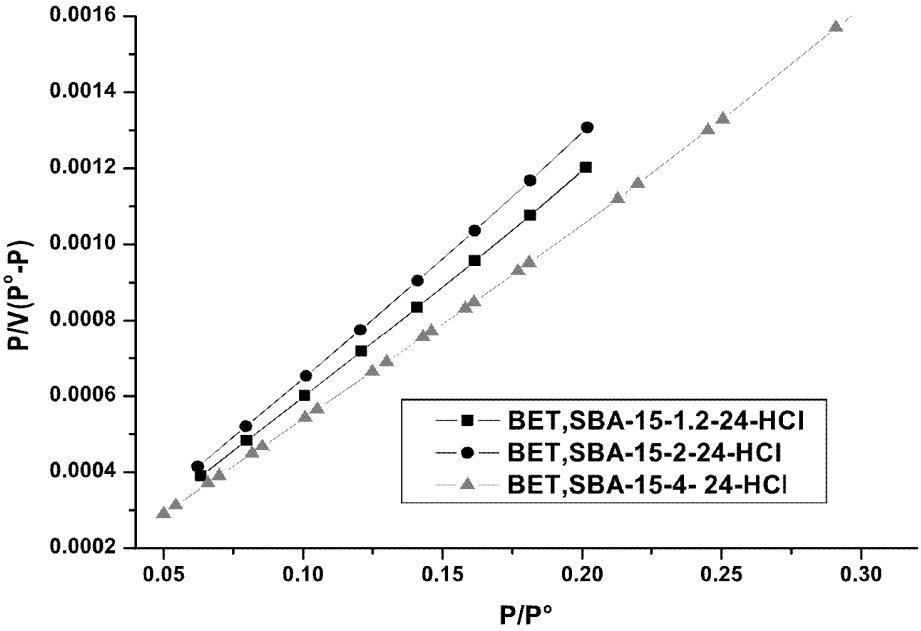
0.0016
0.0014
0.0012
0.0010
0.0008
0.0006
0.0004
0.0002
P/V(P°-P)
0.05
0.10
0.15
0.20
0.25
0.30
P/P°
BET,SBA-15-1.2-24-HCl
BET,SBA-15-2-24-HCl
BET,SBA-15-4- 24-HCl

Fig. 17

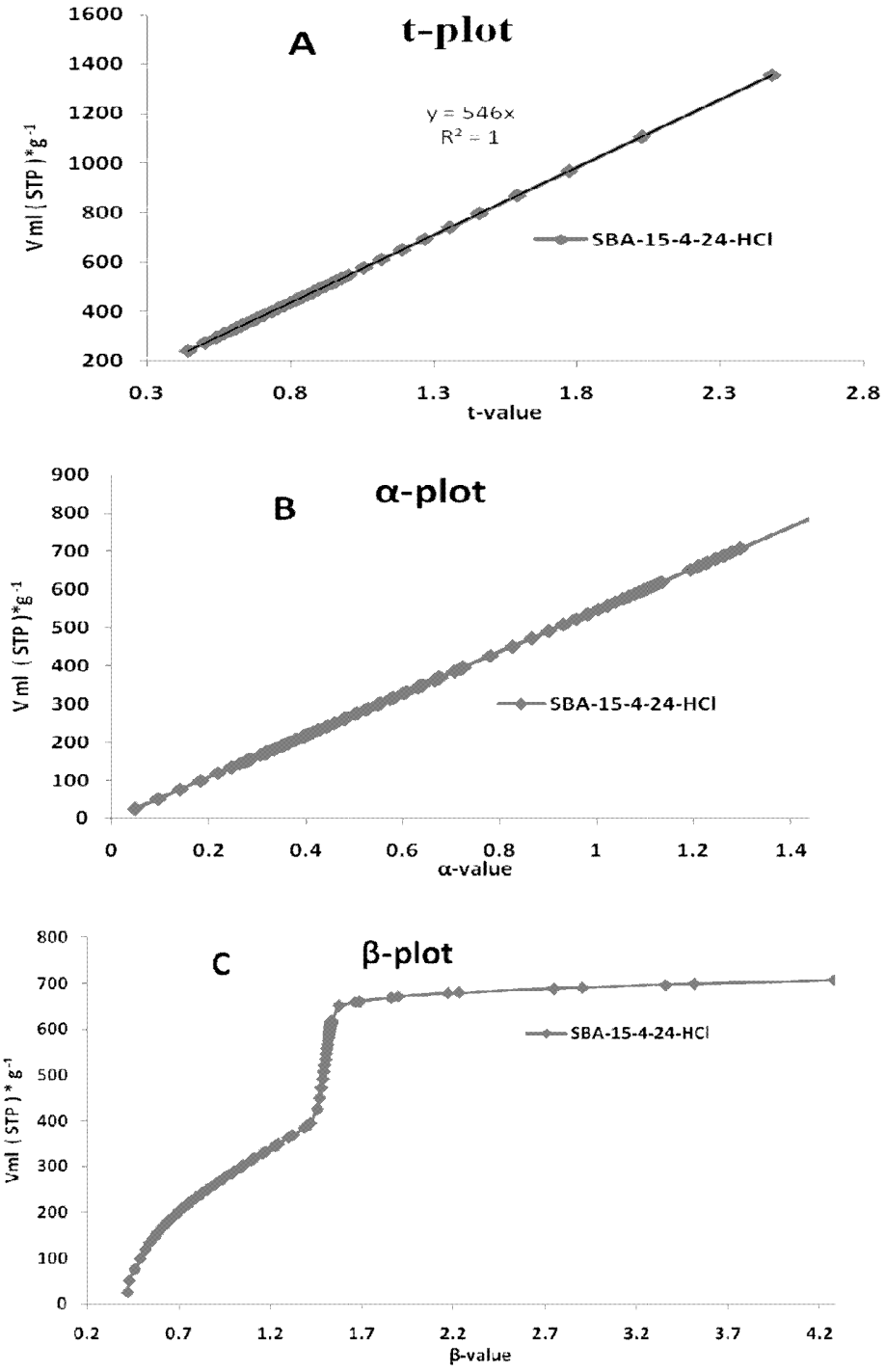
A
t-plot
y = 546x
R² = 1
SBA-15-4-24-HCl
V ml (STP)*g-1
t-value
B
α-plot
SBA-15-4-24-HCl
V ml (STP)*g-1
α-value
C
β-plot
SBA-15-4-24-HCl
Vml (STP) * g-1
β-value

Fig. 18

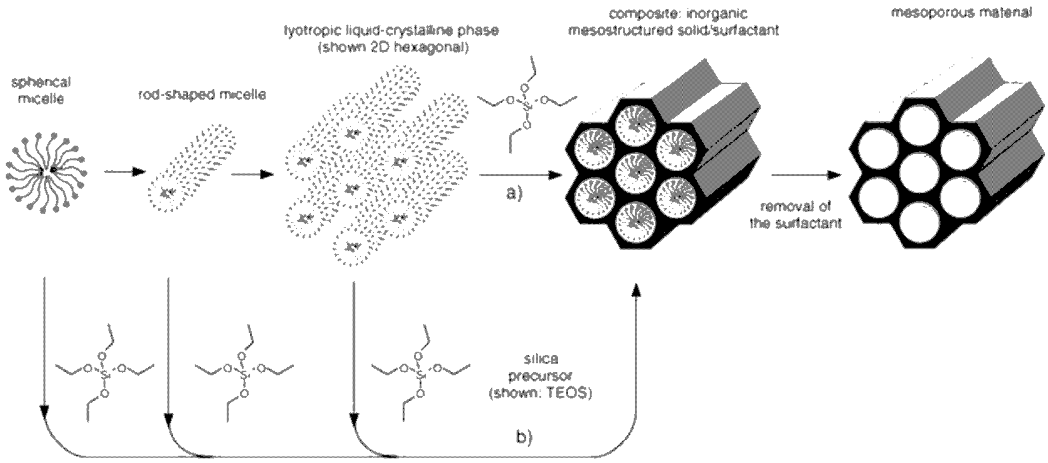
spherical micelle
rod-shaped micelle
lyotropic liquid-crystalline phase (shown 2D hexagonal)
composite: inorganic mesostructured solid/surfactant
mesoporous material
a)
removal of the surfactant
silica precursor (shown: TEOS)
b)

Fig. 19

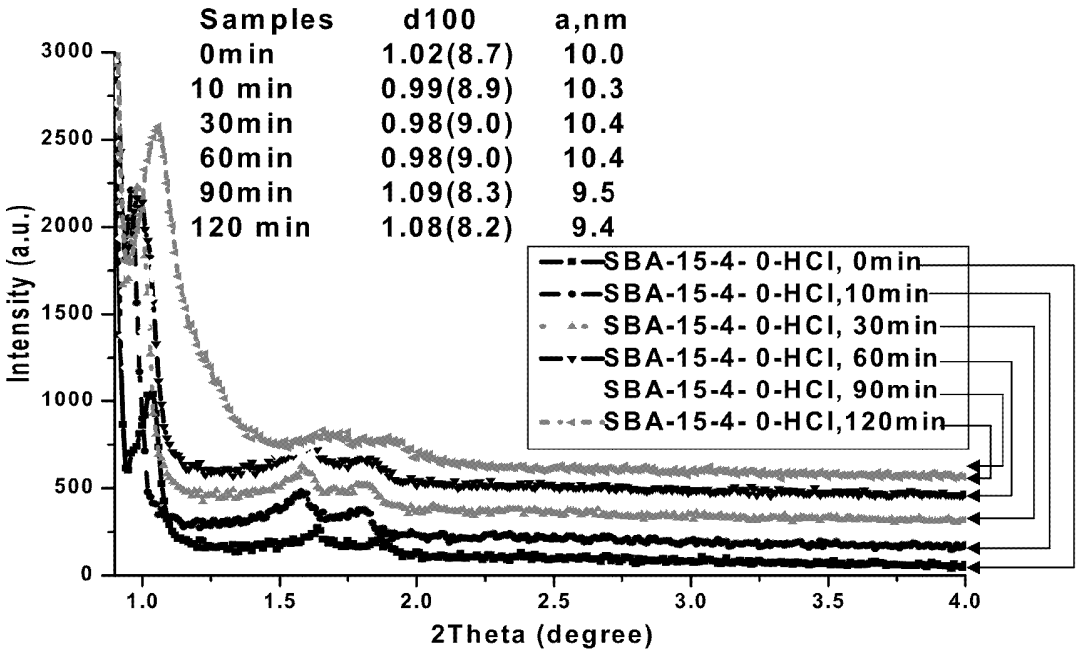
Samples d100 a,nm
0min 1.02(8.7) 10.0
10 min 0.99(8.9) 10.3
30min 0.98(9.0) 10.4
60min 0.98(9.0) 10.4
90min 1.09(8.3) 9.5
120 min 1.08(8.2) 9.4
SBA-15-4- 0-HCl, 0min
SBA-15-4- 0-HCl,10min
SBA-15-4- 0-HCl, 30min
SBA-15-4- 0-HCl, 60min
SBA-15-4- 0-HCl, 90min
SBA-15-4- 0-HCl,120min
Intensity (a.u.)
2Theta (degree)
3000
2500
2000
1500
1000
500
0
1.0
1.5
2.0
2.5
3.0
3.5
4.0

Fig. 20

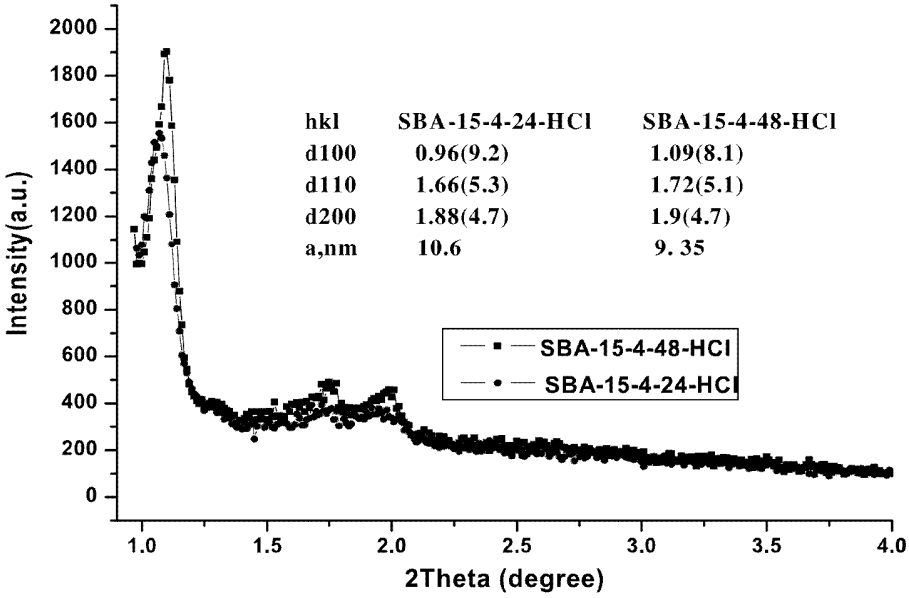
Intensity(a.u.)
2Theta (degree)
hkl SBA-15-4-24-HCl SBA-15-4-48-HCl
d100 0.96(9.2) 1.09(8.1)
d110 1.66(5.3) 1.72(5.1)
d200 1.88(4.7) 1.9(4.7)
a,nm 10.6 9. 35
SBA-15-4-48-HCl
SBA-15-4-24-HCl

Fig. 21

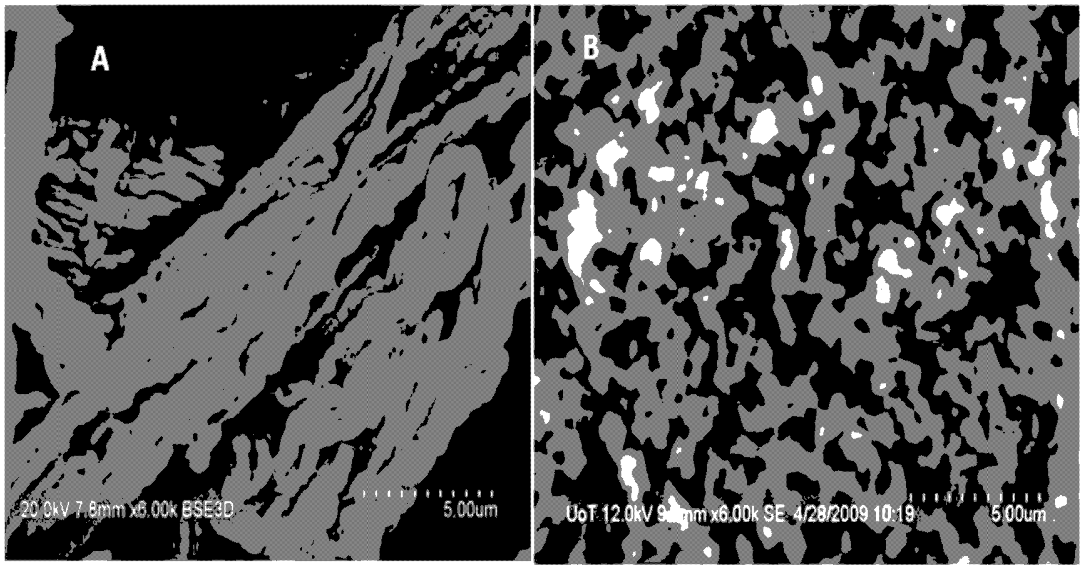
A
20.0kV 7.8mm x6.00k BSE3D
5.00um
B
UoT 12.0kV 9.4mm x6.00k SE 4/28/2009 10:19
5.00um

Fig. 22

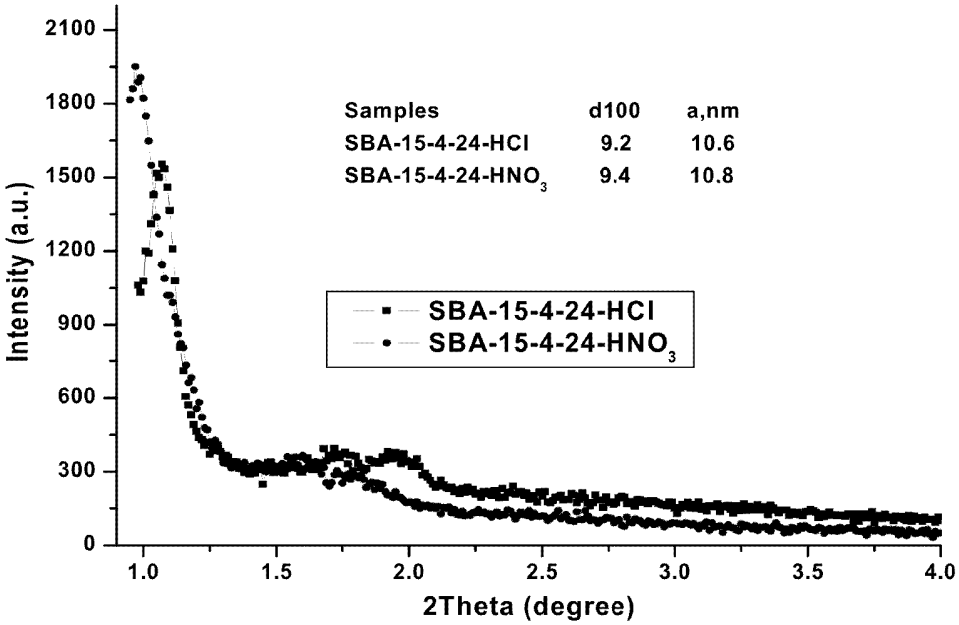
Samples d100 a,nm
SBA-15-4-24-HCl 9.2 10.6
SBA-15-4-24-HNO3 9.4 10.8
SBA-15-4-24-HCl
SBA-15-4-24-HNO3
Intensity (a.u.)
2Theta (degree)
2100
1800
1500
1200
900
600
300
0
1.0
1.5
2.0
2.5
3.0
3.5
4.0

Fig. 23

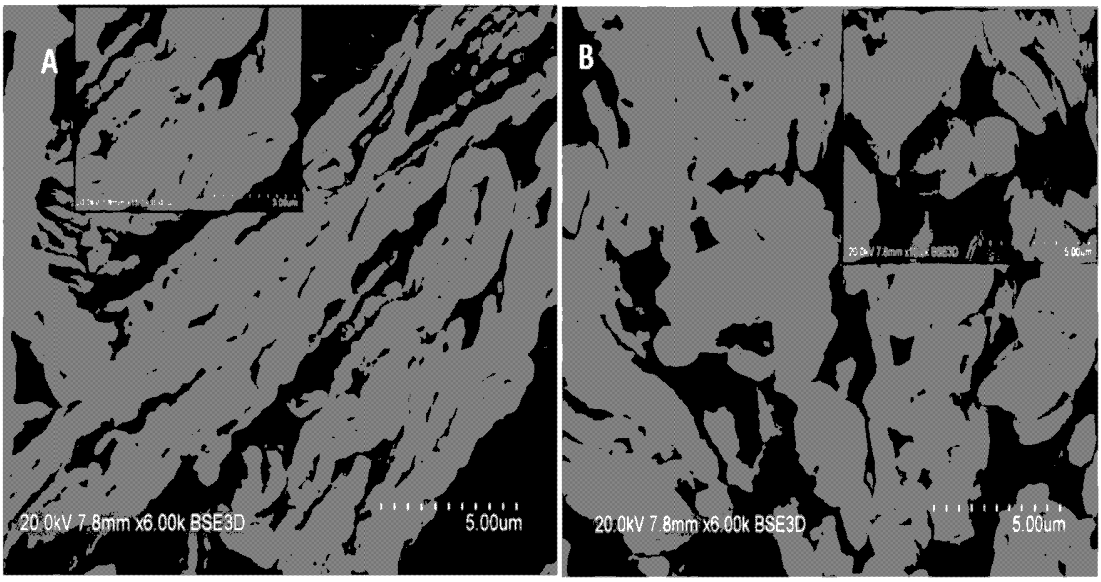
A
20.0kV 7.8mm x6.00k BSE3D
5.00um
B
20.0kV 7.8mm x6.00k BSE3D
5.00um

Fig. 24

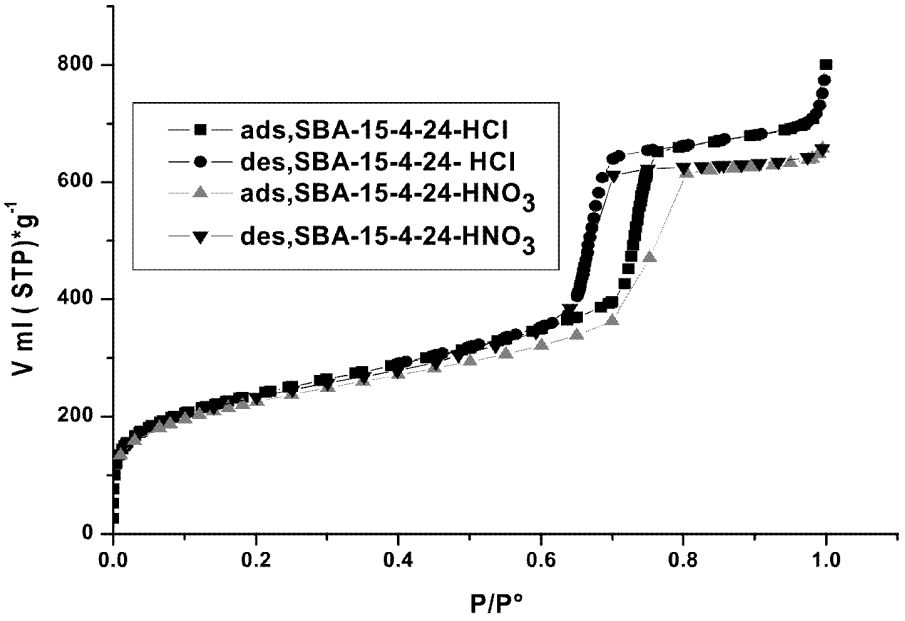
800
600
400
200
0
0.0
0.2
0.4
0.6
0.8
1.0
V ml (STP)*g-1
P/P°
ads,SBA-15-4-24-HCl
des,SBA-15-4-24- HCl
ads,SBA-15-4-24-HNO3
des,SBA-15-4-24-HNO3

Fig. 25

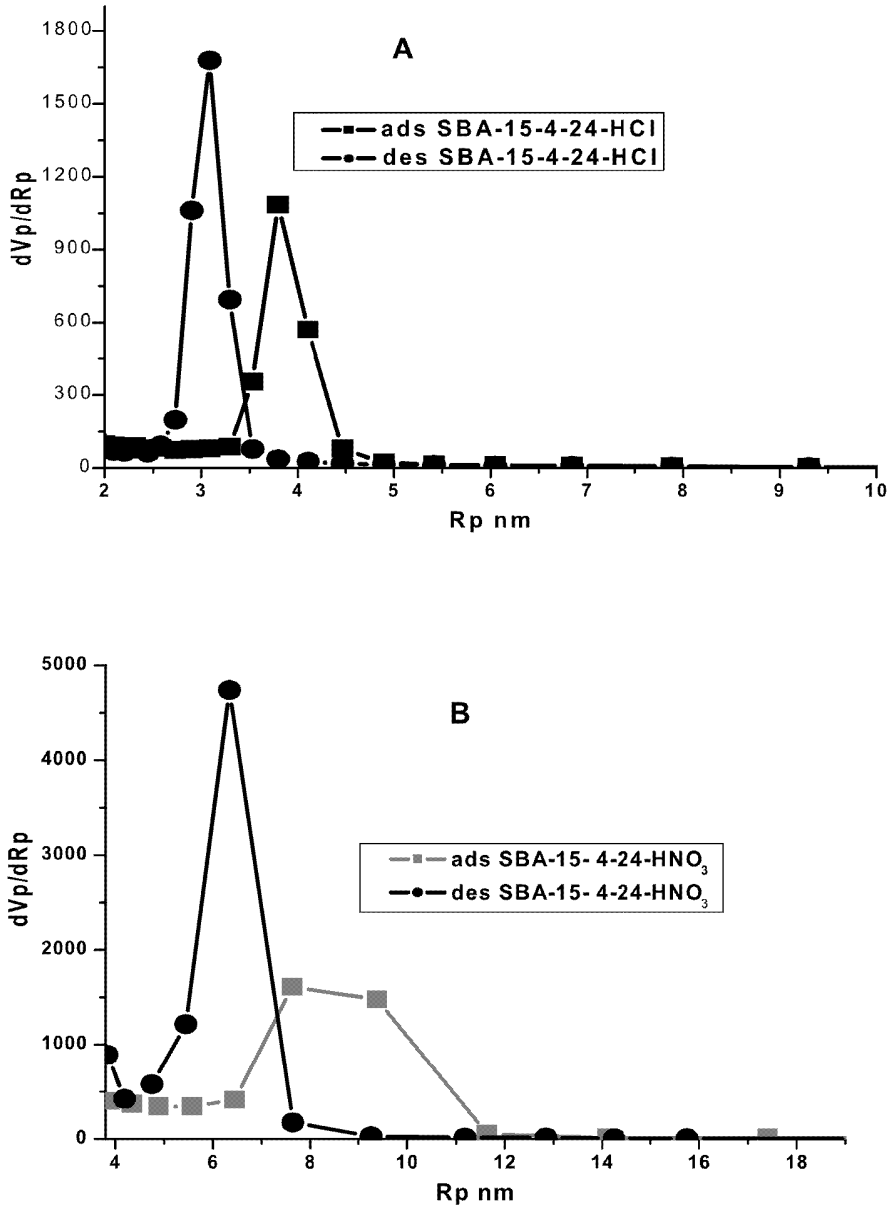
A
ads SBA-15-4-24-HCl
des SBA-15-4-24-HCl
dVp/dRp
Rp nm
B
ads SBA-15- 4-24-HNO3
des SBA-15- 4-24-HNO3
dVp/dRp
Rp nm

Fig. 26

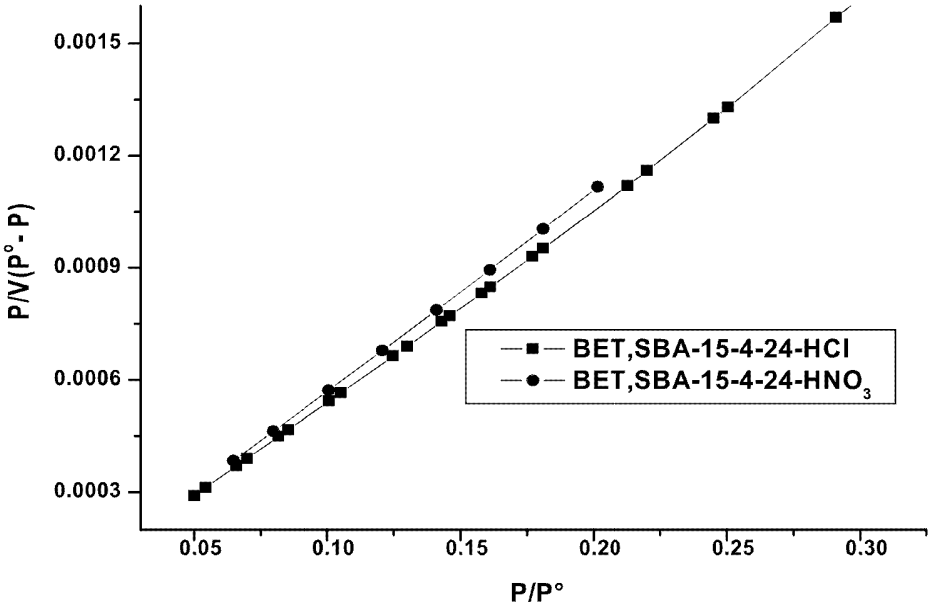
0.0015
0.0012
0.0009
0.0006
0.0003
P/V(P°- P)
0.05
0.10
0.15
0.20
0.25
0.30
P/P°
BET,SBA-15-4-24-HCl
BET,SBA-15-4-24-HNO3

Fig. 27

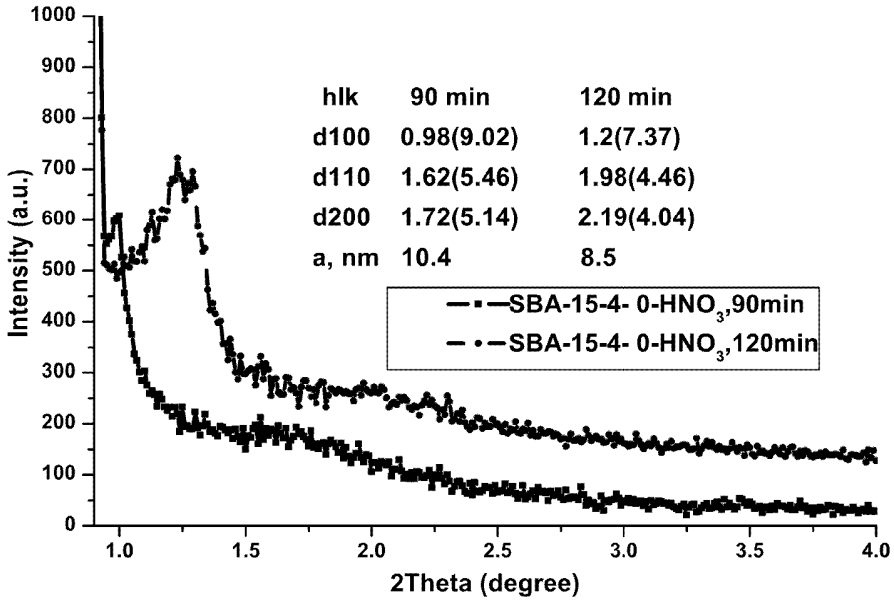
hlk 90 min 120 min
d100 0.98(9.02) 1.2(7.37)
d110 1.62(5.46) 1.98(4.46)
d200 1.72(5.14) 2.19(4.04)
a, nm 10.4 8.5
SBA-15-4- 0-HNO3,90min
SBA-15-4- 0-HNO3,120min
Intensity (a.u.)
2Theta (degree)
1000
900
800
700
600
500
400
300
200
100
0
1.0
1.5
2.0
2.5
3.0
3.5
4.0

Fig. 28

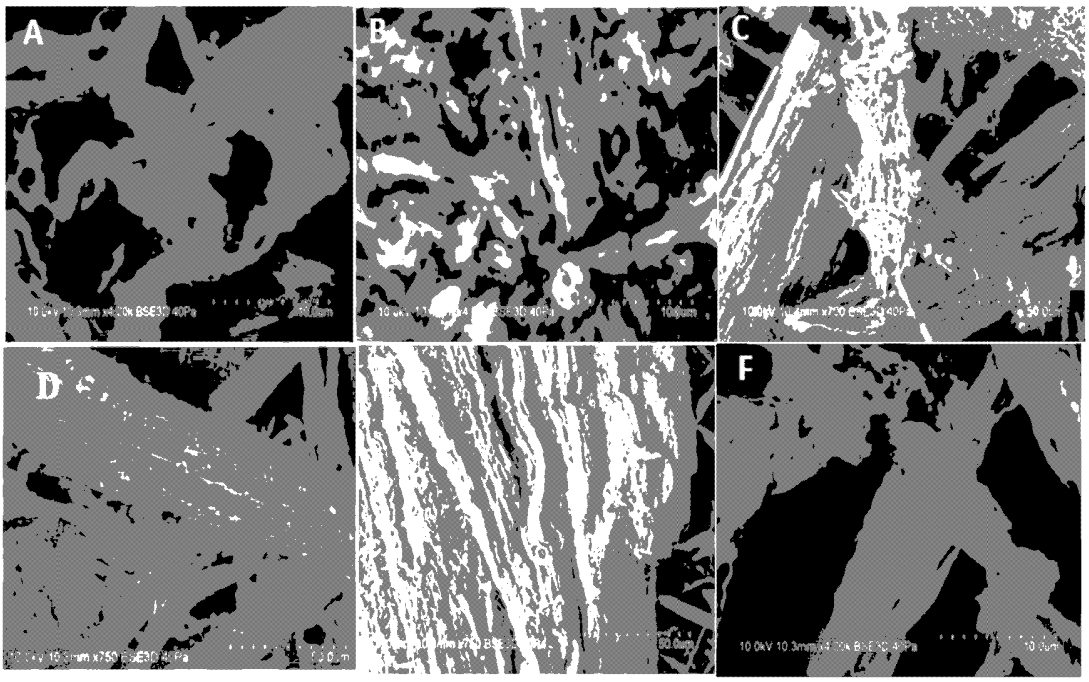

Fig. 29

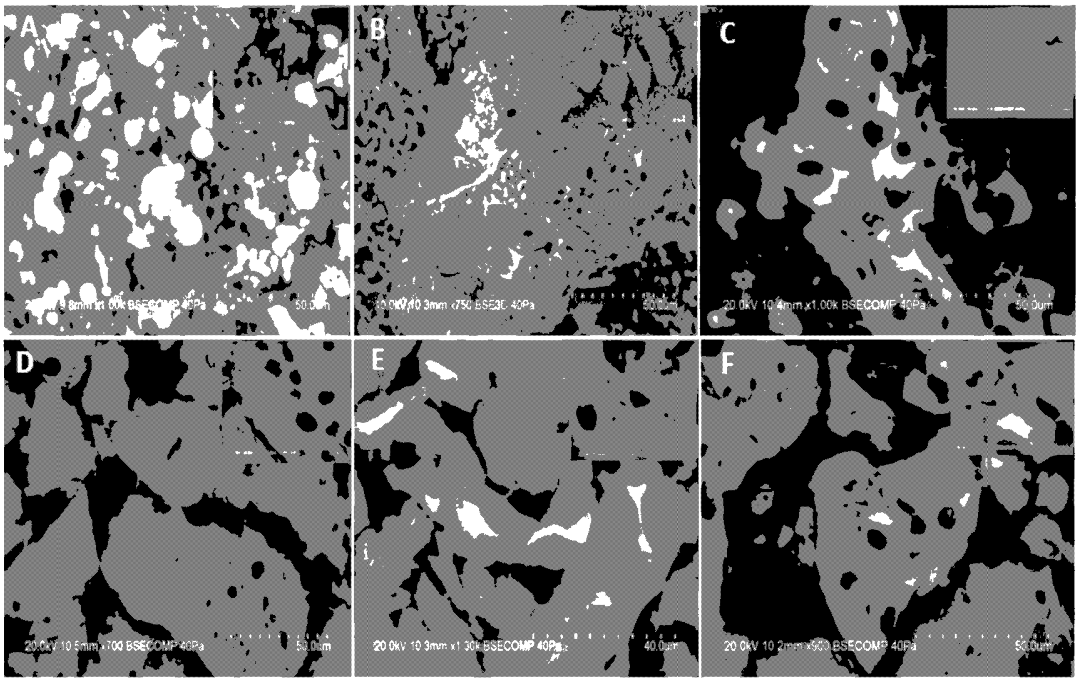

Fig. 30

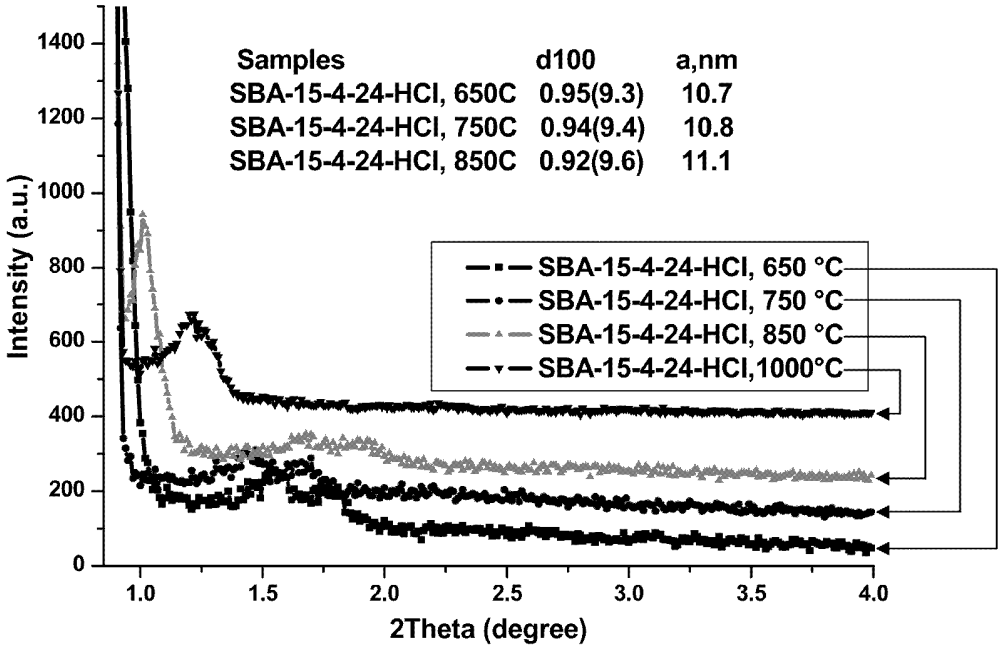
Samples d100 a,nm
SBA-15-4-24-HCl, 650C 0.95(9.3) 10.7
SBA-15-4-24-HCl, 750C 0.94(9.4) 10.8
SBA-15-4-24-HCl, 850C 0.92(9.6) 11.1
SBA-15-4-24-HCl, 650 °C
SBA-15-4-24-HCl, 750 °C
SBA-15-4-24-HCl, 850 °C
SBA-15-4-24-HCl,1000°C
Intensity (a.u.)
2Theta (degree)
0
200
400
600
800
1000
1200
1400
1.0
1.5
2.0
2.5
3.0
3.5
4.0

Fig. 31

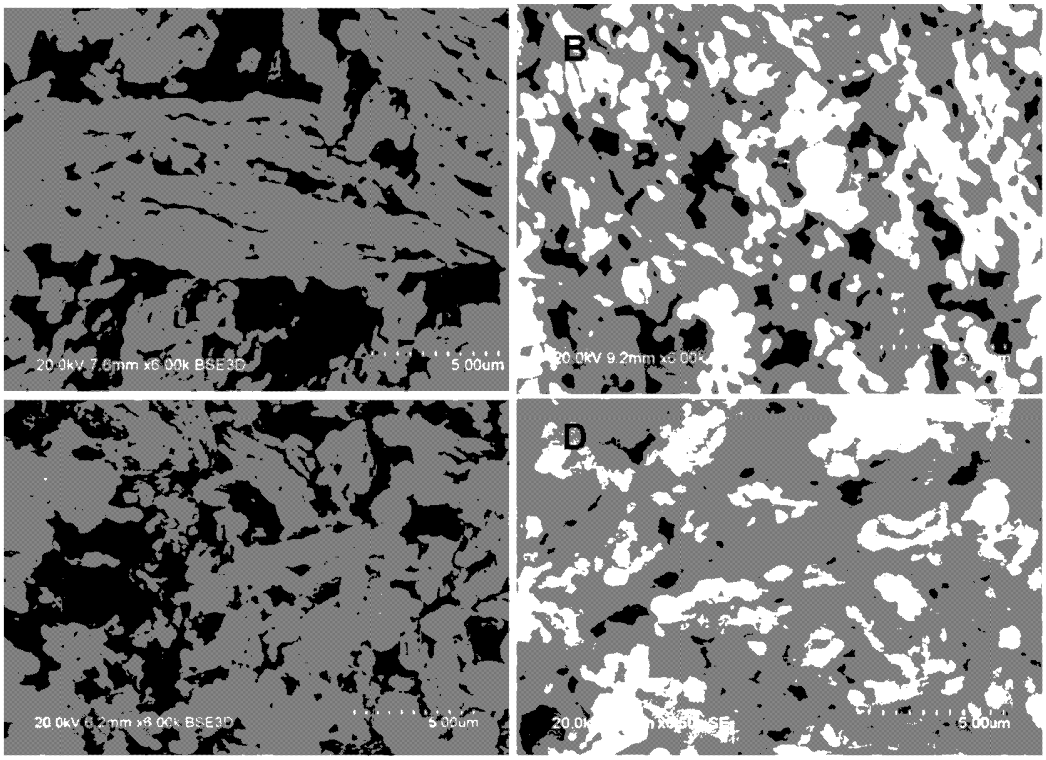

Fig. 32

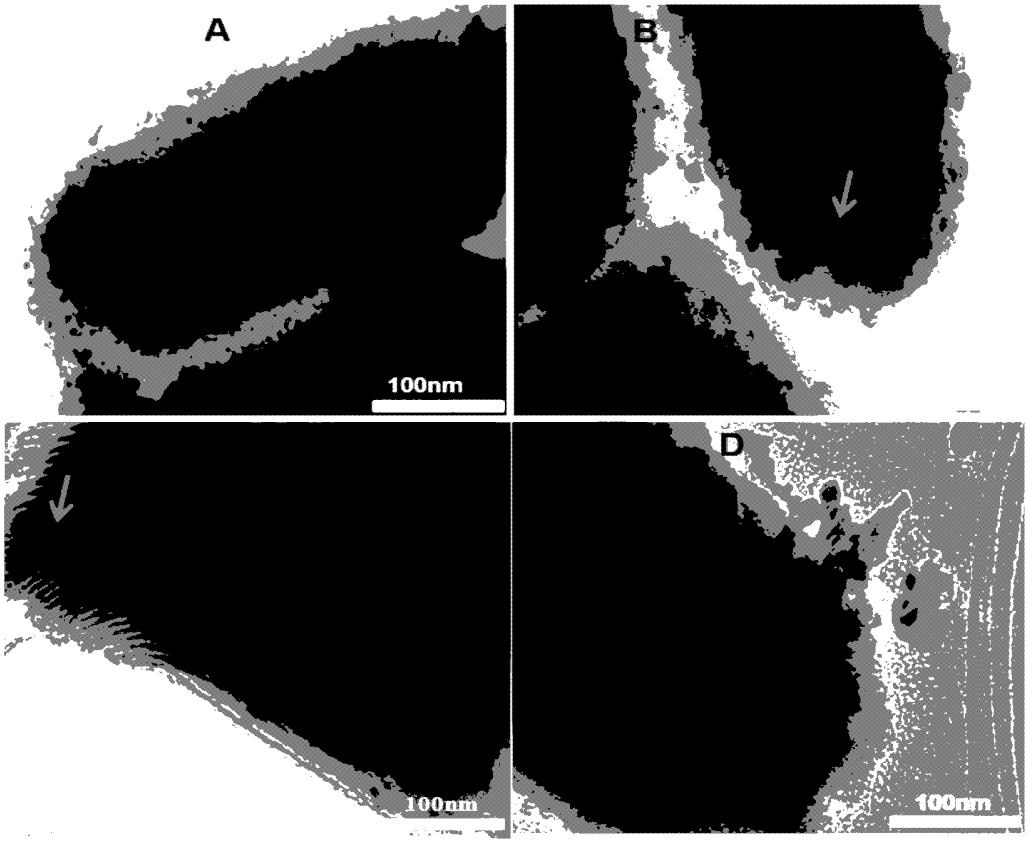

Fig. 33

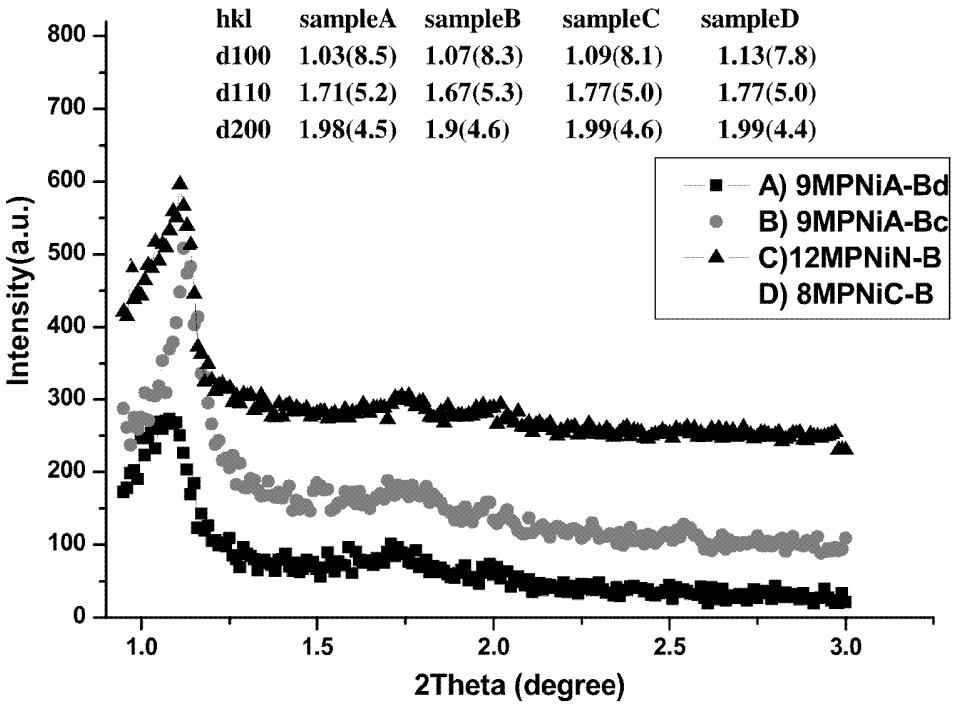
hkl sampleA sampleB sampleC sampleD
d100 1.03(8.5) 1.07(8.3) 1.09(8.1) 1.13(7.8)
d110 1.71(5.2) 1.67(5.3) 1.77(5.0) 1.77(5.0)
d200 1.98(4.5) 1.9(4.6) 1.99(4.6) 1.99(4.4)
A) 9MPNiA-Bd
B) 9MPNiA-Bc
C)12MPNiN-B
D) 8MPNiC-B
Intensity(a.u.)
2Theta (degree)
0
100
200
300
400
500
600
700
800
1.0
1.5
2.0
2.5
3.0

Fig. 34

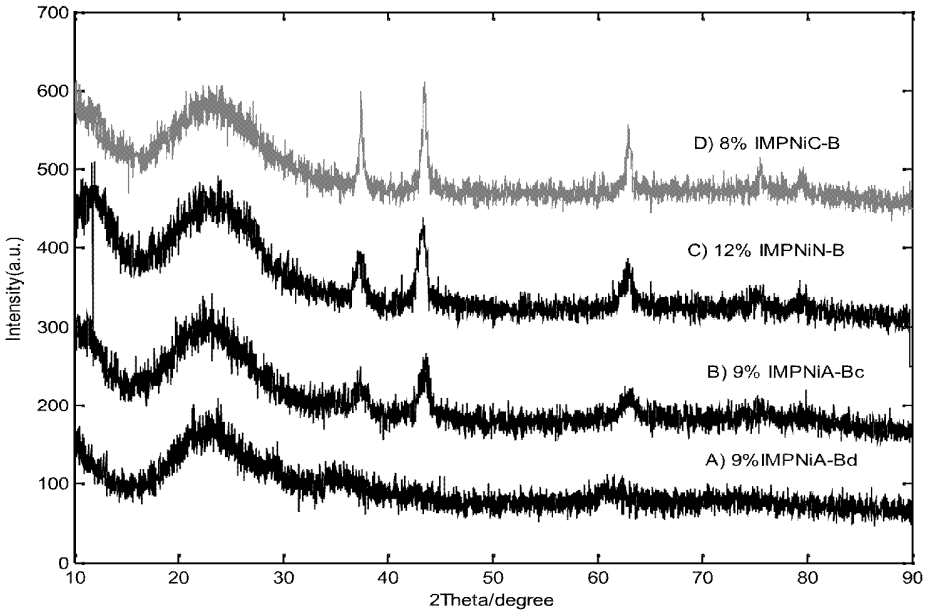
D) 8% IMPNiC-B
C) 12% IMPNiN-B
B) 9% IMPNiA-Bc
A) 9%IMPNiA-Bd
Intensity(a.u.)
2Theta/degree
0
100
200
300
400
500
600
700
10
20
30
40
50
60
70
80
90

Fig. 35

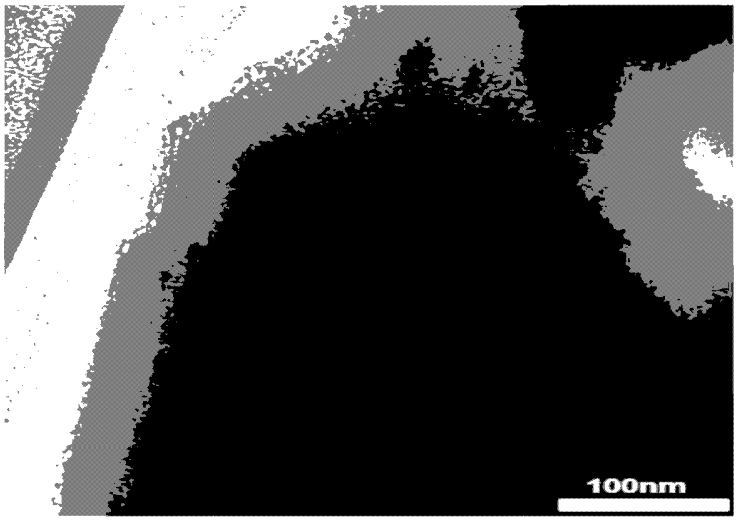

Fig. 36

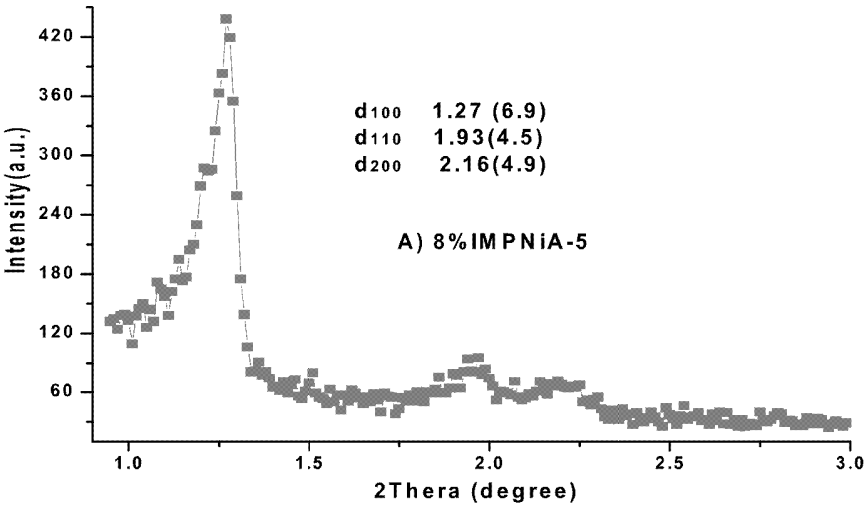
d100 1.27 (6.9)
d110 1.93(4.5)
d200 2.16(4.9)
A) 8%IMPNiA-5
Intensity(a.u.)
2Thera (degree)

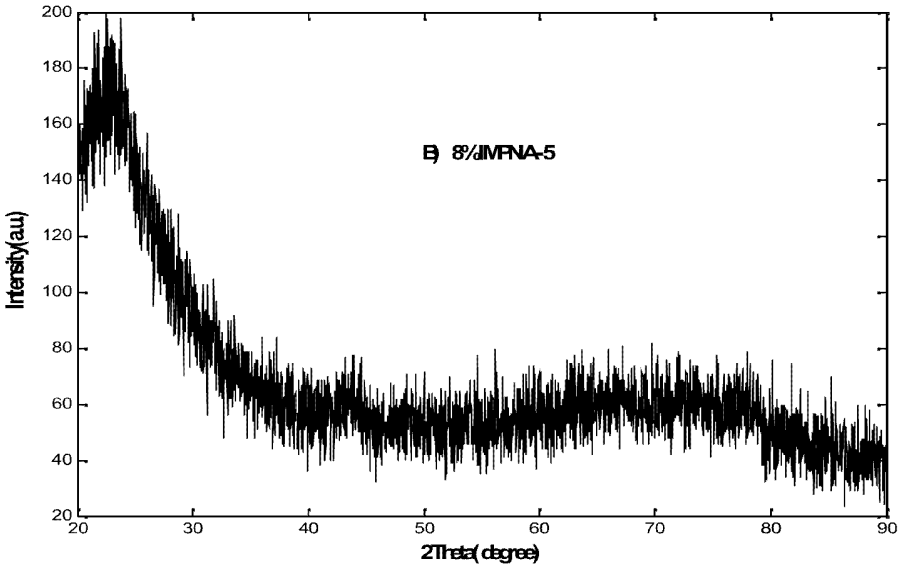
B) 8%IMPNiA-5
Intensity(a.u.)
2Theta(degree)

Fig. 37

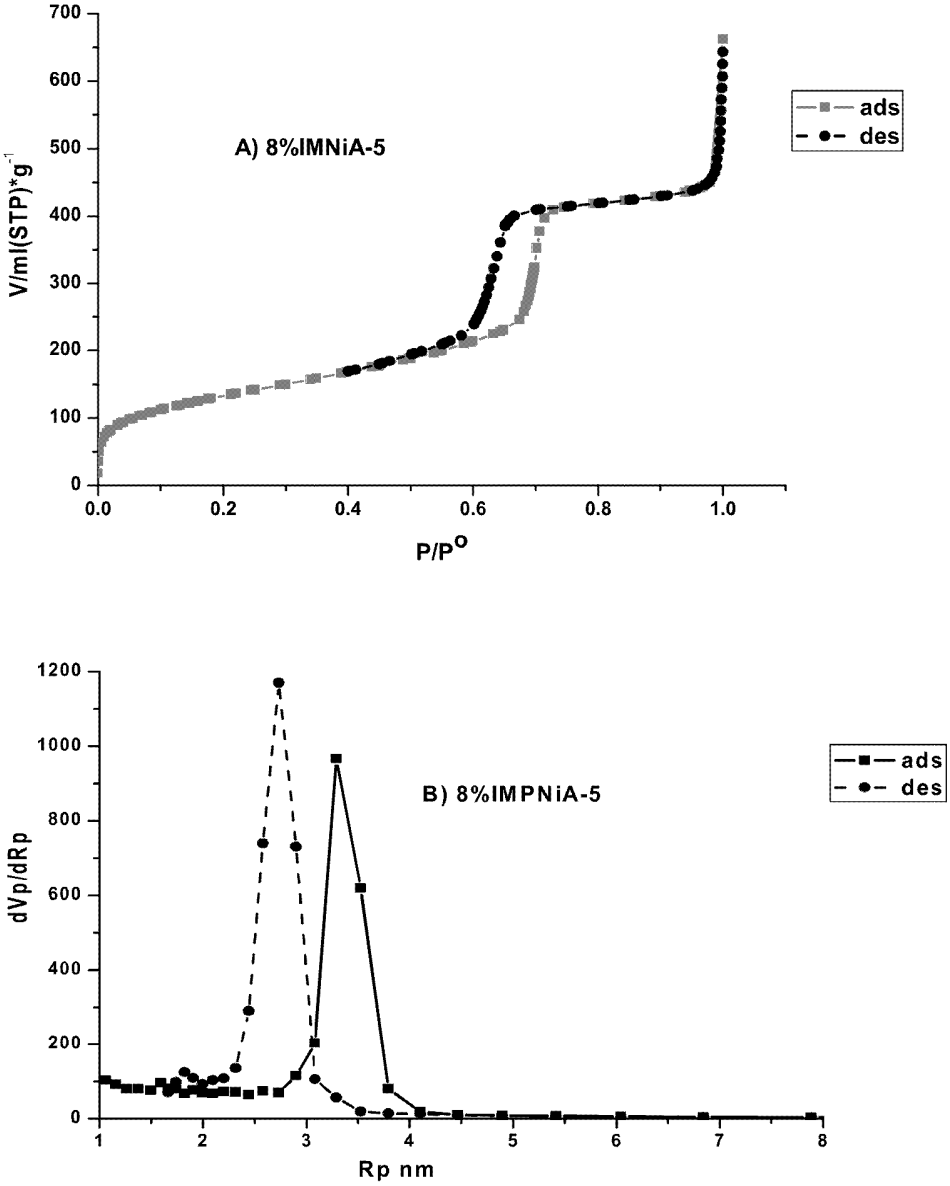
A) 8%IMNiA-5
V/ml(STP)*g-1
P/Po
ads
des
B) 8%IMPNiA-5
dVp/dRp
Rp nm
ads
des

Fig. 38